NATIONAL ADVISORY COMMITTEE FOR AERONAUTICS

TECHNICAL NOTE 3163

USE OF A HOT-WIRE ANEMOMETER IN SHOCK-TUBE INVESTIGATIONS

By Darshan Singh Dosanjh

The Johns Hopkins University

Washington

December 1954

TABLE OF CONTENTS

NATIONAL ADVISORY COMMITTEE FOR AERONAUTICS

TECHNICAL NOTE 3163

USE OF A HOT-WIRE ANEMOMETER IN SHOCK-TUBE INVESTIGATIONS

By Darshan Singh Dosanjh

SUMMARY

The use of the hot-wire anemometer as an instrument for experimental investigations of the transient flow phenomena in a shock tube is examined. The response of a hot-wire to a transient step-function type of change in flow conditions (e.g., shock waves) is experimentally studied and a criterion for predicting the right compensation is postulated and experimentally verified. The advantages and limitations of this somewhat special and, until now, unattempted use of the hot-wire anemometer are stressed.

Besides using the hot-wire anemometer for the actual wave phenomena and for flow studies, it has been very successfully used as a timing and/or triggering device in shock-tube work. It is demonstrated both from theoretical considerations as well as experimental observations that the hot-wire anemometer is satisfactory for timing very weak traveling shock waves, while it can be used for similar purposes for comparatively stronger shocks.

INTRODUCTION

The shock tube as an instrument of research has been gainfully employed in the studies of one-dimensional unsteady flow of gases and the transient wave phenomena by a large number of workers both in this country and abroad. The shock tube has served as an inexpensive and simple source of transient flows of quite heterogeneous thermodynamical properties. The short-duration flows with pressures, temperatures, and densities extraordinarily different from the normal atmospheric conditions are easily made accessible. For instance, one can easily produce, for a short duration, temperatures comparable with surface solar temperatures.

Optical techniques[1] (spark shadowgraphs, schlieren, interferometer, spectroscopes, etc.) have been the main tools employed in shock-tube

[1]References 1 and 2; also private conversation with Research Group at Cornell University, Department of Aeronautics, about some spectroscopic work being done in the region behind traveling shock waves.

research. These techniques have been generally very useful in studying the traveling shocks, their reflection and diffraction, and other allied phenomena. But if there were some fluctuations in the main flow behind these thermodynamic discontinuities (shock waves, contact surfaces, rarefaction waves, etc.), then these instruments shed only a limited amount of quantitative light on the phenomena (ref. 3). For instance, it is well known that because of the breaking characteristics of cellophane (the usual diaphragm material) the contact surface flow is rather turbulent. Qualitative confirmation of the presence of turbulence in this flow is the best that optical techniques have been able to deliver so far. It was to explore the possible eventual use of the hot-wire anemometer for the study of transient mean and/or fluctuating flows and the wave phenomena involved in shock tubes that this present work was undertaken.

The hot-wire is a standard instrument for studying the nature of subsonic and supersonic turbulent flow fields. Almost all of the development and worth-while analysis of this commendable technique are based on the assumption of small fluctuations as compared with the mean flow in which the hot-wire is operated. Ordinarily shock tubes are operated such that there is no mean flow in the system to start with. Then all of a sudden large flow fields are established for a very short duration. If the hot-wire is mounted in the middle of the cross section of the tube at some convenient location and the shock tube is operated, the response of the hot-wire will give the time history of the flow passing over it. So before one is able to study the fluctuations (artificially introduced or naturally present) in the flows behind the principal waves generated in the shock tube, it is necessary to gather some basic information about the response of this instrument to these transient wave fronts and the flow regions behind them.

The hot-wire anemometer and the associated electronic equipment are usually tested on the basis of the validity of certain hot-wire response equations (refs. 4, 5, and 6). The transient response of the hot-wire, when proper electronic compensation is applied, is usually assumed to be identical for transients in flow conditions or in heating current. (Ref. 7 by Betchov seems to show that, because of thermal propagation, the two may be somewhat different.) This plausible assumption was first experimentally verified by the author and others (ref. 8). Since then the technique of experimentation has been considerably improved and most of the results arrived at in the original report have been rechecked and extended. Main conclusions included in the present report are based on data obtained mostly with the experimental arrangement as described here.

Known fluctuations in velocity and temperature are difficult to produce. Wires have been shaken sinusoidally up to 150 to 200 cps in moving

air streams, but the frequency was limited because of the mechanical difficulties.[2] It is believed that the traveling shock wave furnishes an ideal flow field for studying the hot-wire response to a time-step-function change in flow conditions. When a traveling shock wave passes over the hot-wire, the latter experiences a discontinuous step-function variation of the mass flow, pressure, density, stagnation, and ambient temperature, and the flow is uniform and constant thereafter for a few milliseconds until the contact surface or some other wave front (reflected shock or rarefaction wave, etc.) reaches the hot-wire.

When a step-function type of transient (either in current or flow condition) is applied to the hot-wire, because of the thermal lag the response of the hot-wire is exponential (ref. 6). This can be electronically compensated such that the exponential is restored to almost a step function (ref. 8 and fig. 1). The hot-wire anemometer thus can be used to study the transient wave fronts and fluctuations in the flow fields in a shock tube if one knows how to predict the right compensation values (for constant-current operation). The criterion for predicting the compensations has been suggested and verified within an acceptable experimental agreement.

Ultimate time resolution of the hot-wire and the associated equipment is usually estimated electrically (square-wave technique, ref. 4). Hot-wire response to a shock wave offers an alternate way of experimentally determining this ultimate time resolution by recording its response to a controlled step-function type of change in flow conditions. This has been done for the equipment used in this work (see also ref. 8).

In shock-tube studies, one of the most important instrumentation problems is the controlled timing of the transient phenomena. Usually the primary shock wave is used as the basis for the design and operation of a transducer which changes some property of the shock front into a suitable electric pulse. This pulse, after sharpening and amplification, is utilized for triggering and/or timing purposes. Since the exponential response of the hot-wire to any sudden changes in flow conditions can be sharpened either by compensating amplifiers or by differentiating the signal, the hot-wire anemometer has been successfully used to time various transient phenomena in a shock tube.

Most of the experimental work in shock tubes does not include any systematic studies at the lower end of the spectrum of shock strength. This, by and large, is due to the limitations of the existing timing devices. When the hot-wire is used at elevated temperatures, it is predominantly mass flow sensitive. This characteristic of hot-wires has

---

[2]Unpublished personal communication regarding work done on low frequency shaking of hot-wires at the National Bureau of Standards in the early 1930's.

been successfully used to time very weak shocks (drift velocity of a few feet per second) nearing virtually a sound speed. The experimental triggering and timing system actually used is described in the text. (For details see ref. 9.)

It is experimentally demonstrated over a limited range of shock strengths that the hot-wire anemometer can be used to measure transient temperature jumps. Also the mass-flow and temperature jumps which occur simultaneously in case of a shock wave can be separated. This is achieved by using two different heating currents through the same wire, with the same shock strength used twice consecutively (ref. 5). The difference between the observed results and the expected ones is discussed. Hot-wires have also been used in detecting and timing rarefaction waves.

Since this technique has further potentialities, the discussion included about the response of the hot-wire in various regions of the shock-tube flows at times exceeds the range and regions actually investigated experimentally. This ground work may facilitate the work of those who may choose to use this technique to extend the scope of the present investigation.

The author is indebted to Drs. Francis H. Clauser and Leslie S. G. Kovásznay for their encouragement and many helpful suggestions. Mr. Richard Swartley's help with the experimental work is gratefully acknowledged.

This work was supported under the combined sponsorship of the Bureau of Ordnance, Department of the Navy, and the Department of the Air Force. Since April 1, 1953, the sponsorship has been entirely by the Air Force. The author appreciates this much needed financial assistance.

The present report is based on Part I of a dissertation (ref. 10) submitted by the author to the Faculty of Philosophy of The Johns Hopkins University in conformity with the requirements for the degree of Doctor of Philosophy. It has been made available to the National Advisory Committee for Aeronautics for publication because of its general interest.

SYMBOLS

Hot-Wire Symbols

$$a_v(t) = \frac{R_v - R_e}{R_e} = \alpha_e(T_v - T_e)$$

$$a_w(t) = \frac{R_w - R_e}{R_e} = \alpha_e(T_w - T_e)$$

C	heat capacity of wire, ergs/deg
d	diameter of wire
$E(T_w)$	stored energy in wire, CT_w
Δe	voltage fluctuation or jump
H	heat loss from wire per unit time
I	heating current through hot-wire
I_o	characteristic current of wire (a calibration constant used in range where King's equation of heat loss is assumed valid)
k	heat conductivity of gas
l	length of wire
M^*	time constant of wire for small fluctuations (linearized theory)
$n = \frac{C}{\alpha R_f}$	
$R_e(t)$	equilibrium resistance at $T_e(t)$
R_f	reference resistance at T_f
R_o	wire resistance at room temperature without any current through it
$R_v(t)$	wire resistance at $T_v(t)$
$R_w(t)$	wire resistance at $T_w(t)$
$T_e(t)$	equilibrium temperature attained by wire if unheated
T_f	reference temperature (usually at 273° K)
$T_v(t)$	virtual wire temperature that would be attained in absence of thermal lag
$T_w(t)$	instantaneous temperature of hot-wire (average along wire)
t	time
U_o	characteristic velocity of wire (a calibration constant of wire used in range where King's equation of heat loss is assumed valid)

W heat generated in wire per unit time

α temperature coefficient of resistivity at reference temperature

$$\alpha_e = \frac{\alpha}{1 + \alpha(T_e - T_f)}$$

μ viscosity of gas

Shock-Tube Parameters

a local speed of sound

$$a_{vc}(t) = \frac{R_{vc} - R_{oc}}{R_{oc}}$$

$$a_{v2}(t) = \frac{R_{v2} - R_{e2}}{R_{e2}} = \frac{R_{v2} - R_{o2}}{R_{o2}} \quad \text{if} \quad R_{e2} = R_{o2}$$

C_p specific heat at constant pressure

C_v specific heat at constant volume

K Knudsen number, λ/d

M Mach number of flow corresponding to region indicated by subscripts, u/a

$M_{2,c}^*(t)$ time constant for large step function in flow conditions when wire is operated "hot"

$M_{ou}^*(t)$ time constnat for large step function when wire is operated "cold" at velocity u

Nu Nusselt number, $H/\pi l k(T_w - T_e)$

P pressure ratio across diaphragm, p_R/p_1

Pr Prandtl number, $\mu C_p/k$

p_R pressure in compression chamber

R resistance of hot-wire at corresponding T

Re Reynolds number, $\rho u d/\mu$

$R_v(t)$ corresponding resistance at $T_v(t)$

S measure of shock strength, $p_2/p_1 > 1$

T, ρ, p temperature, density, and pressure, respectively

$T_v(t) = \begin{cases} T_{v1} = \text{Constant for } t < 0 \\ T_{v2} = \text{Constant for } t \geqq 0 \end{cases}$ operating equilibrium temperature of wire after wave front under study has passed over wire

U_s primary shock speed

$U_{s'}$ reflected shock speed

u velocity of flow

x coordinate along axis of tube

$\gamma = \frac{C_p}{C_v} = 1.4$ for air

λ molecular mean free path

ρu mass flow behind wave under study

$\sigma = \frac{\gamma + 1}{\gamma - 1} = 6$ for air

Subscripts:

c contact-surface region ending at foot of rarefaction wave and corresponding parameters

e equilibrium value of parameter

o stagnation parameters

R region ahead of head of centered rarefaction wave; before bursting of diaphragm, compression chamber as a whole

r region between head and tail of centered rarefaction wave

v "virtual" parameters, that is, value of various parameters if there had been no lag due to thermal capacity of wire or if fluctuations were infinitely slow

1 region and corresponding parameters in front of primary shock wave; before shock wave is generated, conditions in expansion chamber as a whole

2 region from primary shock wave to start of contact-surface region and corresponding parameters

3 region between reflected shock and reflecting wall and corresponding parameters

BASIC WAVE MODEL IN SHOCK TUBE

A shock tube usually consists of a long metallic pipe or box separated into two sections by a membrane across which a pressure differential can be established. The high-pressure side is called the compression chamber and the low-pressure side, the expansion chamber. When a desired pressure ratio is attained, the membrane is ruptured, generating a pressure wave propagating down the expansion chamber. Within a short distance from the membrane (a few diameters of the tube), the pressure wave steepens into a sharp pressure discontinuity (shock wave). The simple wave model and the associated regions of flow assumed in the subsequent analysis of shock-tube phenomena and the behavior of hot-wires are reproduced in figure 2. Mainly it consists of:

(a) A centered rarefaction wave moving to the left in the compression chamber.

(b) A plane shock wave (that will be referred to as the primary shock wave) moving at constant speed to the right in the expansion chamber.

(c) A contact surface (the boundary between masses of the gases previously on the two sides of the membrane) following the shock wave into the expansion chamber.

(d) A reflected shock from the closed far end of the expansion chamber, traveling upstream. If the end is open, the reflected wave will be a rarefaction wave.

Some of the other wave fronts in the shock tube are overlooked here because they do not play a prominent role in the scope of this work.

The usual simplifying assumptions in the analysis of the various waves and the associated flow phenomena are as follows:

(1) Perfect gas with γ constant.

(2) The membrane, or what is commonly called a diaphragm, is a plane boundary that is instantaneously removable without loss of energy.

(3) The flow in various regions of the shock tube is isentropic and one dimensional.

(4) There is no diffusion across the contact surface.

(5) The regions labeled R, 1, 2, and c as shown in figure 2 are assumed to be constant.

The operation of both the compression and the expansion chamber with air in them will be indicated by the notation Air/Air.

The quantitative values of the various thermodynamic parameters (mass flow, temperature, etc.) in the various regions of interest are required for their subsequent application in the determination of the hot-wire response. However, only the relevant relations without any extensive derivations will be included. (For details see refs. 1 and 10.)

Flow Region Behind Primary Shock Wave (State 2)

State 2 is the region behind the primary shock wave and the contact surface (fig. 2). All the following relations refer to the coordinate system in which the medium ahead of the shock front is at rest.

Let the shock strength

$$S = \frac{p_2}{p_1} = \frac{\text{Pressure behind shock wave}}{\text{Pressure in front of shock wave}}$$

and the primary shock speed

$$U_s = a_1\sqrt{\frac{1 + \sigma S}{1 + \sigma}} \tag{1}$$

where

$$\sigma = \frac{\gamma + 1}{\gamma - 1}$$

A plot of U_s versus S is given in figure 3.

The mass flow behind the shock wave in region 2 is given as

$$\frac{\rho_2 u_2}{\rho_1 a_1} = \frac{(\sigma - 1)(S - 1)}{\sigma + S}\sqrt{\frac{1 + \sigma S}{\sigma + 1}} \tag{2}$$

A plot of $\rho_2 u_2/\rho_1 a_1$ versus S is given in figure 4.

The temperature ratio is

$$\frac{T_2}{T_1} = \frac{S(\sigma + S)}{1 + \sigma S} \tag{3}$$

Since later the hot-wire will be assumed to respond to stagnation temperatures, it is desirable to obtain the corresponding relations (ref. 8). For the flow behind the primary shock wave, the energy equation is

$$C_p T_2 + \frac{1}{2} u_2^2 = C_p T_{o2}$$

or

$$\frac{T_{o2}}{T_2} = 1 + \frac{\gamma - 1}{2}\left(\frac{u_2}{a_2}\right)^2 \tag{4}$$

One can get

$$\frac{T_{o2}}{T_1} = \frac{S(6 + S)}{1 + 6S} + \frac{5}{7}\frac{(S - 1)^2}{1 + 6S}$$

or

$$\frac{T_{o2} - T_1}{T_1} = \frac{2}{7}(S - 1) \tag{5}$$

where $S > 1$. Relation (5) gives the theoretical rise in stagnation temperature behind the primary shock wave traveling in still air. The plot of T_{o2} versus S (also for other temperatures of possible interest) is given in figure 5.

Contact-Surface Region (State c)

State c is the region that contains the gas which, to start with, was in the compression chamber. As figure 2 shows, it ends at the foot of the centered rarefaction wave. The contact-surface flow is of considerable interest in shock-tube work. The sudden expansion of the gas in the compression chamber cools the gas considerably, thus reducing the local speed of sound, which in turn yields higher Mach number flows. Assuming that there is no change in entropy through the rarefaction wave generated because of this sudden expansion, one can solve the remaining continuity and momentum equations by the method of characteristics (ref. 11) such that the unknown physical quantities through the wave can be related to the known quantities ahead of the wave. If the centered rarefaction wave moving to the left in a gas at rest (shock-tube case) is considered under the assumptions that the expansion of the gas in the compression chamber is adiabatic and

$$\left.\begin{aligned} p_c &= p_2 \\ u_c &= u_2 \end{aligned}\right\} \tag{6}$$

then for Air/Air operation,

$$P = \frac{p_R}{p_1} = S\left[1 - \frac{S - 1}{\sqrt{7(1 + 6S)}}\right]^{-7} \tag{7}$$

The derivation of this basic equation is given in almost all of the shock-tube references listed. The physical quantities such as temperature, pressure, density, speed of sound, wave speeds, and particle velocities throughout regions r, c, and 2 are related to known quantities in regions R and 1 through relation (7) which connects the pressure ratio across the diaphragm to the shock strength. From the consideration of Mach number $M_c = \frac{u_c}{a_c}$, and making use of the boundary conditions (6) and the fact the expansion is assumed adiabatic, one can get

$$\frac{T_c}{T_R} = \left[1 - \frac{S - 1}{\sqrt{(\sigma + 1)(1 + \sigma S)}}\right]^2 \tag{8}$$

It has been experimentally observed that the hot-wire responds to the stagnation temperature of the flow. With that end in view, an expression for the stagnation temperature in the contact-surface flow can be obtained

from the consideration of the energy equation of the contact-surface flow. One gets

$$\frac{T_{oc}}{T_1} = \frac{T_{oc}}{T_R} = \left(1 + \frac{\gamma_R - 1}{2}\left\{\frac{2}{\gamma_R - 1}\left[\frac{1}{1 - \frac{S - 1}{\sqrt{(\sigma + 1)(1 + \sigma S)}}} - 1\right]\right\}^2\right)\left[1 - \frac{S - 1}{\sqrt{(\sigma + 1)(1 + \sigma S)}}\right]^2 \qquad (9)$$

Plots of T_c and T_{oc} versus S are given in figure 5.

In calculating hot-wire voltage signals for pure temperature response, one has to consider the fact that the hot-wire reaches equilibrium at approximately the stagnation temperature of the flow behind the primary shock wave before the contact surface washes over it. So the decrease in resistance due to the cooling of the wire will start from the elevated temperature. Therefore $T_{o2} - T_{oc}$ is more useful. From relations (5) and (9) one can get

$$\frac{T_{oc} - T_{o2}}{T_{o2}} = \left(1 + 2\left\{5\left[\frac{1}{1 - \frac{S - 1}{\sqrt{7(1 + 6S)}}} - 1\right]\right\}^2\right)\left[1 - \frac{S - 1}{\sqrt{7(1 + 6S)}}\right]^2\left[\frac{2}{7}(S - 1) + 1\right]^{-1} - 1 \qquad (10)$$

One also can obtain the mass flow in the contact surface given by

$$\frac{\rho_c u_c}{\rho_1 a_1} = P\left[1 - \frac{S - 1}{\sqrt{(\sigma + 1)(1 + \sigma S)}}\right]^{\sigma - 1}\frac{(\sigma - 1)(S - 1)}{\sqrt{(\sigma + 1)(1 + \sigma S)}} \qquad (11)$$

A plot of this is given in figure 4. For an Air/Air operation the ratio of relation (11) to (2) is ρ_c/ρ_2. From the consideration of the ordinary gas equation

$$\frac{\rho_c}{\rho_2} = \frac{T_2}{T_c}$$

Since $T_2 > T_c$, one has $\rho_c > \rho_2$. While there is no mass flow across the contact-surface discontinuity, it involves a sudden temperature and density discontinuity between the mass of the gas which originally belonged on the two sides of the diaphragm. This fact has an interesting bearing on the Reynolds numbers in adjacent regions 2 and c of the flow (figs. 6 and 7).

Reflected Shock and Region Behind It (State 3)

In the conventional arrangement in shock-tube work, the primary shock wave travels through the medium which is at rest in front of it. If the far end of the shock tube is closed by a completely solid and rigid wall parallel to the shock front, the shock will be totally reflected and will travel upstream against the drift velocity of the primary (incident) shock wave. The gas in contact with the rigid wall must be at rest. The reflected shock thus has a strength such that the drift velocity due to the primary shock heading toward the closed end is canceled by the reflected shock. While the primary shock accelerates the medium from the speed zero to u_2, the reflected shock decelerates it back to zero. Thus the reflected shock differs from the primary shock in that the state in front of the reflected shock wave is identical with the state behind the primary shock wave. Let the reflected shock strength $S' = p_3/p_2$. From the Rankine-Hugoniot relations for the incident and reflected shock and the condition that

$$u_2 = u_2'$$

(where primed parameters are associated with the reflected shock) one can obtain the speed of the reflected shock with respect to the shock tube as

$$U_{s'} = a_1 \frac{2S + (\sigma - 1)}{\sqrt{(\sigma + 1)(\sigma S + 1)}}$$

The temperature behind the reflected shock is

$$\frac{T_3}{T_1} = \frac{S(\sigma + S)}{1 + \sigma S} \frac{(\sigma + 2)S - 1}{\sigma + S} \left(\frac{2}{\sigma + 1} + \frac{\sigma - 1}{\sigma + 1} \frac{1}{S} \right) \tag{12}$$

A plot of this is given in figure 5.

Rarefaction Waves in Shock Tube

Centered rarefaction wave propagating in compression chamber (region r).- From the viewpoint of the hot-wire anemometer as a timing device, the centered rarefaction wave (region r) is also of some interest. It originates because of the sudden adiabatic expansion at the abrupt breaking of the diaphragm between the expansion and compression chamber. Such a wave represents a continuous disturbance for $t > 0$ where $t = 0$

is the time of rupture. If the problem is analyzed by the method of characteristics, one can arrive at the following conclusions:

(1) The head of the rarefaction wave travels with the speed of sound of the medium at rest in the compression chamber.

(2) The temperature change across the rarefaction front and the mass flow per unit area initiated by a centered rarefaction are given by

$$T = \frac{T_r}{T_R} = \left(\frac{2}{\gamma_R + 1} - \frac{1}{\sigma_R}\frac{X}{\tau}\right)^2 \tag{13}$$

and

$$m = \frac{\rho_r u_r}{\rho_R a_R} = \frac{2}{\gamma_R + 1}\left(\frac{X}{\tau} + 1\right)\left(\frac{2}{\gamma_R + 1} - \frac{1}{\sigma_R}\frac{X}{\tau}\right)^{\frac{2}{\gamma_R - 1}} \tag{14}$$

where

$$X = \frac{x}{L}$$

$$\tau = \frac{a_R t}{L}$$

and L is the length of the compression chamber. For the desired hot-wire use as a timing device, T_r/T_R and $\rho_r u_r/\rho_R a_R$ are of main interest. These are plotted in figures 8 and 9 for various times after the diaphragm is ruptured, namely, for $\tau = 0.20$, 0.25, 0.5, 0.75, and 1.0, against various locations in the shock tube. Interaction of these plots with the corresponding temperature and mass flows in the contact surface (relations (8) and (11), respectively) sets the limit to the region of application of relations (13) and (14).

For the head of the rarefaction wave, at $X_R = \frac{x}{a_R t} = -1$, one gets

$$\left(\frac{dT}{dx}\right)_{x=-1} = -\frac{2}{\sigma_R} \tag{15}$$

Similarly,

$$\left(\frac{dm}{dx}\right)_{x=-1} = \frac{2}{\gamma_R + 1} \tag{16}$$

The head of the rarefaction thus represents a discontinuity in temperature and mass flow. The hot-wire responds to both temperature and mass-flow change. The rarefaction initiates cooler flow. If the hot-wire is used at an elevated temperature, both the mass-flow and temperature changes involved give signals of the same sign. Thus one can use the hot-wire technique to clock the speed of the rarefaction wave. Since the head of the rarefaction travels at the speed of sound in the still gas in the compression chamber, one can measure the sound speeds in various gases rather easily with the hot-wire technique provided the hot-wire is used at an elevated temperature.

Rarefaction originating at open end of shock tube.- If the shock tube is operated with the extreme end of the expansion chamber open (fig. 2), a rarefaction wave originates when the primary shock wave leaves the open end. This is due to the pressure behind the traveling primary shock wave being higher than the atmospheric pressure surrounding the shock tube. If the flow behind the primary shock wave is supersonic, the open end does not influence the quasi-steady flow inside the shock tube. But for the subsonic range (i.e., $M_2 < 1$) a rarefaction wave is propagated toward the inside of the shock tube starting at the instant the primary shock wave leaves the open end (fig. 2). This wave is, in general, transmitted as a rarefaction wave, at least until it encounters the contact surface inside the shock tube. The propagation of this rarefaction wave has been studied experimentally (procedure and results to be discussed later), especially from the point of view of its speed, that is, the time of its appearance at fixed stations along the axis of the shock tube under different working pressure ratios, and so forth. For the detection of the time of arrival, it is sufficient to consider only the first characteristic of the wave originating at the open end. It will further be assumed that the flow behind the primary shock is subsonic and that the position of the detecting station is at such a distance from the open end that the contact-surface flow or the principal reflected rarefaction wave does not reach that station prior to this rarefaction front under investigation. The first characteristic of this rarefaction wave travels at the speed of sound in the region of transmission. Based on these assumptions the time of arrival of the first characteristic at any station can be predicted.

Suppose ξ and η are the coordinates of the detecting station (which, in this case, will be a hot-wire mounted along the axis of the shock tube). Then, as shown in figure 10,

$$r = a_2 t = \sqrt{x^2 + y^2} \tag{17}$$

$$\left.\begin{aligned} y &= \eta \\ x &= \xi + u_2 t \end{aligned}\right\} \tag{18}$$

where u_2 is the particle speed and a_2 is the speed of sound in region 2.

Therefore from relations (17) and (18), the velocity of propagation of the rarefaction front moving toward the inside from the open end of the shock tube is

$$V_{ri} = \frac{\sqrt{\xi^2 + \eta^2}}{t}$$

$$= \frac{a_2^2 - u_2^2}{u_2 \cos\theta \pm \sqrt{a_2^2 - u_2^2 \sin^2\theta}} \tag{19}$$

Retaining the sign which gives positive velocity of propagation, for $\theta = 0$,

$$V_{ri} = a_2 - u_2 \tag{20}$$

For the outside of the shock tube, a similar procedure gives the velocity of propagation as

$$V_{ro} = \frac{a_2^2 - u_2^2}{-u_2 \cos\theta \pm \sqrt{a_2^2 - u_2^2 \sin^2\theta}} \tag{21}$$

Retaining the sign which gives the positive velocity, for $\theta = 0$,

$$V_{ro} = a_2 + u_2 \tag{22}$$

For $\theta = 90^\circ$, that is, at the open end, from relations (19) and (21)

$$V_r = \sqrt{a_2^2 - u_2^2} \tag{23}$$

If a hot-wire mounted in the middle of the shock tube as a detecting device is used, then, when the primary shock wave passes over the hot-wire, it will register the jump and the response will stay steady until the rarefaction wave passes over it (fig. 1). The total time interval between the instant of jump due to the shock wave and the time the cooling due to rarefaction is registered will be

$$t = \frac{\xi}{U_s} + \frac{\sqrt{\xi^2 + \eta^2}}{V_{ri}} \tag{24}$$

If the hot-wire was mounted in the wall of the shock tube, then

$$t = \frac{\xi}{U_s} + \frac{\xi}{V_{ri}} \tag{25}$$

For the hot-wire mounted outside the shock tube along the axis

$$t = \frac{\sqrt{\xi^2 + \eta^2}}{V_{ro}} - \frac{\xi}{U_s} \tag{26}$$

where ξ is the horizontal distance from the open end. (Experimental verification of these time intervals will be discussed later.)

The rarefaction wave completely overtakes the whole shock front at about an equivalent length of a diameter of the shock tube downstream from the open end. The decay of the shock front becomes very evident after that.

SOME RELEVANT FEATURES OF HOT-WIRE RESPONSE

Steady-State Response of a Hot-Wire

If a wire, through which some heating current is passing, is immersed in a flowing fluid, the wire responds to the changes in the heating current or in the cooling (or heating) effects of the flow according to certain response equations.

In order to derive these equations the conservation of energy is assumed, that is, the difference between electric heat input and heat loss due to the forced convection (including radiation and free convection, etc.) equals the increased thermal energy in the wire:

$$W - H = C \frac{dT_w}{dt} \tag{27}$$

where

H heat loss from wire per unit time

W energy input in the wire per unit time

For the steady case

$$W - H = 0 \tag{28}$$

The well-known investigation of heat loss from the cylindrical wire placed in an incompressible ($M \longrightarrow 0$) flow conducted by King (ref. 12) gives for heat loss

$$H = l(T_w - T_e)\left(k_e + \sqrt{2\pi k_e C_p \rho u d}\right)$$

or

$$H = (T_w - T_e)(A + B\sqrt{u}) \tag{29}$$

where

$$A = k_e l$$

$$B = l\sqrt{2\pi k_e C_p \rho d}$$

Using relation (28)

$$I^2 R_w = (T_w - T_e)(A + B\sqrt{u}) \tag{30}$$

This can be further transformed into (refs. 4, 5, and 10)

$$\frac{I^2}{I_o{}^2} = \frac{2a_w}{1 + a_w}\left(1 + \sqrt{\frac{u}{U_o}}\right) \tag{31}$$

This is a steady-state equation which governs the hot-wire heat-loss behavior in a steady stream of flow. The characteristic constants I_o and U_o are functions of temperature and pressure or density of the flow and are experimentally determined by the calibration of the wire (see section "Calibrating Facility"). If the flow conditions of the calibrating jet are different from those of the flow under investigation, then I_o and U_o either will need modification or, in more extreme cases, may exhaust their usefulness and thus may have to be discarded for an alternative approach. The variation of these constants is usually small if the operating conditions are not radically different from the calibrating conditions. The variation of U_o due to the actual flow being of a substantially different density can be taken into account rather simply by expressing relation (31) in the form

$$\frac{I^2}{{I_o}^2} = \frac{2a_w}{1 + a_w}\left(1 + \sqrt{\frac{\frac{\rho}{\rho_f}u}{\left(\frac{\rho}{\rho_f}u\right)_o}}\right) \tag{32}$$

where ρ_f is some reference density and ρ is the density of the actual flow. Supposing $U_o = 10$ feet per second at normal atmospheric density, then, if the density of the flow was, say, one-half the normal atmospheric density, U_o will be 20 feet per second. The function U_o does not depend upon the material of the wire and for constant temperature $U_o d$ = Constant. The characteristic constant I_o is different for different types of wires (fig. 11). Since in shock-tube flows the temperatures vary considerably from the normal room temperature, the dependence of k_e on temperature has to be taken into account. (Variations of C_p with moderately high temperatures may be neglected.) It is sometimes advantageous to put the heat-loss equation (31) into an alternative form valid under widely varying conditions:

$$Nu = a + b\sqrt{P_e} \tag{33}$$

where a and b are constants and the Peclet number $Pe = PrRe$. When centimeter-gram-second units are used then Nusselt's number

$$Nu = \frac{0.2389\ I^2 R_w}{\pi l k_e\left(T_w - T_e\right)}$$

Therefore,

$$\frac{0.2389\ I^2R_w}{\pi l k_e \left(T_w - T_e\right)} = 0.318 + 0.798\sqrt{Pe}$$

If $Pr = 0.72$, which for diatomic gases is a close value over a wide range of temperatures (ref. 13), then

$$\frac{0.2389\ I^2R_w}{\pi l k_e \left(T_w - T_e\right)} = 0.318 + 0.677\sqrt{Re} \tag{34}$$

Besides the forced convection, the heat loss is influenced quite appreciably by free convection, radiation, and conduction through ends.

For hot-wires used in low-density wind tunnels or low-density operation of shock tubes, the heat loss due to free convection is substantial. If the hot-wire is heated to a certain temperature under normal atmospheric conditions, then much less current is needed to heat the same wire to the same temperature under partial vacuum conditions. To calibrate this effect a platinum wire ($d = 0.0001$ inch) and a tungsten wire ($d = 0.00015$ inch) were mounted in a shock tube. They were heated to $a_w = 0.5$ and $a_w = 0.1$ at various pressures within the range 760 to 0.15 millimeter of mercury. The corresponding cold resistance was measured at each pressure and the operating resistance calculated for the different overheating ratios. The currents needed to heat the wires to these overheating ratios were measured. These wires were mounted both vertical and horizontal to the base of the shock tube. Since no appreciable difference was noticed between the performance of these two orientations of the wires, only the data for vertical wires are reproduced here.

Even in still air, there is always heat loss. This may be due to free convection or molecular conduction.

The measure of free convection is the so-called Grashof number (ref. 14)

$$Gr = \frac{g\rho^2 d^3\left(T_w - T_e\right)}{\mu^2 T_e}$$

where g is the acceleration due to gravity and T_e is the gas temperature surrounding the wire.

From relation (33) (for $\sqrt{Re} = 0$) and for constant temperature of the gas

$$\frac{I^2 R_w}{l(T_w - T_e)} \propto a\left[\frac{g\rho^2 d^3 (T_w - T_e)}{\mu^2 T_e}\right] \tag{35}$$

This could be written as

$$\frac{R_l \alpha_l}{l} I^2 \frac{1 + a_w}{a_w} \propto a\left(\frac{g\rho^2 d^3 a_w}{\mu^2 \alpha_e T_e}\right) \tag{36}$$

If the temperature of the gas is constant, then for the same wire

$$I^2 \frac{1 + a_w}{a_w} \propto a\left(a_w \rho^2\right) \tag{37}$$

The examination of the data from the point of view that free convection is entirely influenced by Grashof number failed to correlate the data for $a_w = 0.5$ and $a_w = 0.1$ (see ref. 10). Because of the smallness of the diameter of the wire, the Grashof number even at atmospheric pressure is very small in magnitude (approximately 10^{-6}) and the normal free-convection effect (with usual free-convection velocity, and the associated buoyancy effects) is considerably reduced (ref. 14).

Free convection is also affected by the molecular conductivity through the dimensionless quantity known as the Knudsen number

$$K = \frac{\lambda}{d}$$

where

λ molecular mean free path

d characteristic length (diameter of wire)

Since λ is inversely proportional to the density of the gas, for the same wire, K is greater at lower densities. This shows no influence of overheating ratio but does involve density.

Relation (35) can be written as

$$\frac{\sigma\alpha_e}{d^2} I^2 \frac{a_w + 1}{a_w} \propto a\left(\frac{\lambda}{d}\right) \tag{38}$$

where σ is the specific resistivity of the material of the wire. The data are plotted as shown in figure 12 and the values of d, α_e, σ, and λ have been assumed as indicated.

The decrease in the amount of current needed to heat the wire to the same temperature under partial vacuum is striking.

The heat-loss behavior of both tungsten and platinum wires agrees for large values of K (low densities), that is, where the mean free path is large compared with the characteristic length.

For comparatively higher densities, however, the agreement for platinum wire for the two overheating ratios is poor. This disagreement is not fully understood.

Linearized Unsteady Response to Fluctuations

The approach used is that of reference 10. From the consideration of energy conservation, relation (27) was written. If one assumes that the flow can be split into mean motion and the fluctuations (Δ quantities), and since mean flow satisfies the steady-state relation (28), one gets

$$\Delta W - \Delta H = C \frac{d(\Delta T_w)}{dt} \tag{39}$$

where

$$\Delta H = \frac{\partial H}{\partial T_w} \Delta T_w + \frac{\partial H}{\partial T_e} \Delta T_e + \frac{\partial H}{\partial(\rho u)} \Delta(\rho u)$$

$$\Delta W = \left(\frac{\partial W}{\partial I}\right)\Delta I + \left(\frac{\partial W}{\partial T_w}\right)\Delta T_w$$

Collecting and dividing by the coefficients of ΔT_w, and from the knowledge of the explicit expressions for W and H, one can obtain the expression

$$M^* = \frac{C}{\frac{\partial H}{\partial T_w} - \frac{\partial W}{\partial T_w}}$$

$$= n \frac{a_w}{I^2} \tag{40}$$

where

$$n = \frac{C}{\alpha R_f}$$

$$a_w = \frac{R_w - R_e}{R_e}$$

The thermal-lag constant n is a universal constant of the wire as it is directly related to its physical properties. For a specific material it varies with the fourth power of the diameter of the wire.

The voltage fluctuations across the wire terminals can be due to resistance and/or current fluctuations

$$\Delta e = I \Delta R + R_w \Delta I \tag{41}$$

Using relation (41) along with the assumed heat-loss law (King's incompressible case), relation (39) can be written as

$$-F \Delta(\rho u) + G \Delta T_e = \Delta e + M^{**} \frac{d(\Delta e)}{dt} \tag{42}$$

where F and G, the sensitivity coefficients, and M^{**} are given by

$$\left.\begin{aligned} F &= \frac{\bar{e}aEZ}{2\rho u} \\ G &= \alpha R_f IE \frac{\bar{R}_w}{R_e} \\ M^{**} &= \frac{M^*}{1 + 2a_w\epsilon} \end{aligned}\right\} \qquad (43)$$

and

$$Z = \frac{1}{1 + \sqrt{\frac{(\rho u)_o}{\rho u}}}$$

Here $(\rho u)_o$ is the calibration constant and

$$E = \frac{1 - \epsilon}{1 + 2a_w\epsilon}$$

$$\epsilon = \frac{R_w}{Z_S + R_w} = \frac{\bar{e}}{e_{open}}$$

where

Z_S impedance of current source

$\bar{e}$ mean voltage drop across the wire, $\bar{I}\bar{R}_w$

e_{open} open-circuit voltage of hot-wire supply circuit if hot-wire is removed

If the alternating-current source impedance of the hot-wire terminals is infinite, then $\epsilon \longrightarrow 0$ and $E = 1$ and therefore

$$\left.\begin{aligned} F &= \bar{e}a_w Z/2\overline{\rho u} \\ M^* &= na_w/I^2 \\ G &= \bar{I}R_f \alpha R_w/R_e \end{aligned}\right\} \tag{44}$$

If $\bar{R}_w \longrightarrow \bar{R}_e$, then

$$G = \bar{I}\alpha R_f \tag{45}$$

which is the case when the current passed through the wire placed in the flow does not raise the temperature or resistance of the wire appreciably higher than the equilibrium temperature which the wire assumes without any current through it.

If the conditions vary extremely slowly or the wire has no thermal heat capacity, then the left-hand side of equation (42) is the static response of the wire and one can write

$$\Delta e_v = \Delta e + M^* \frac{d(\Delta e)}{dt} \tag{46}$$

where Δe_v is the virtual voltage fluctuation which the wire, without any thermal lag, would have assumed and M^* is the usual time constant of the wire at particular operating conditions. Equation (46) is equivalent to the differential equation obeyed by a circuit containing an inductance and resistance or resistance and capacitance arranged as an integrating device. Such equivalent circuits can be used as "dummy hot-wires" (ref. 4).

Response to a Finite Step Function

The principal application of hot-wires is to turbulence measurements where the fluctuations usually are small compared with the mean motion and the unsteady hot-wire response equation is linearized resulting in a time constant M^* which is a function of the average operating conditions (relation (44)). If a traveling shock or any other transient wave passes over a hot-wire placed in the shock tube, both the mass flow and the ambient temperature change as a step function in time. This fact

enables one to solve the exact equation without resorting to the perturbation method and results in a simple rule that the time constant may be determined by the operating conditions that would be assumed in a steady state after the jump.

For this type of derivation the following assumptions are made:

(1) The current I remains constant (reasonably well justified by the hot-wire equipment used).

(2) Thermal condition of the wire can be characterized by a single temperature T_w (thermal wave propagation along the wire is negligible). This means that the distribution shape of the temperature along the wire does not change (except for a constant) under different operating conditions.

(3) The shock fronts, contact surface, and reflected shock front are all plane.

(4) King's heat-loss law applies for the incompressible range (low Mach numbers) and Kovasznay's empirical heat-loss relation applies for the supersonic range considered. (The limitations of this assumption will be dealt with later.)

(5) The temperature which the wire will assume if it was not heated at all will be called the equilibrium temperature and it is approximately equal to stagnation temperature. It is assumed that the hot-wire responds to stagnation temperature.

Primary shock wave.- The heat generated at any time is

$$W = I^2R_f\left[1 + \alpha\left(T_w - T_f\right)\right] \tag{47}$$

The heat loss after the primary shock has passed is

$$H = \left(T_w - T_{o2}\right)\left(A + B\sqrt{\rho_2 u_2}\right) \tag{48}$$

The hot-wire transient response equation (27) becomes

$$I^2R_f\left[1 + \alpha\left(T_w - T_f\right)\right] - \left(T_w - T_{o2}\right)\left(A + B\sqrt{\rho_2 u_2}\right) = C\frac{dT_w}{dt} \tag{49}$$

After equilibrium between wire and flow has been established, $\frac{dT_w}{dt} \longrightarrow 0$ and $T_w \longrightarrow T_{v2}$

$$I^2R_f\left[1 + \alpha\left(T_{v2} - T_f\right)\right] - \left(T_{v2} - T_{o2}\right)\left(A + B\sqrt{\rho_2 u_2}\right) = 0 \tag{50}$$

Subtracting equation (50) from (49) and eliminating $A + B\sqrt{\rho_2 u_2}$, one gets

$$T_{v2} = T_w + M_2^* \frac{dT_w}{dt} \tag{51}$$

where

$$M_2^* = \frac{C}{I^2R_f} \frac{T_{v2} - T_{o2}}{1 + \alpha\left(T_{o2} - T_f\right)}$$

$$= \frac{n}{I^2} a_{v2} \tag{52}$$

with

$$a_{v2} = \frac{R_{v2} - R_{o2}}{R_{o2}}$$

In this special case when the mass flow $\rho_2 u_2$ and temperature T_{o2} are constant in time, except for discontinuous jumps from the ambient condition, M_2^* still remains constant except that its value must be computed with the steady-state operating conditions which the wire assumes "long" after the transient occurs. This means that wire response will still be an exponential function of time and that ordinary electronic thermal-lag compensation should give proper compensation if the time constant is set according to $M_2^* = n \frac{a_{v2}}{I^2}$. This has been checked to be so as described in reference 8 and rechecked again (see "Analysis of Experimental Data"). A typical compensated and uncompensated oscillogram is reproduced in figure 1. If the fluctuations in the flow behind

this main jump are being studied, this relation for compensations is applicable only if the fluctuations are small as compared with the mean flow.

Contact surface.- After the shock has passed, the wire adjusts to the conditions behind the shock and when the contact discontinuity reaches the hot-wire it experiences another step-function change in flow conditions. The temperature of the wire before the contact surface reaches it is T_{v2}, and after equilibrium with the contact surface is established the wire temperature becomes T_{vc}. Following a procedure similar to the one used for the derivation of equation (51), one gets

$$T_{vc} = T_{v2} + M_c^* \frac{dT_{v2}}{dt} \tag{53}$$

where

$$M_c^* = \frac{n}{I^2} a_{vc} \tag{54}$$

with

$$a_{vc} = \frac{R_{vc} - R_{oc}}{R_{oc}}$$

Comparing relations (52) and (54),

$$\frac{M_2^*}{M_c^*} = \frac{a_{v2}}{a_{vc}} \tag{55}$$

where a_{v2} and a_{vc} are the new equilibrium overheating ratios which the wire acquires in the flow behind shock and contact surface, respectively. From the calculations (details to follow in the next section), $a_{v2} > a_{vc}$ by approximately 20 to 30 percent for the same shock strength S. This means that lesser compensations will be needed for the contact-surface region.

So far the discussion has centered around the jumps due to the main wave fronts (shock waves, contact surface, and rarefaction wave). If there are fluctuations present (natural or artificially introduced) in the flows behind the main fronts, the linearized theory will hold again, with the difference that the new equilibrium operating conditions a_{v2} and a_{vc} are different from the original a_w. This affects the sensitivity coefficients of the hot-wire response (relations (44) and (45)).

COMPUTATION OF EXPECTED VOLTAGE SIGNALS FROM HOT-WIRE OPERATED IN SHOCK TUBES

The contents of this section are in general helpful for the operation of the hot-wire anemometer and the design of the associated equipment for use in the shock-tube work. It gives the order of magnitude of voltage signals expected from the various regions of the flow under some standard operating conditions. Until otherwise stated, the following assumptions have been made:

(1) For the subsonic range of flow, King's heat-loss relation is considered valid. This means that Mach number effects on the heat-loss behavior of the hot-wire used in subsonic flows are overlooked.

(2) The wire responds to stagnation temperatures.

(3) The hot-wire is heated from a current source of infinite impedance.

Region Behind Primary Shock

The flow behind a shock wave has temperature and density higher than that of the region ahead of it. Since the calibration constants of the hot-wire U_o or $(\rho u)_o$ and I_o are functions of temperature, for high-strength shocks they have to be modified. The alternative, of course, is to resort to the actual physical dimensions and so forth of the wire; while for this case one does not need to calibrate the wire, one has to rely on the measured length and diameter of the wire which are rather poorly defined and vary from sample to sample. So to calculate the jump signals due to response of the hot-wire to a traveling shock wave, one is offered a relative choice at best. Calculations carried out by both methods did not show any pronounced difference. Since the aim of these calculations is only the estimate of the order of magnitude of the signals involved, the choice is not critical. The approach elaborated here

is the one using the physical dimensions of the wire. In conventional shock-tube work there is no flow to start with, that is, $\sqrt{\rho u} = 0$. Therefore, from relation (34), the heat loss for no flow is given in centimeter-gram-second units by

$$Nu_1 = \frac{0.2389\ I^2 R_w}{\pi l k_e \left(T_w - T_e\right)} = 0.318 \tag{56}$$

Since because of the passage of the shock wave $\sqrt{Re}$ jumps to $\sqrt{Re_2}$, one gets

$$Nu_2 = \frac{0.2389\ I^2 R_w}{\pi l k_{o2} \left(T_{v2} - T_{o2}\right)} = 0.318 + 0.677\sqrt{Re_2} \tag{57}$$

where

$$Re_2 = \rho_2 u_2 d/\mu_{o2}$$

For constant-current operation

$$\frac{Nu_2}{Nu_1} = \frac{R_{v2}}{R_w} \frac{k_1}{k_{o2}} \frac{T_w - T_1}{T_{v2} - T_{o2}}$$

and

$$\beta_2 = \frac{R_{v2}}{R_w} \frac{R_w - R_1}{R_{v2} - R_{o2}}$$

where

$$\beta_2 = \frac{Nu_2}{Nu_1} \frac{k_{o2}}{k_1} \tag{58}$$

therefore

$$R_{v2} = \frac{R_{o2}}{1 - \frac{1}{\beta_2} \frac{a_w}{a_w + 1}} \tag{59}$$

From relation (56),

$$I^2 = \frac{0.318\pi k_1 l a_w}{0.2389 R_w \alpha_1} \tag{60}$$

If the respective values of l and R_1 are selected, then for various operating overheating ratios, the corresponding currents can be calculated. The values assumed for the tungsten wire of $d = 0.00015$ inch are $R_1 = 10$ ohms, $l = 0.2$ centimeter, and $k_1 = 5.71 \times 10^{-5}$ cal cm^{-1} sec^{-1} $^oC^{-1}$. If the shock strength S is known, then $\sqrt{Re_2}$ and Nu_2 can be calculated and, since T_{o2} is known from relation (5), corresponding air conductivities k_{o2} are obtained from reference 15 and β_2 can be calculated from relation (58). Since T_{o2} is known, R_{o2} can be found. As a_w is known at the start, R_{v2} can be calculated from relation (59). Also a_{v2} can be calculated. The voltage jump for constant-current operation is

$$\Delta e = I\left(R_w - R_{v2}\right) \tag{61}$$

where Δe is positive if $R_w < R_{v2}$ and negative if $R_w > R_{v2}$.

The shock tube can be operated in many different ways. For instance, one can keep the expansion chamber at normal atmospheric pressure and pressurize the compression chamber or one may partially evacuate the expansion chamber and keep the compression chamber at normal atmospheric conditions (or higher). The method of operation has a striking effect on the $\sqrt{Re}$ of the flows (figs. 6 and 7).

The calculations of Δe's as a function of shock strengths with a_w as a parameter presented here assume that the shock tube is operated with the expansion chamber at normal atmospheric conditions. Notice that there are combinations of a_w and S where no signal is available (fig. 13). The shock wave represents a mass-flow as well as a temperature jump and the hot-wire is sensitive to both these changes. While the temperature jump tends to increase the resistance, the mass flow reduces it. These signals are of opposite polarity. Thus in between there must be a "neutral" point where these two signals cancel out, giving no response at all. The point is well borne out by the oscillogram produced in figure 14. Corresponding to the intermediate current there is hardly any jump, while the largest and the smallest currents have jumps of the opposite polarity. Needless to say, while the hot-wire is used for timing

purposes, one should avoid working in the neighborhood of this region. It is advantageous, as a matter of fact, to stay as far away from it as possible. However, when the wire is used for actual flow studies this presents very little difficulty. On the contrary, at times it may be advantageous to operate closer to this point in order to avoid large voltage signals. Notice the extremely large signals obtainable by operating the hot-wire with a considerable current through it at extremely weak shock waves. In the author's opinion this is the region where the hot-wire is uniquely well suited for timing shock-wave speeds, and so forth.

During the course of the work described in this report by chance a tungsten wire was found with a resistance of exactly 10 ohms. The wire was calibrated and actually used for measuring jump voltages for low-strength shocks at overheating ratios of 0.5 and 0.3. The expansion chamber was at atmospheric pressure. The amount of signals obtained (fig. 13(a)) verifies the order-of-magnitude calculations for the jump signals.

Tungsten wires oxidize at much lower temperatures than platinum wires. Based on personal experience, the author would advise against the use of tungsten wires beyond an overheating ratio $a_w = 0.7$. For very weak shocks platinum wires are more desirable since one can heat them to higher overheating ratios without their oxidizing.

Contact-Surface Flow

The contact-surfact flow follows the flow behind the primary shock front, thus introducing another sudden change in temperature, mass flow, and Mach number. The hot-wire comes into equilibrium with this flow. But in this case the initial conditions are the equilibrium conditions due to the flow behind the primary shock wave. The Reynolds numbers of the hot-wire jump from $\sqrt{Re_2}$ to $\sqrt{Re_c}$. As the Mach number effects ($M_c < 1$) will again be neglected, the corresponding Nu_c is calculated from King's heat-loss equation. By a similar procedure to that followed for the flow behind the shock wave,

$$R_{vc} = \frac{R_{oc}}{1 - \frac{1}{\beta_c} \frac{a_{v2}}{1 + a_{v2}}} \tag{62}$$

where

$$\beta_c = \frac{Nu_c}{Nu_2} \frac{k_{oc}}{k_{o2}}$$

Knowing R_1 and T_{oc} one can find R_{oc} and thus R_{vc} can be determined from relation (62), and the voltage jump is given by

$$\Delta e = I\left(R_{v2} - R_{vc}\right) \tag{63}$$

Since $R_{v2} > R_{vc}$ these signals are negative and increase with the increasing overheating ratio initially used (fig. 13(b)). The values of $\sqrt{Re_c}$ used here are the ones calculated with the expansion chamber at normal atmospheric conditions (ref. 9).

If one wants to use the contact surface as the principal front to start the triggering circuit, one should operate it such that the shock-wave signal is positive in polarity and the associated electronic equipment should be so arranged that it overlooks the signal due to the shock wave and does not trip the thyratron tube until the negative signal from the contact surface activates the system (ref. 9).

Pure Temperature Response

From the consideration of the sensitivity of the hot-wire (relations (44) and (45)) one observes that, if the operating resistance of the hot-wire is very close to the equilibrium resistance of the wire without any current through it, the temperature sensitivity dominates and the hot-wire acts like a resistance thermometer. If the operating temperature of the wire is not much different from the gas surrounding it (i.e., "small" current) and if the current is assumed constant, then the voltage change is given by

$$\begin{aligned} \Delta e &= \pm I\,\Delta R \\ &= \pm I R_1 \alpha_1\,\Delta T \end{aligned} \tag{64}$$

where ΔT is the change in temperature of the gas passing over the hot-wire. If the resistance of the wire is, say, 10 ohms, the current through it is 4 milliamperes, and $\alpha = 0.0035$ then the voltage jump per degree jump in temperature is $\Delta e = 0.14$ mv/°C. The temperature jumps across the shock wave, contact surface, and reflected shock are of such magnitudes (fig. 5) that one can obtain fairly large voltage signals from the timing hot-wire even for moderately strong shock waves.

However, the temperature jumps across the strong waves are so large that, even if one operates the wire at relatively high temperatures, the

temperature response dominates and the signal is positive. The oscillographic record of the hot-wire response reproduced in figure 15 demonstrates this clearly. The initial jump (A) is due to the shock wave and after a millisecond or so the contact surface arrives at the hot-wire and cools it. The turbulent nature of the contact-surface flow (B) is evident.

The break in the first jump is due to the firing of the spark (D), the output of which was purposely applied to the oscilloscope.

HOT-WIRE RESPONSE TO TRANSIENT SUPERSONIC FLOW

REGIONS IN SHOCK TUBE

In shock-tube investigations, the transient supersonic flows are very easily produced. There are two regions of such flows which are of main interest:

(1) Flow behind the primary shock wave (region 2).

(2) Flow in the contact surface (region c).

While the pressure and particle velocity are the same in both the regions, the temperature and density are quite different. Therefore, for the same shock strength the Reynolds numbers and Mach numbers in these regions differ quite substantially.

Hot-wire techniques have been recently extended to supersonic flows. Kovasznay's empirical law of heat loss obeyed by the hot-wire placed in a supersonic stream is given by

$$H = \pi l k_e \left(T_w - T_e\right)\left(A\sqrt{\frac{\rho u d}{\mu_o}} - B\right)\left(1 - C\,\frac{T_w - T_e}{T_o}\right) \tag{65}$$

where A, B, and C are nondimensional constants. For low-temperature loading

$$\frac{T_w - T_e}{T_o} \longrightarrow 0$$

$$Nu = \frac{H}{\pi l k_e\left(T_w - T_e\right)} = \left(A\sqrt{\frac{\rho u d}{\mu_o}} - B\right)$$

The heat loss is still dependent on the Reynolds number. The negative intercept in the plot of Nu versus $\sqrt{Re}$ (ref. 16) is different from the low-speed heat-loss law (King's case). Experimental studies of heat transfer from bodies in a high-speed rarefied gas stream (i.e., Reynolds number lower than the range at which Kovasznay worked) show that this negative intercept in reality does not occur. Starting near the origin Nu versus $\sqrt{Re}$ is parabolic in this lower range of Re and joins with Kovasznay's empirical curve (i.e., if fig. 7 in ref. 17 is replotted as Nu versus $\sqrt{Re}$).

For the study of heat transfer from bodies in high-speed and low-density flows, in addition to Reynolds number and Mach number, the Knudsen number $K = \lambda/d$ becomes important, where λ is the molecular mean free path and d is the characteristic length (diameter of the wire in the present case).

The parameter K can be related to M and Re as (refs. 17 and 18)

$$K = 1.5 \frac{M}{Re}$$

One usually uses the Knudsen number as a criterion for deciding in which type of flow one is operating (i.e., continuum, slip, or free molecular). When the Knudsen number is small ($K < 0.01$) the effect of the molecular motion on the flow is negligible and the gas may be treated as a continuum. For large values of Knudsen number ($K \geq 10$) the molecular motion is all important and the phenomena can be completely described in terms of free molecules. The realm of flow with Knudsen number $0.01 < K < 10$ is usually classified as the slip-flow region. In such a flow the gas no longer sticks to the surface but slips over the surface with definite velocity.

The shock tube can be operated in a number of ways. The method of operation has rather a striking effect on the Reynolds number obtained. This in turn has an effect on the Knudsen number and the heat loss from the wire. Calculations of Reynolds numbers and Knudsen numbers were carried through for the flow behind the shock wave and contact surface for the following cases:

(1) The expansion chamber at atmospheric conditions and the compression chamber at higher pressures (figs. 6 and 16).

(2) The expansion chamber partially evacuated and the compression chamber at atmospheric pressure (figs. 7 and 17).

A few salient features are stated here.

(a) The Reynolds number in the contact surface $Re_c = \frac{\rho_c u_c d}{\mu_{oc}}$ is higher than the corresponding one in the region behind the shock $Re_2 = \frac{\rho_2 u_2 d}{\mu_{o2}}$. This is due to the higher density and lower temperature (i.e., lower viscosity coefficient μ_o, ref. 19) in the contact-surface flow.

(b) When the shock tube is operated with the expansion chamber open to the atmosphere, the Reynolds numbers are higher than the corresponding ones for the expansion chamber operated at low pressures.

(c) Based on the criterion discussed above, the numerical values of the Knudsen number show that it is only when the shock tube is operated with the expansion chamber at normal atmospheric pressure that the flow over the hot-wire can be treated as a continuum. When the expansion chamber is operated at low densities, K is small and one operates the hot-wire in or very close to the slip-flow conditions for a large range of shock strength.

Because of the small characteristic length (diameter of the wire $d = 0.00015$ inch), even at normal temperature and pressure, $K = 0.02$ with $\lambda = 8.5 \times 10^{-6}$ centimeter.

Most of the turbulence investigations conducted with the hot-wire technique in the main stream of a supersonic wind tunnel have $K \approx 0.02 \rightarrow 0.04$. This is also the range in which Kovasznay worked to establish the empirical heat-loss law (relation (65)) which breaks down for $K \approx 0.1$. According to the cirteria agreed upon, this lies in the slip-flow region.

Thus while operating the hot-wire in shock tubes one should decide the heat-loss relation to be used (and therefore the estimated signals, etc.) according to the operating range of Reynolds number, Mach number, and Knudsen number.

EXPERIMENTAL EQUIPMENT AND TECHNIQUE

The experimental arrangement consists of the following functional units:

(1) Shock tube

(2) Hot-wire equipment

(3) Triggering and timing

(4) Mounting of hot-wires

(5) Recording

(6) Calibrating facility

Relevant features of each unit are summarized in the subsections which follow.

Shock Tube

The shock tube consists of a steel box of uniform cross section (approximately 6 by 4 inches inside) with the 6-inch side laid horizontal (fig. 18) to allow the largest path of the beam of light through the flow under investigation. The total length of the shock tube is 29 feet. The compression chamber is 6 feet long and the expansion chamber consists of seven sections (fig. 19).

The construction of the shock tube is weld free and, as this was intended to be a functional rather than a precision shock tube, the minimum amount of machining was employed. Most of the shock tube is constructed of ordinary cold-rolled steel plates. The plates are bolted together with 1/16-inch rubber gasket as sealing material. Dowel pins are used to keep the box square and alined (fig. 18).

The construction of the glass section is somewhat different. This is the only completely machined part in the whole shock tube. The glass window extends from the top to the bottom plate and one can have any section of the glass free from bolts with a maximum clear view of 4 by 11 inches.

The compression chamber is capable of withstanding considerable internal pressures. It has been used at 125 pounds per square inch.

The high pressure is measured with a 12-inch-diameter pressure gage graduated from 0 to 250 pounds per square inch.

When the expansion chamber is used under vacuum the pressure is measured by a mercury manometer, absolute pressure gages (0 to 20 millimeters; 0 to 100 millimeters, Wallace and Tiernan), and a McLeod gage (0.01 to 50 millimeters). Among them the full range of low-pressure measurement, which one may feasibly require in shock-tube work, is covered. The overlapping of their ranges is used to check one against the other.

The shock tube is provided with a spring-loaded, solenoid-activated mechanism with a thin pointed needle to puncture the diaphragm.

General performance of this simply constructed shock tube is very satisfactory whether it is used at high pressures or with expansion under partial vacuum. The expansion chamber has been used at pressures lower than 1/10 millimeter of mercury. (For details see ref. 10.)

Hot-Wire Equipment

The hot-wire equipment used in this investigation is that designed by Kovasznay. (For any detailed information see ref. 20.) The equipment consists of functional units such as control unit, calibration unit, and compensating amplifier, assembled together.

The control unit controls the heating current through the wire and makes it possible to measure the resistance of the wire.

The calibrating unit contains a direct-current potentiometer which makes it possible to measure the current through the wire.

The compensating amplifier is the most critical part of the hot-wire equipment. The amplifier in this equipment is a five-stage push-pull type with total gain, without compensation, of approximately 10,000. The compensation adds another factor of 250 making the total amplification at high frequencies a maximum of 2.5×10^6. The compensation is resistance-capacitance type. For limiting the noise there is a five-step low-pass filter.

Main units in the hot-wire equipment and the allied instruments are shown in the block diagram (fig. 20).

Triggering and Timing

From the discussion of the hot-wire behavior and of the expected voltage signals and their polarities under various operating conditions in different flow regions in the shock tube, one is easily convinced that the hot-wire anemometer is admirably suited for timing transient wave phenomena. Depending upon its operating conditions, the hot-wire is sensitive to temperature and/or mass-flow fluctuations. The shock front involves a sudden jump in both temperature and mass flow. If the response of the hot-wire to a traveling shock front is differentiated, it gives a fairly sharp pulse which can be used to synchronize the transient wave phenomena in the shock tube with the passage of the shock wave over the hot-wire. (See fig. 21.) If the hot-wire is operated such that it is predominantly mass flow sensitive, then the auxiliary arrangement shown in figure 22 is used in conjunction with the temperature unit. This arrangement makes it possible to measure the speed of very weak

shocks (S = 1.01) and also strong shocks (S = 20). (For more details about the circuit, the scope, and advantages of this timing device see refs. 9 and 10.)

Mounting of Hot-Wires

The hot-wire anemometer has been used for two distinctly different purposes, namely, for actual flow studies and as a transducer for timing the wave phenomena generated in the shock tube. Thus two different types of probes were called for.

The most successful timing hot-wire probe is shown in figure 23. The construction and mounting details are evident from the drawing (or see ref. 9). Both tungsten (d = 0.00015 inch) and platinum (d = 0.0001 inch) wires have been successfully used.

The probes used for actual flow studies are constructed as shown in figure 24. The mounting of these probes differs according to the configuration of the shock tube used. If the shock tube is used with the extreme end open, then the mounting arrangement shown in figure 25 is used; but, if the expansion chamber is used under partial vacuum or with the extreme end closed, then the probe arrangement shown in figure 26 is employed. Both platinum (d = 0.0001 inch) and tungsten (d = 0.00015 inch) wires have been used.

Recording

Essentially there are three different types of recording operations performed in this work. They are:

(1) Shock-speed measurements

(2) Shadowgraph records

(3) Oscillographic records

If desired, they can all be used simultaneously, but for convenience of operation most of the time only two were recorded simultaneously. Combinations recorded simultaneously were

(a) The time the shock wave takes between two fixed stations and the shadowgraph

(b) The time the shock wave takes between two fixed stations and the oscillograms

The arrangement and the procedure followed in each of these major categories will be summarized below.

Method of measuring shock speeds.- Two timing hot-wires are mounted at two stations some known distance apart. The output of the timing wire nearer to the diaphragm is fed to the triggering unit connected to the "start" of the chronograph. The output of the second station (which is downstream from the first station) is fed to the triggering unit connected to the "stop" of the chronograph (fig. 27). This chronograph records in intervals of 1 microsecond. The time taken by the shock wave to traverse the distance between these two stations is recorded by the chronograph. Thus the speed of the corresponding shock is calculated. There are six available holes for mounting the timing hot-wires. The distance between the first hot-wire (located some 13 feet down from the diaphragm) and the second one could be anywhere between 19.7 and 70 inches depending upon the configuration of the shock tube being used.

To insure that the response of the two wires was as alike as possible, the wires were matched for their resistance and for the currents needed to heat both to the same temperature. As the timing hot-wire system has no bridge for measuring resitances, the main hot-wire set was used for matching wires.

Shadowgraphs.- The arrangement used to take shadowgraphs of the traveling shock waves and the allied flow fields is reproduced in figure 19. The short-duration (1 microsecond) high-intensity point source of light is obtained by a sudden high-voltage (about 5,000 volts) discharge of a coaxially arranged set of six condensers, with a total capacity of 0.12 microfarad, across a narrow gap between two semispherical electrodes (ref. 21). To trip the spark a sudden large current is passed through the spark coil connected to the central needle electrode. This generates a tiny spark which ionizes the gap and the intense discharge between electrodes follows. To take a shadowgraph of a traveling shock at a predetermined instant and location, one synchronizes the tripping of the spark with the help of a pickup device (timing hot-wire in this case) and a delay generator (fig. 19). The delay can be preset in intervals of 10 microseconds. In the earlier setup, however, the required delay was generated by a simple resistance-capacitance circuit which worked very well for low delay times (up to about 500 microseconds) but developed progressively higher scatter for larger delays.

The light source is used either with a collimating lens or without one as the need dictates. The collimation of the light is achieved by an $f = 4.5$ and 500-millimeter focal-length lens with the point source of light at the focal point of the lens. This gives a parallel beam of light approximately 4.5 inches in diameter, thus covering the full height of the glass section.

Oscillographic records.- For taking oscillograms the main hot-wire equipment was used. Most of the oscillograms are single-sweep records of the hot-wire response over a period of a few milliseconds. The problem essentially is to bring the response of the hot-wire conveniently on the face of the oscilloscope. For that one has to start the horizontal sweep at a time somewhat ahead of the arrival of the wave front at the hot-wire station. This necessitates the knowledge of the approximate delay to be applied to the output of the triggering hot-wire. After this first problem of positioning the time axis, one has to calibrate the vertical scale such that the response signal from the hot-wire neither jumps off the screen nor is so squeezed that no quantitative measurement can be effected with any degree of accuracy. For deciding both of these questions the knowledge of the shock speed and the expected voltage signal (fig. 13) helps. It will take an extremely long time to record a set of oscillograms if one has to calculate the jump in each case. After a while experience becomes a good guide.

The block diagram (fig. 20) demonstrates the arrangement used to take oscillograms. For sweeping the signal across the oscilloscope once and only once, the output from the triggering unit is fed to the oscilloscope through a single-shot thyratron-tube circuit. If the ordinary oscilloscope (Dumont Type 304 H R) is used, it is advantageous to intensify the beam temporarily by applying a flat-top pulse to the Z input (ref. 8). If the high-intensity high-voltage cathode-ray oscilloscope (Tektronix Type 513 D) is used, this is not necessary. Both types have been used during the course of this work. A polaroid camera was used most of the time. If very fast sweep records were required (sweep time of approximately 100 microseconds), the high-intensity oscilloscope with an $f = 1.5$ lens and Tri X film was used.

The operational procedure for taking oscillograms is as follows: The amplitude and frequency of the calibrating sine wave are adjusted according to the dictates of the shock strength and operating condition of the hot-wire. A short preexposure is given. It improves the quality of the polaroid pictures and also gives a reference grid in the background. Then the calibrating sine wave is driven across by the manual triggering while the camera shutter is kept open on B. After that the shutter is closed. Then the spot is moved toward the upper or lower part of the screen. This is decided purely on the basis of the polarity of the expected jump. If the expected jump is downward, the spot is moved to the upper half of the screen. The pressure across the diaphragm is adjusted to the desired value. The triggering unit, intensifying unit, chronograph, and so forth are all reset to receive the pulse. The shutter is opened and the puncturing mechanism is actuated by the person operating the camera. In this way he can coordinate the opening of the shutter and the firing of the shock tube. After the trace flashes across the screen, the shutter is closed. The corresponding time of traverse of the shock wave between two detecting stations is recorded by the chronograph.

Calibrating Facility

Only the hot-wires used for actual flow studies need to be calibrated. The wire is placed in the stream of air issuing out of a 1/2-inch-diameter open jet which is supplied by a vacuum-cleaner motor. The velocity of the jet can be varied by controlling the voltage supplied to the motor and is measured by a total-head tube mounted in about the middle of the jet, almost a diameter from the opening. The hot-wire is also mounted parallel to, and very close to, the total-head tube. The total head is connected to an inclined alcohol manometer. At each voltage adjustment (velocity) the height of the alcohol column is recorded. Also the hot-wire bridge is balanced for the same temperature by readjusting the current. The total pressure is given by

$$\Delta p = \frac{1}{2}\rho u^2$$

or

$$u = 58.3\sqrt{\Delta h} \text{ fps} \tag{66}$$

where Δh is the vertical height in inches of the ethyl-alcohol column. The constants of the wire U_o and I_o are found by plotting (ref. 8)

$$I^2 \frac{1 + a_w}{2a_w} \text{ versus } \sqrt{u}$$

Typical calibration curves for platinum Wollaston (d = 0.0001 inch) and tungsten (d = 0.00015 inch) wires are reproduced in figure 11.

Another function of the calibration is to find n, the universal constant of the wire. This is done by the square-wave technique. The square-wave current is passed through the wire which distorts it. This is restored to a square wave by applying the needed compensation. Knowing a_w, M^*, and I^2 at some setting of the velocity, one can calculate n from the relation

$$M^* = n \frac{a_w}{I^2}$$

ANALYSIS OF EXPERIMENTAL DATA

So far, experimental data have been taken to examine the following aspects of the use of the hot-wire anemometer in shock-tube studies:

(1) The response of a hot-wire to a sudden step-function type of change in flow conditions and the criterion for the proper compensation.

(2) Ultimate time resolution of the hot-wire and the allied equipment.

(3) Measurement of the absolute temperature jump across a shock wave passing over the hot-wire.

(4) Separation of the simultaneous jump in mass and temperature associated with a shock front.

(5) Measurement of the shock speeds.

(6) Measurement of the time of arrival at various locations inside the shock tube of the rarefaction front originated at the open end.

Response to a Sudden Step-Function Change and Criterion for Predicting Proper Compensation

The compensation involves usually a suitably arranged circuit which has differentiating properties and has increasing amplification for increasing frequencies, thus counteracting the integrating effects of the hot-wire response. Various arrangements have been used to achieve this end (ref. 20).

In turbulent-flow investigations, the proper compensation is known from the calibration of the wire under known average conditions. However, when the hot-wire is operated in a shock tube, there is no such apparent recourse for foretelling the proper compensation.

If a traveling shock wave passes over a hot-wire mounted in the shock tube, both mass flow and temperature change as a step function in time. In the previous discussion of the hot-wire response to a step function it has been established that the time constant may be determined by the operating conditions that would be assumed in a steady state after the jump. If the wire is operated at elevated temperature, after the jump its temperature falls; that is, its overheating ratio drops. This effect

is enhanced by the fact that the temperature of the flow behind the shock is higher than normal atmospheric temperature. So both of these changes reduce

$$a_{v2} = \frac{R_{v2} - R_{o2}}{R_{o2}}$$

to values considerably smaller than the overheating ratio (i.e., a_w) that was started with. The stronger the shock, the more marked is this difference. So the compensations required are (eq. (52))

$$M_2^* = n \frac{a_{v2}}{I^2}$$

In spite of the voltage signal jump the current I is supposed to remain constant. Because of the finite impedance of the direct-current heating circuit, however,

$$M_2^* = n \frac{a_{v2}}{I^2\left(1 + 2a_{v2}\epsilon\right)}$$

(see section "Linearized Unsteady Response to Fluctuations"). For low equilibrium overheating ratios a_{v2} or small values of ϵ, this feedback correction is negligible.

All of the quantities on the right-hand side are experimentally (from calibration, oscillogram, etc.) determinable. So M_2^* can be computed purely from experimental data. By taking compensated oscillographic records of the hot-wire response, one can, by trial and error, find the proper compensations.

After the shock has passed and steady conditions have been established, one can obtain, for the flow behind the shock wave,

$$\frac{I^2}{I_{o2}{}^2} = \frac{2a_{v2}}{1 + a_{v2}}\left(1 + \sqrt{\frac{u_2}{(u_2)_o}}\right) \tag{67}$$

by a similar procedure to that followed in the derivation of relation (31) (refs. 4 and 10).

Here the wire constants I_{o2} and $(u_2)_o$ are modified from the ones obtained at normal atmospheric conditions:

$$\left.\begin{aligned} I_{o2}^2 &= I_o^2 \frac{k_{e2}}{k_e} \\ (u_2)_o &= \frac{\rho_1}{\rho_2} \frac{k_{e2}}{k_e} U_o \end{aligned}\right\} \tag{68}$$

If the heating current I, the calibration constants n, I_o, and U_o, and the shock strength (i.e., the mass flow and temperature of the flow) are known, then from relation (70) the equilibrium overheating ratio a_{v2} can be calculated and the theoretical value of the required compensation can be obtained, as

$$M_2^* = n \frac{a_{v2}}{I^2}$$

These three different ways of getting the compensation (viz, computed, observed, and theoretical) have been compared with each other. Two distinctly different approaches to data collecting were followed for this purpose:

(a) Overheating ratios a_w (for the same wire) were kept constant and the shock strength S was varied.

(b) The shock strength S was kept the same and the initial overheating a_w was varied.

For case (a) the results are reproduced in figure 28. The initial overheating was $a_w = 0.5$. The current and n remain the same. For each shock strength, the equilibrium overheating a_{v2} is different. The higher the shock strength, the lower is this value. Therefore for stronger shock strengths the compensation decreases. The computed, observed, and theoretical values of the compensation agree within 10 to 15 percent. For high-strength shocks and constant-current operation the required compensations are very small.

The conclusions for case (b) were essentially the same as reached previously (ref. 8). Since the shock strength is kept constant and the initial overheating is varied, the current through the wire is different

for each overheating ratio. After equilibrium conditions are established, a_{v2} is higher for higher overheating ratios, but the corresponding current is higher too. The over-all effect of these two changes on

$$M_2^* = n \frac{a_{v2}}{I^2}$$

is that the required compensation somewhat increases if one goes from an overheating ratio of, for example, $a_w = 0.2$ to $a_w = 0.9$, keeping the shock strength the same for all the oscillograms.

The unheated (or heated by very low current) wire has a time constant which is dependent on the mass flow (refs. 4 and 8). The relationship between compensation needed, for the same shock strength and the same wire, operated once at an elevated temperature and then with very small current through it, is

$$M_{ou}^* = \frac{M_2^*}{1 + a_{v2}} \tag{69}$$

where M_{ou}^* is the time constant when the wire is operated without any current at velocity u (or mass flow ρu).

For weak shock strengths the temperature jumps are very small. Therefore the voltage signal was low. Because of the noise level of the hot-wire equipment it was not possible to judge the right compensation from the compensated oscillograms. So the experimental points shown for M_{ou}^*, the cold compensation, are for $S \geq 1.25$ (fig. 28).

However, for weak shock strengths it is possible to find the right compensation by graphic means from the uncompensated exponential oscillograms of the hot-wire response.

Notice that these observed values of compensations for cold operation are somewhat lower than the corresponding values of M_2^*. The higher the shock strength, the greater is the mass flow. This reduces the required compensations.

In conclusion, the hot-wire response to a step-function type of transient in flow conditions is exponential in time and can be compensated back to almost a step function if the compensation is set according to

$$M_2^* = n \frac{a_{v2}}{I^2}$$

where the equilibrium overheating ratio a_{v2} is determined by the assumed validity of the King's heat-loss law (relation (29)) which is linear with temperature difference but nonlinear with mass flow.

Behind the main traveling shock wave the mass and temperature of the flow are constant. The agreement between the expected and experimentally observed values of compensation shows that the hot-wire is essentially a linear instrument in its temperature response. However, this does not mean that the hot-wire is a linear instrument for large fluctuations in general. These predicted compensations will apply for fluctuations in the flow behind the shock wave only if these fluctuations are small compared with the mean flow.

It may be pointed out that if the temperature difference as it occurs in King's relation is large then even the temperature response may not be linear (ref. 16).

Ultimate Time Resolution of Hot-Wire and Associated Electronic Equipment

The electronic thermal-lag compensation of a hot-wire involves additional amplification proportional to frequency (at higher frequencies). For perfect compensation this would require infinite amplification for infinite frequency. The total amplification in any amplifier must be finite; therefore, the frequency limit of the thermal-lag compensation is also finite. The finite frequency appears in the time domain as a finite rise time for the step function. Depending on particular applications, the sharp rise (high-frequency response) or a noise-free operation may be more desirable. The increase in random-noise power is proportional to the area under the frequency-response curve. To limit the noise low-pass filters are used which limit the frequency response. (For more details see ref. 20.) The filter used in the present studies had a limit of about 70 kilocycles. Since the upper bound of the passable frequency band is rather high, to resolve the rise time, one has to take oscillographic records with very small sweep times. This puts severe demands on the photography of these fast single-sweep traces. As mentioned before, this problem was solved by using an f = 1.5 lens in conjunction with a high-intensity oscilloscope and Tri X film.

To start with one has to find the right compensation by trial and error, and then keeping the same operating conditions one has to stretch out the horizontal time base. Location of the jump clearly on the oscilloscope face did not require much effort with the improved pickup and delay unit and the records could be repeated without perceptible scatter. A typical oscillogram is shown in figure 29. The relevant data are given in the figure legend.

The lower part of figure 29 is the response of the equipment to a 10-kilocycle square wave passed through a dummy hot-wire with a time constant of 0.2 millisecond. This compensation is applied to restore the distorted square wave. The amplitude of the square wave is the same as that of the jump due to the shock wave. The oscilloscope reference grid is calibrated for time and amplitude with a 50-kilocycle sine wave. The calibrating sine-wave signal was itself calibrated for frequency against the 60 cycles from the line.

The rise time with square-wave technique is slightly smaller than the one observed by the response of a hot-wire to a traveling shock wave. The initial rise in the hot-wire trace is fairly steep, but after about 10 microseconds it rounds off. The same type of flattening was observed before (ref. 8). However, if the rise time is taken as given by two-thirds of the total rise, then this time is of the order of 10 microseconds and the two techniques agree rather well.

Absolute Temperature Measurements

If the same hot-wire (characterized by the same R_f, I_o, $(\rho u)_o$, and n) is operated twice with two different heating currents for shock waves of the same strength (i.e., the same T_{o2} and $\rho_2 u_2$), then under equilibrium conditions attained after the jump one gets

$$(I')^2 R_f \left[1 + \alpha\left(T_{v2}' - T_f\right)\right] = \left(T_{v2}' - T_{o2}\right)\left(A + B\sqrt{\rho_2 u_2}\right) \tag{70}$$

$$(I'')^2 R_f \left[1 + \alpha\left(T_{v2}'' - T_f\right)\right] = \left(T_{v2}'' - T_{o2}\right)\left(A + B\sqrt{\rho_2 u_2}\right) \tag{71}$$

where the primes refer to the two different overheating ratios.

Taking ratios of these relations (for details see refs. 8 and 10), one gets

$$\left(T_{o2} - T_1\right) = \frac{1}{\alpha_1}\left\{\frac{(I')^2 R_{v2}'\left(R_{v2}'' - R_1\right) - (I'')^2 R_{v2}''\left(R_{v2}' - R_1\right)}{R_1\left[(I')^2 R_{v2}' - (I'')^2 R_{v2}''\right]}\right\} \tag{72}$$

where

$$\alpha_1 = \frac{\alpha}{1 + \alpha\left(T_1 - T_f\right)}$$

or for $I' \gg I''$ and $R_{v2}' > R_{v2}''$

$$\left(T_{o2} - T_1\right) = \Delta T = \frac{\Delta R}{\alpha_1 R_1} \tag{73}$$

Most of the quantities on the right-hand side of equation (72) are directly measurable. However, one has to determine R_{v2}'' and R_{v2}' from the oscillographic records of the hot-wire response. The equilibrium resistance R_{v2} is computed as follows:

The height of the jump due to the shock wave represents a voltage change Δe across the wire. The root-mean-square value of the sine-wave calibrating signal is known in millivolts. The peak-to-peak value for the sinusoidal voltage is $2\sqrt{2}$ times the root-mean-square value. Therefore, the scale of the records is established. This experimental voltage jump in reality is smaller than what it would have been if the heating-current source had infinite impedance. The finite impedance of the heating circuit acts like a negative feedback by reducing both the sensitivity and the thermal lag. From the known circuit characteristics and the initial operating overheating ratio, one can find

$$E = \frac{1 - \epsilon}{1 + 2a_w\epsilon} \tag{74}$$

where

$$\epsilon = \frac{R_w}{R_w + Z_s}$$

For cold operation $a_w \longrightarrow 0$; therefore, $E = 1 - \epsilon$.

From this, the corrected voltage jump $\Delta e_{corrected}$ can be found and

$$\Delta R = \pm \frac{\Delta e_{corrected}}{I} \tag{75}$$

The positive sign is used when the wire gives a voltage jump corresponding to increase in resistance (temperature response) and the negative sign, corresponding to decrease in resistance (mass flow response). Then

$$R_{v2} = R_{v1} \pm \Delta R \tag{76}$$

When little heating current is used, the wire is predominantly temperature sensitive and

$$R_{v2}'' = R_{v1}'' + \Delta R \tag{77}$$

and, when the wire is operated at elevated temperatures, the wire is predominantly mass flow sensitive and

$$R_{v2}' = R_{v1}' - \Delta R \tag{78}$$

Knowing R_{v2}'', R_{v2}', and the corresponding currents, one can find ΔT from relation (72). However, for these calculations a representative value had to be assumed for α, the temperature coefficient of resistivity. The value of α was not measured for every hot-wire used. Some previous measurements showed that values of α given in handbooks are invariably higher than the values experimentally found. In these calculations, for tungsten wires $\alpha = 0.0035$ and for platinum Wollaston wires $\alpha = 0.003$ have been used.

Mass-Flow and Temperature Separation

When a shock wave passes over a hot-wire, the latter experiences a sudden temperature and mass-flow change. Its operating resistance suddenly changes yielding a voltage jump. Depending upon their operating conditions, hot-wires are sensitive to both temperature and mass-flow fluctuations. If these fluctuations occur simultaneously (as in a shock wave), they can be quantitatively separated into temperature and mass-flow jumps (ref. 5).

By subtracting relations (70) and (71), one gets

$$A + B\sqrt{\rho_2 u_2} = \frac{(I')^2 R_{v2}' - (I'')^2 R_{v2}''}{T_{v2}' - T_{v2}''} \tag{79}$$

where

$$\left.\begin{aligned} A &= k_{e2} l \\ B &= l\sqrt{2\pi k_{e2} C_p d} \end{aligned}\right\} \tag{80}$$

where k_{e2} is the heat conductivity of the air at equilibrium temperature of the flow behind the shock wave and C_p is assumed constant. Now,

$$\frac{A^2}{B^2} = \frac{k_{e2}}{2\pi C_p d} = \left(\rho_2 u_2\right)_o \tag{81}$$

Therefore relation (79) becomes

$$\rho_2 u_2 = \left(\rho_2 u_2\right)_o \left[\frac{(I')^2 R_{v2}' - (I'')^2 R_{v2}'}{2 I_{o2}^2 \left(R_{v2}' - R_{v2}''\right)} - 1 \right]^2 \tag{82}$$

where

$$I_{o2}^2 = \frac{A}{2\alpha R_f} = \frac{k_{e2} l}{2\alpha R_f}$$

The calibration of the wire is usually conducted in the flow with normal atmospheric conditions (see section "Calibrating Facility"), and the constants of calibration are

$$\left.\begin{aligned} I_o^2 &= \frac{k_e l}{2\alpha R_f} \\ (\rho u)_o &= \frac{k_e}{2\pi C_p d} \end{aligned}\right\} \tag{83}$$

If these constants are compared with the shock-tube case (for the same wire)

$$\frac{\left(\rho_2 u_2\right)_o}{(\rho u)_o} = \frac{k_{e2}}{k_e}$$

or

$$\frac{\left(\frac{\rho_2}{\rho_f} u_2\right)_o}{\left(\frac{\rho}{\rho_f} u\right)_o} = \frac{k_{e2}}{k_e}$$

If ρ_f, the reference density, is taken to be the atmospheric density, then $\rho = \rho_f$ and

$$\left(\frac{\rho_2}{\rho_f} u_2\right)_o = U_o \frac{k_{e2}}{k_e} \tag{84}$$

Also

$$I_{o2}^2 = I_o^2 \frac{k_{e2}}{k_e} \tag{85}$$

Therefore relation (82) becomes

$$\sqrt{\frac{\rho_2 u_2}{\rho_f}} = \sqrt{\frac{U_o k_e}{k_{e2}}} \frac{1}{I_o^2} \left[\frac{(I')^2 R_{v2}' - (I'')^2 R_{v2}''}{2\left(R_{v2}' - R_{v2}''\right)} - I_o^2 \frac{k_{e2}}{k_e} \right] \tag{86}$$

If the shock tube is operated such that the density in the expansion chamber is lower than atmospheric, that is, $\rho_1 < \rho_f$, then relation (84) can be written as

$$\left(\frac{\rho_2}{\rho_1} \frac{\rho_1}{\rho_f} u_2\right)_o = U_o \frac{k_{e2}}{k_e}$$

or

$$\left(\frac{\rho_2}{\rho_1} u_2\right)_o = \frac{\rho_f}{\rho_1} \frac{k_{e2}}{k_e} U_o$$

and relation (86) becomes

$$\sqrt{\frac{\rho_2}{\rho_1} u_2} = \sqrt{\frac{\rho_f}{\rho_1} U_o \frac{k_e}{k_{e2}}} \frac{1}{I_o^2} \left[\frac{(I')^2 R_{v2}' - (I'')^2 R_{v2}''}{2\left(R_{v2}' - R_{v2}''\right)} - I_o^2 \frac{k_{e2}}{k_e} \right] \quad (87)$$

Knowing the operating conditions, the shock strength, and thus the expected temperature, one can find k_{e2}/k_e (ref. 15). The rest of the quantities on the right-hand side of equation (87) are experimentally determinable. Thus it is possible to calculate the mass-flow jump behind the primary shock wave.

While the finite circuit correction for temperature records is comparatively small, it is considerable for mass-flow oscillograms, since the initial overheating ratio a_w is large. This correction gets progressively smaller if the operating temperature of the wire is so arranged that it is only moderately higher than the expected temperature of the flow behind the shock wave. In this case the overheating ratios will be low and jumps will be comparatively smaller too. But this technique of experimentation results in the difference $\left(R_{v2}' - R_{v2}''\right)$ being a very small quantity. This small quantity, as a difference of two large quantities, is very touchy to calculate and thus the scatter in the calculated values of mass flows increases considerably. On the other hand, if the high operating overheating ratios are used, the difference $R_{v2}' - R_{v2}''$ (though still small) gets to be comparatively larger than the case cited above. However, the evaluation of R_{v2}' itself is done from a large signal and a slightly wrong estimate of the amplitude of the actual jump or the calibrating signal and/or the feedback correction contributes to the scatter in the calculated values. The oscillographic records selected to calculate the mass flows, as reproduced here, used the combination of a temperature trace with very low current (platinum wire, $d = 0.0001$ inch) and mass flow traces with initial overheating ratio of $a_w = 0.5$ to 0.9. The computed mass-flow values are plotted against the corresponding measured shock strength. The scatter of the measured quantities is approximately 20 percent from the theoretically expected values.

Besides such uncertainties as measuring the initial current under no-flow conditions (which is rarely true) and the use of the modified I_o and U_o, the author feels that the principal difficulty lies in the technique of measurement and calculation. The equilibrium resistance R_{v2}' due to the mass-flow response and R_{v2}'' due to the temperature response fall closer together and they differ progressively less and less as the shock is stronger. This makes the personal error in setting the calibrating voltage and reading the amplitude of the jump and/or of the calibrating voltage rather an important factor, as all these plausible errors have a strong effect on $R_{v2}' - R_{v2}''$ and thus on $\frac{\rho_2}{\rho_1} u_2$.

It may be added here that during the process of collecting data with any calibrated wire if its resistance showed a trend to increase by more than 0.01 ohm the wire was rejected for any quantitative mass-flow or temperature investigations.

A set of calculations of $\frac{\rho_2}{\rho_1} u_2$ based on the same data as used for temperature calculations (fig. 30) is reproduced in figure 31. The scatter is quite evident. On the average the agreement with the theoretically expected values is fair.

Shock-Speed Measurements

In the section "Recording" the techniques of measuring shock speeds, taking shadowgraphs, and so forth have already been detailed. The chief interest in these measurements is the use of the hot-wire anemometer as a timing device which has made it possible to time shocks as weak as could be generated ($S = 1.01$) while it has been successfully operated at $S = 20$ and it is believed that the upper limit is safely higher than this. The thinnest diaphragm material obtainable was of thickness 0.0007 inch. In the shock tube (6- by 4-inch cross section), it could stand about 3 lb/sq in. With this diaphragm 1/2-pound-per-square-inch overpressure was used in the compression chamber and the time for the corresponding speed measurement was recorded. Because of the breaking characteristics of the diaphragm material at such low loadings there was some scatter from one shock to the other in the measurement of very low shock speeds. To keep the diaphragm material dry, it was stored in a box with silica gel.

But for this difficulty in the mechanics of producing weak shocks, even weaker "shocks" could have been timed, since a hot-wire operated at elevated temperatures is sensitive even to normal speech. If controlled very weak "shocks" could be generated by accelerating a piston, the hot-wire anemometer could be a very useful instrument for investigating the phenomena.

During the course of this work the following interesting observation was made. It is rather common practice among shock-tube workers to use two thin sheets of diaphragm material, if a single thicker sheet capable of withstanding the desired pressure is not available. When shock waves were being timed, a double thickness of diaphragm material was used not suspecting that anything unusual would happen. Quite surprisingly the recorded speeds were those of weak shock waves (almost the speed of sound). An oscillograph record, shown in figure 32, revealed that a very weak wave preceded the main shock about 1 millisecond at the measuring station 15 feet from the diaphragm. Apparently the double diaphragm, in bursting, generated a double wave. This phenomenon consistently repeated itself, but disappeared when a single diaphragm of equivalent strength was used.

The author would thus advise against the use of more than one sheet of diaphragm since it is doubtful if other timing devices will reveal the possible presence of a weak shock preceding the main front. It is evident that the stronger shock will eventually catch up with the weaker one; but, if this happens after the working section, it clearly could lead to erroneous results.

Incidentally, since the first jump is undercompensated, this double trace is a perfect demonstration of the fact that for weaker shocks larger compensations are needed than for stronger shock waves if the initial overheating ratio is the same (fig. 28).

For the measurement of shock speeds the thickness of the diaphragm was varied according to the overpressure used. For the case when the expansion chamber was partially evacuated, the thickness used varied anywhere between 0.0003 and 0.005 inch. Below 100 millimeters of pressure, 0.005-inch thickness was used. It would have been advantageous if 0.004-inch thickness were commercially available.

The results of the measurements are shown in figure 33. These are average points. However, the scatter in the same shock speed measured more than once was surprisingly little.

Rarefaction-Wave-Speed Measurements

The origin and the cause of the rarefaction wave generated at the open end and the relations for the expected time intervals of its arrival at various locations inside the shock tube were discussed previously. For experimental check the hot-wire anemometer was used to detect the arrival of the first characteristic at the location of the hot-wire. Hot-wires were mounted at various distances from the open end and mass-flow and temperature oscillograms were taken. The time calibration was affected by the 10-kilocycle sine wave. The time between the appearance

of the shock wave and the rarefaction wave was measured from the oscillograms (fig. 1). These oscillograms show the initial jump due to the primary shock wave and then some time later the arrival of the rarefaction cools the wire. This time interval between the arrival of the two wave fronts is the experimentally observed time. This time also can be theoretically calculated from relations (24) and (26):

$$t = \frac{\xi}{U_s} + \frac{\sqrt{\xi^2 + \eta^2}}{V_{ri}}$$

$$t = \frac{\sqrt{\xi^2 + \eta^2}}{V_{ro}} - \frac{\xi}{U_s}$$

The agreement is good. Because of the nature of the calibration time base and the personal error in reading it, however, the accuracy is not better than 3 to 5 percent. These measurements were carried out under two different experimental arrangements as follows.

(1) The hot-wire was kept fixed at one station and shocks of different strengths were used and the corresponding oscillograms recorded. The experimental results are reproduced in figure 34(a).

(2) The shock strength was kept the same and the position of the hot-wire was varied. The experimentally observed time of arrival of the rarefaction wave at these stations is shown in figure 34(b). The arrangement used to mount the hot-wire for such studies is shown in figure 25.

The passage of a shock wave over the hot-wire probe mounted in the glass section is demonstrated in figure 35.

Hot-wires were also mounted along the axis but outside the open end (0 to 6 inches). The time interval between the arrival of the shock wave and the rarefaction wave was measured (fig. 34(b)). This can be done only so far as the rarefaction has not affected the central part of the shock wave. After this has happened, the total jump previously obtained inside the shock tube for the same shock strength falls in amplitude and is not constant. This is due to the alteration of the shock front due to the expansion wave.

A few typical shadowgraphs taken at controlled delay settings are reproduced (fig. 36). The zero delay setting is at the open end of the

shock tube. The shock front just emerging from the open end is quite straight (fig. 36(a)). The curving of the shock front is very evident and the central part is affected by the rarefaction about 4 inches down from the open end (cross section of the shock tube is 4 by 6 inches). The rarefaction clearly originates at the open end and its growth links it with the curving of the shock front (ref. 22 and fig. 36(b)).

The vortex generated at the corners of the open end shows up very distinctly and proceeds rather slowly as compared with the particle velocity behind the central part of the shock front (fig. 36(c)).

CONCLUDING REMARKS

This experimental study has shed considerable light on the behavior of the hot-wire anemometer exposed to transient traveling wave fronts (shock waves, contact surface and rarefaction waves) and their associated flow fields. As an instrument the hot-wire anemometer certainly has encouraging possibilities for investigation of turbulence or some such fast fluctuations in these transient flow fields. However, the type of the associated equipment of which the hot-wire will form an integral part may have to be decided according to the nature of the problem under study. There are two types of hot-wire sets in use:

1. Constant current (heating circuit with large impedance)

2. Constant temperature (negative feedback) (ref. 23)

The constant-current arrangement is more commonly used in turbulence research than the constant-temperature system. The constant-current system has been used to advantage in the present investigation for study of the response of a hot-wire to a sudden step-function change in flow conditions, the ultimate time resolution of the equipment, measurement of required compensations, measurement of absolute temperatures, and for the detection and timing of various wave fronts generated in the shock tube. If a hot-wire is operated at elevated temperatures and the flow conditions jump from zero to high fluctuations in mass flow (the conventional shock-tube operation), then the temperature of the wire falls. This reduces the sensitivity of the hot-wire to any subsequent mass fluctuations. However, if the constant-temperature system is used, it is the current which fluctuates and not the operating temperature of the wire. (Nevertheless, the ambient temperature of the flow will still jump.) For such large negative feedback signals, the constant-temperature

system will be superior. Also one does not need to know the time constant as the negative feedback suppresses it. It cannot be said, however, that this arrangement will not have its own inherent difficulties.

The Johns Hopkins University,
Baltimore 18, Md., December 3, 1953.

REFERENCES

1. Lobb, R. K.: A Study of Supersonic Flows in a Shock Tube. Rep. No. 8, Inst. Aerophys., Univ. of Toronto, May 1950.

2. Bleakney, Walker, and Taub, A. H.: Interaction of Shock Waves. Rev. Modern Phys., vol. 21, no. 4, Oct. 1949, pp. 584-605.

3. Kovasznay, Leslie S. G., and Clarken, Patricia C.: Experimental Investigation of Optical Methods for Measuring Turbulence. Tech. Rep. 42, Project Squid, Contract N6ori-105, Task Order III, Office of Naval Res.; Res. and Dev. Command, Dept. Air Force; and Johns Hopkins Univ.; Jan. 1, 1952.

4. Kovasznay, Leslie S. G.: Turbulence Measurements. High Speed Aerodynamics and Jet Propulsion. Vol. IX, Sect. F., Princeton Univ. Press (Princeton), 1954.

5. Corrsin, Stanley: Extended Applications of the Hot-Wire Anemometer. NACA TN 1864, 1949.

6. Kovásznay, L.: Calibration and Measurement in Turbulence Research by the Hot-Wire Method. NACA TM 1130, 1947.

7. Betchov, R.: Theorie non-lineaire de l'anemometre a fil chaud. Verhand. Kon. Ned. Akad. Wetensch. (Amsterdam), vol. 52, no. 3, 1949, pp. 195-207. (Available in English translation as NACA TM 1346.)

8. Dosanjh, Darshan S., Kovasznay, Leslie S. G., and Clarken, Patricia C.: Study of Transient Hot-Wire Response in a Shock Tube. CM-725, Dept. Aero., The Johns Hopkins Univ., Mar. 12, 1952.

9. Dosanjh, Darshan S.: Use of the Hot Wire Anemometer as a Triggering and Timing Device for Wave Phenomena in a Shock Tube. (To be published in Rev. Sci. Instr.)

10. Dosanjh, Darshan S.: I - Use of the Hot Wire Anemometer in Shock Tube Investigations. II - Interaction of Travelling Shock With Grids. Ph. D. dissertation, The Johns Hopkins Univ., 1953.

11. Courant, R., and Friedrichs, K. O.: Supersonic Flow and Shock Waves. Interscience Publishers, Inc. (New York), 1948.

12. King, Louis Vessot: On the Convection of Heat From Small Cylinders in a Stream of Fluid: Determination of the Convection Constants of Small Platinum Wires With Applications to Hot-Wire Anemometry. Phil. Trans. Roy. Soc. (London), ser. A, vol. 214, Nov. 12, 1914, pp. 373-432.

13. Hilsenrath, Joseph: Dry Air - Prandtl Number $\eta c_p/k$. NBS-NACA Tables of Thermal Properties of Gases, Table 2.44, July 1950.

14. McAdams, William H.: Heat Transmission. Second ed., McGraw-Hill Book Co., Inc., 1942.

15. Nuttall, R. L.: Dry Air - Thermal Conductivity k/k_0. NBS-NACA Tables of Thermal Properties of Gases, Table 2.42, July 1950.

16. Kovasznay, Leslie S. G., and Tornmarck, Sven I. A.: Heat Loss of Hot-Wires in Supersonic Flow. Bumblebee Ser., Rep. No. 127, Contract NOrd-8036, Bur. Ord., Dept. Navy, and Dept. Aero., The Johns Hopkins Univ., Apr. 1950.

17. Stalder, Jackson R., Goodwin, Glen, and Creager, Marcus O.: Heat Transfer to Bodies in a High-Speed Rarefied-Gas Stream. NACA Rep. 1093, 1952. (Supersedes NACA TN 2438.)

18. Stalder, Jackson R., Goodwin, Glen, and Creager, Marcus O.: A Comparison of Theory and Experiment for High-Speed Free-Molecule Flow. NACA Rep. 1032, 1951. (Supersedes NACA TN 2244.)

19. Morey, F. C.: Dry Air - Coefficients of Viscosity η/η_0, ν/ν_0. NBS-NACA Tables of Thermal Properties of Gases, Table 2.39, July 1950.

20. Kovásznay, Leslie S. G.: Development of Turbulence-Measuring Equipment. NACA TN 2839, 1953.

21. Kovásznay, Leslie S. G.: High Power Short Duration Spark Discharge. Rev. Sci. Instr., vol. 20, no. 9, Sept. 1949, pp. 696-697.

22. Elder, F. K., Jr., and de Haas, N.: Schlieren Studies of Initial Conditions at the Open End of a Cylindrical Shock Tube. CM-728, Appl. Phys. Lab., The Johns Hopkins Univ., Apr. 1952.

23. Kovasznay, Leslie S. G.: Simple Analysis of the Constant Temperature Feedback Hot-Wire Anemometer. CM-478, Dept. Aero., The Johns Hopkins Univ., June 1, 1948.

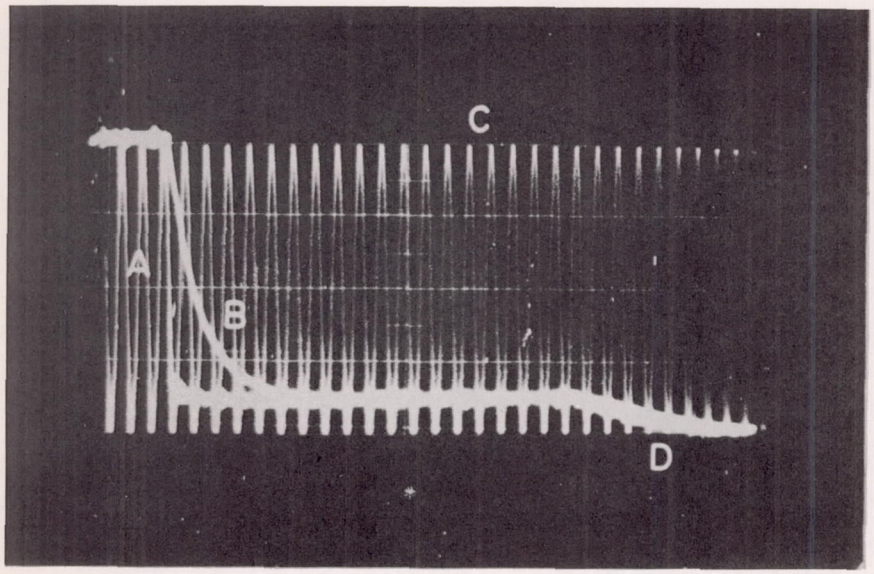

Figure 1.- Uncompensated and compensated response of a hot-wire to a traveling shock wave. Platinum Wollaston wire, d = 0.0001 inch; R_e = 19.12 ohms; R_w = 28.77 ohms; I = 16.24 milliamperes; S = 1.175; location of hot-wire inside open end, 12.25 inches. A, compensated response; compensation, 0.17×10^{-3} second. B, uncompensated response. C, calibrating signal; amplitude, 36 millivolts root mean square; frequency, 10 kilocycles. D, rarefaction wave.

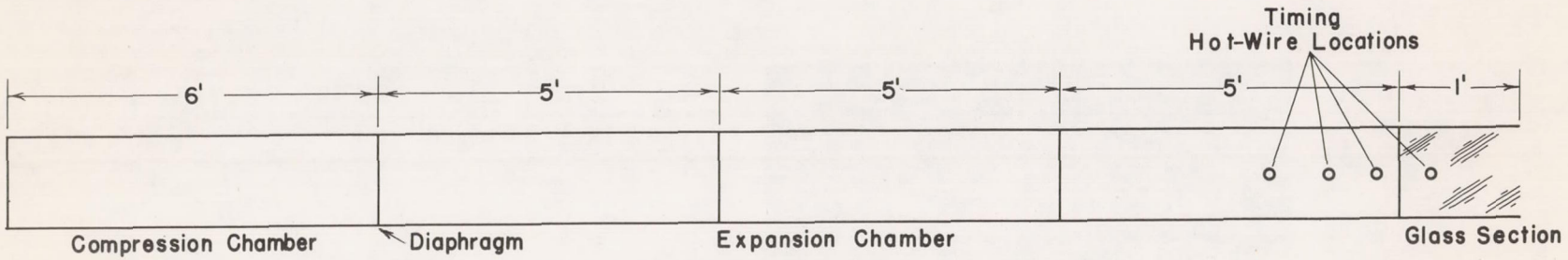

Shock Tube

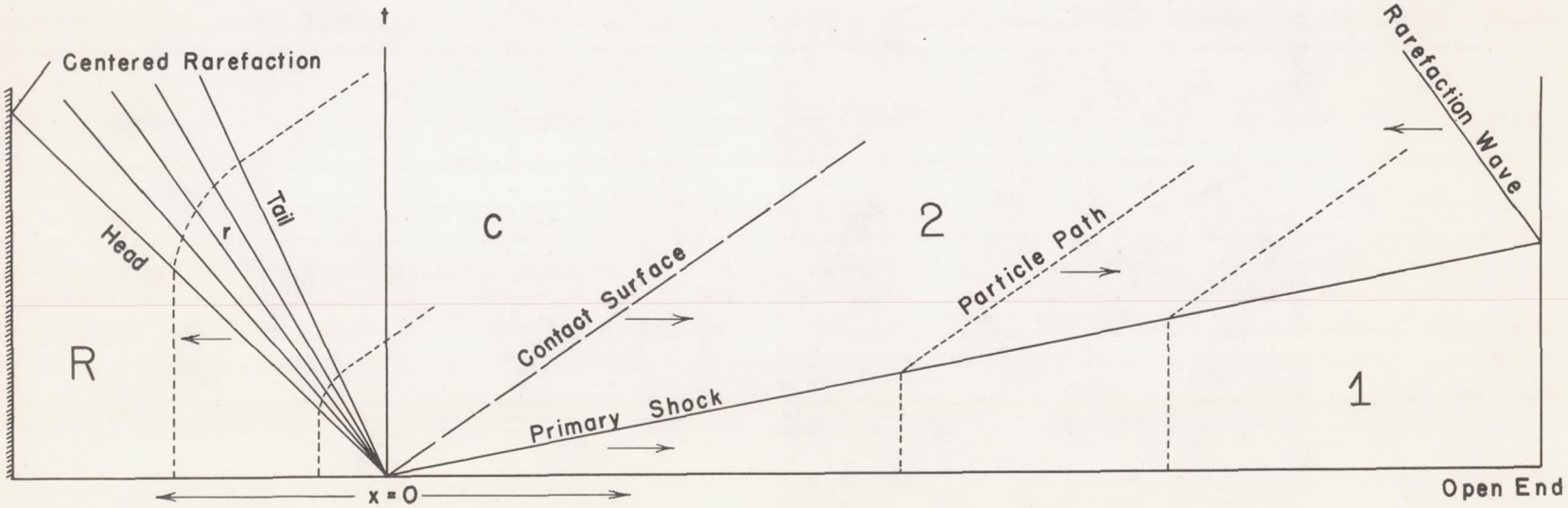

Figure 2.- The (x-t) diagram of wave system produced in a shock tube.

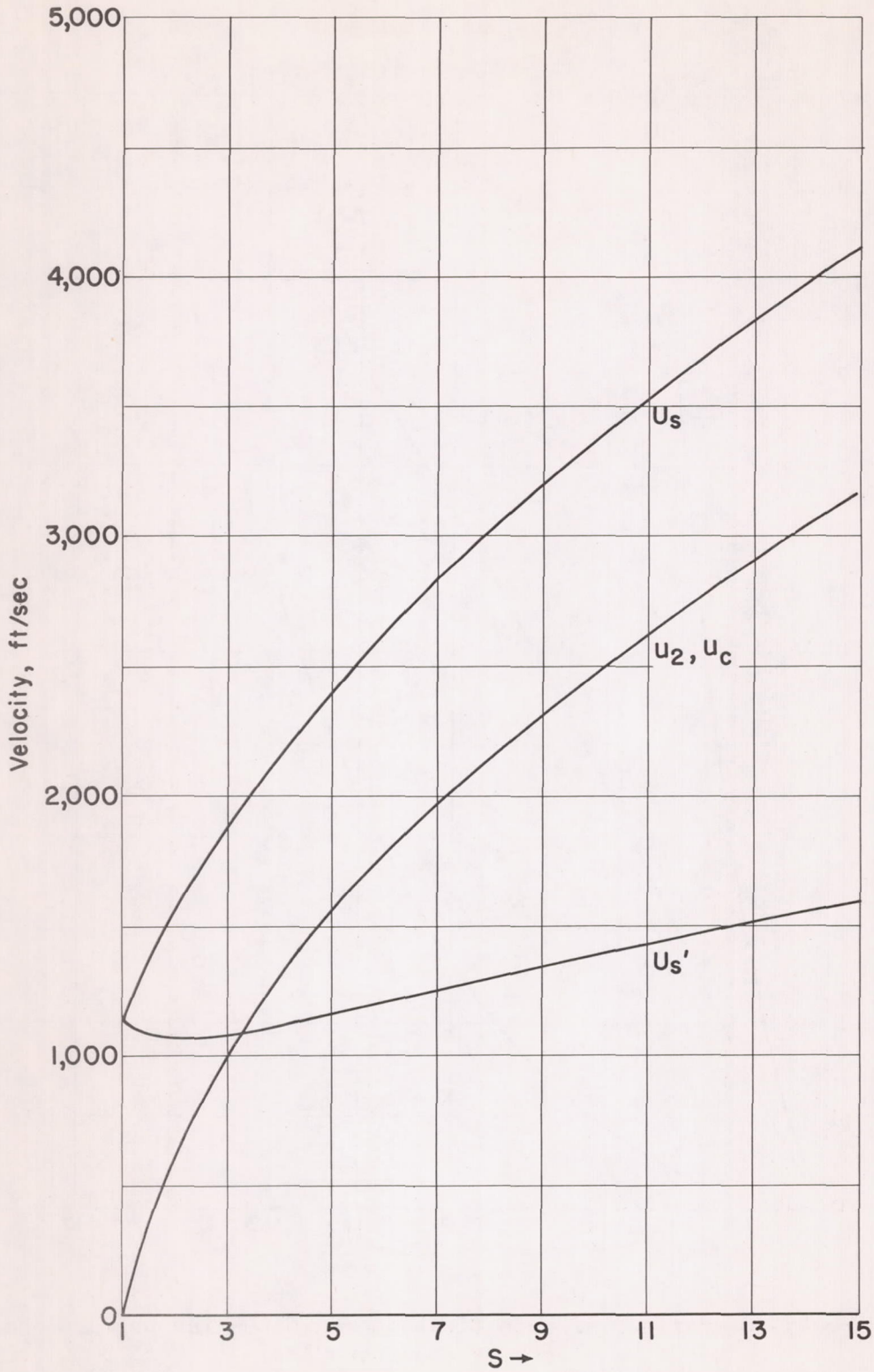

Figure 3.- Particle and wave velocities in a shock tube as a function of shock strength. a_1 = 1,141 feet per second; Air/Air.

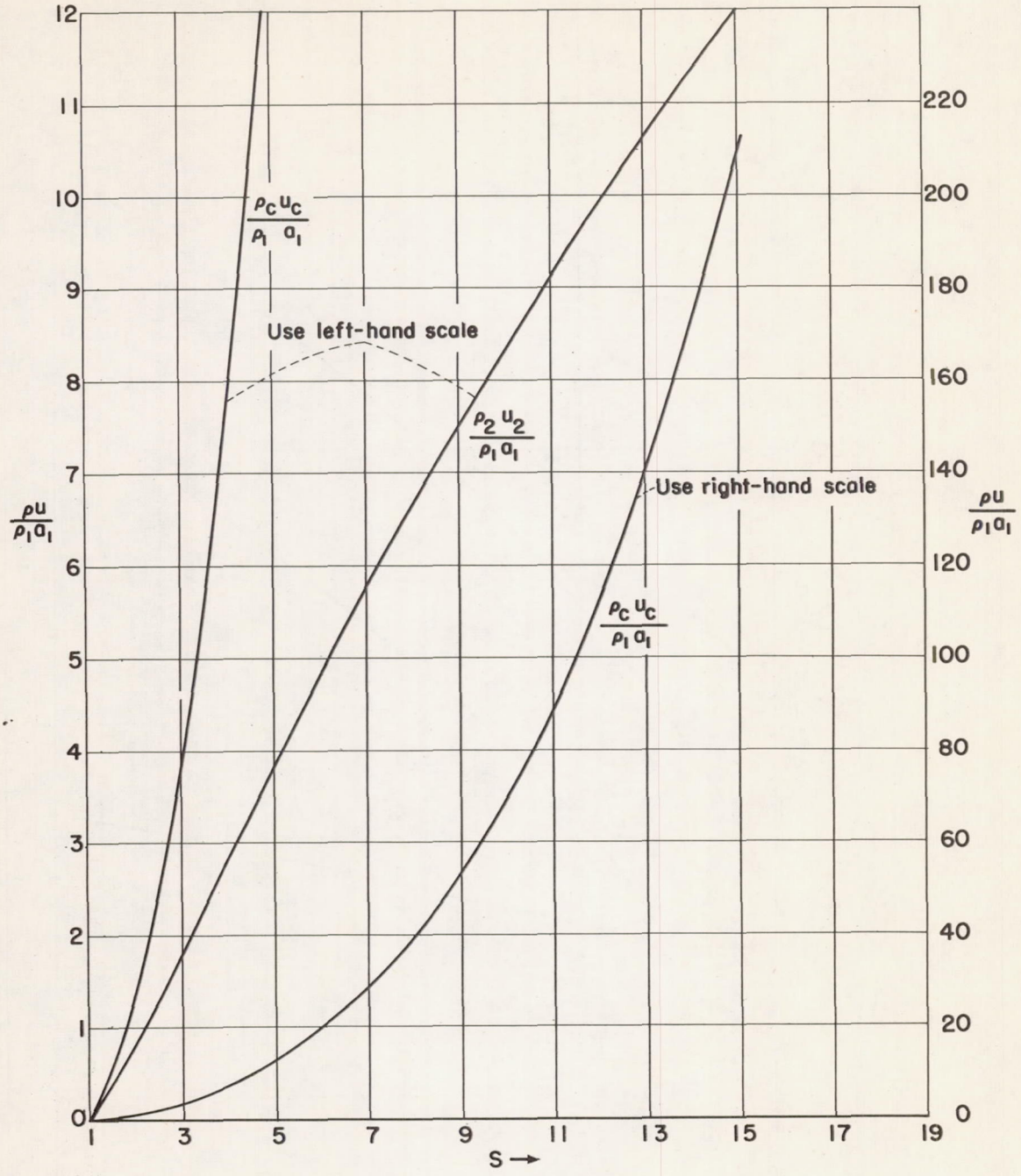

Figure 4.- Comparison of mass flows in region behind primary shock and contact-surface flow.

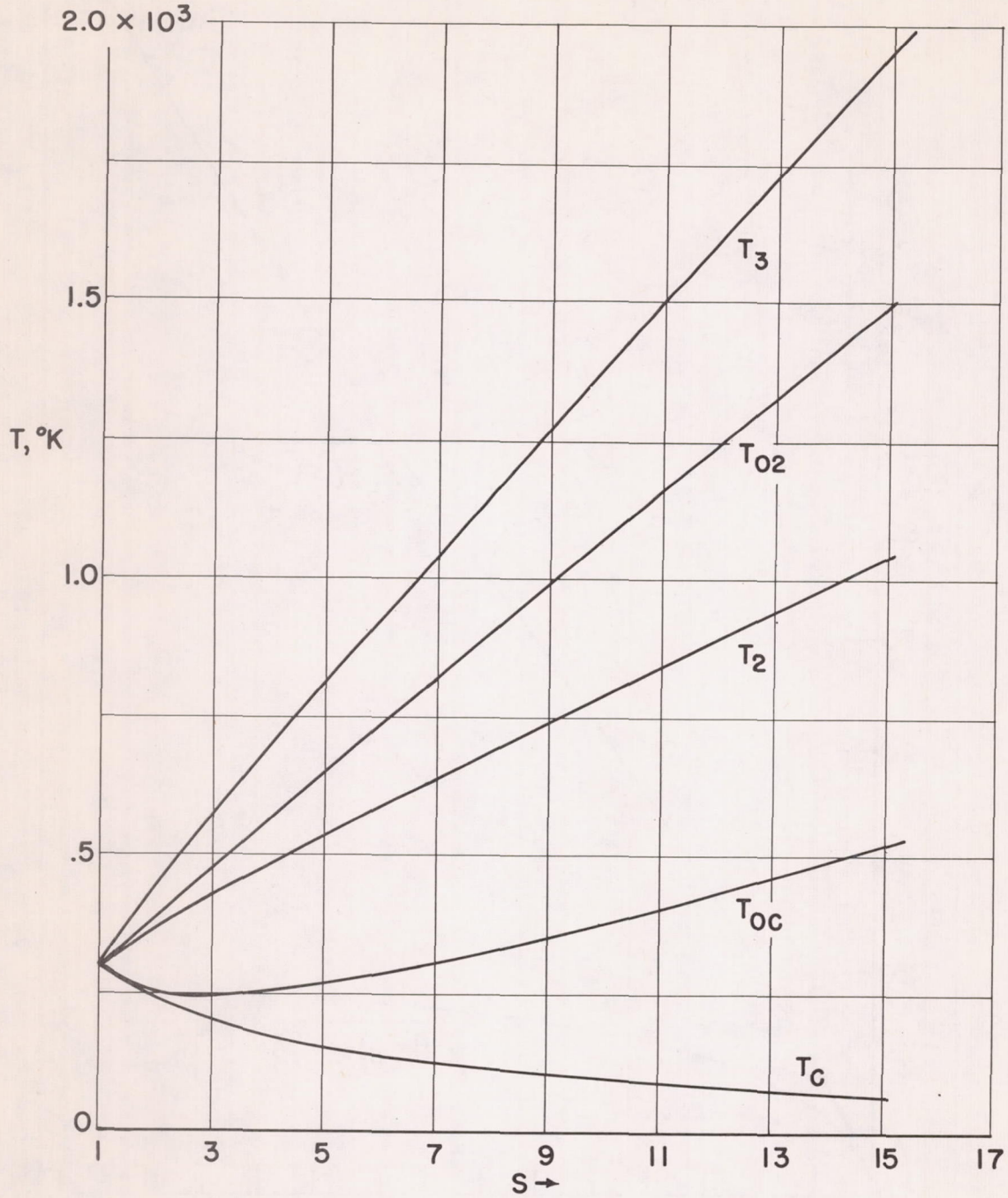

Figure 5.- Temperatures versus shock strength. $T_1 = 299^\circ$ K; Air/Air.

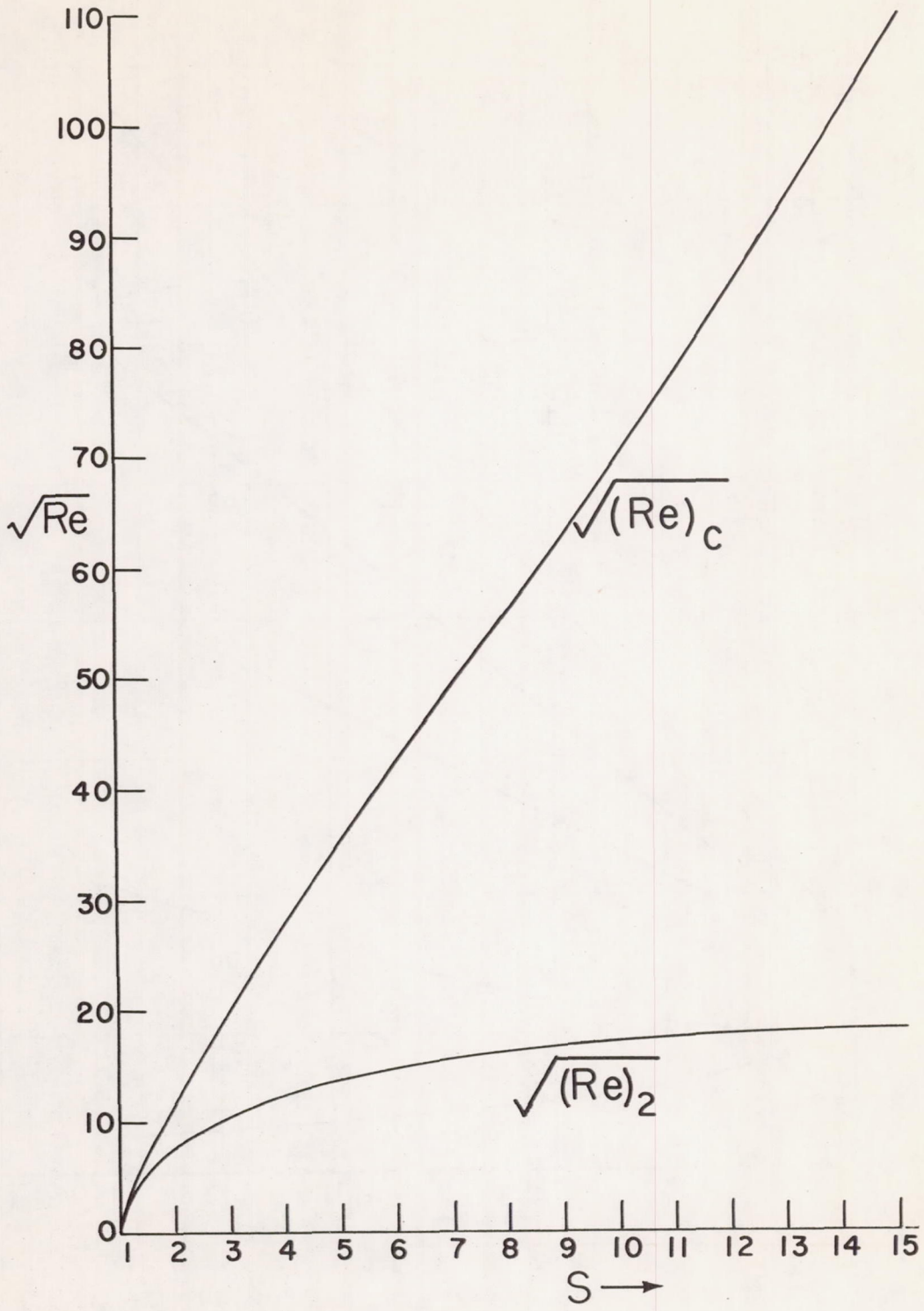

Figure 6.- Reynolds number $\sqrt{Re}$ versus shock strength. Expansion chamber at atmospheric pressure; compression chamber at higher pressure; d = 0.00015 inch (characteristic length); Air/Air.

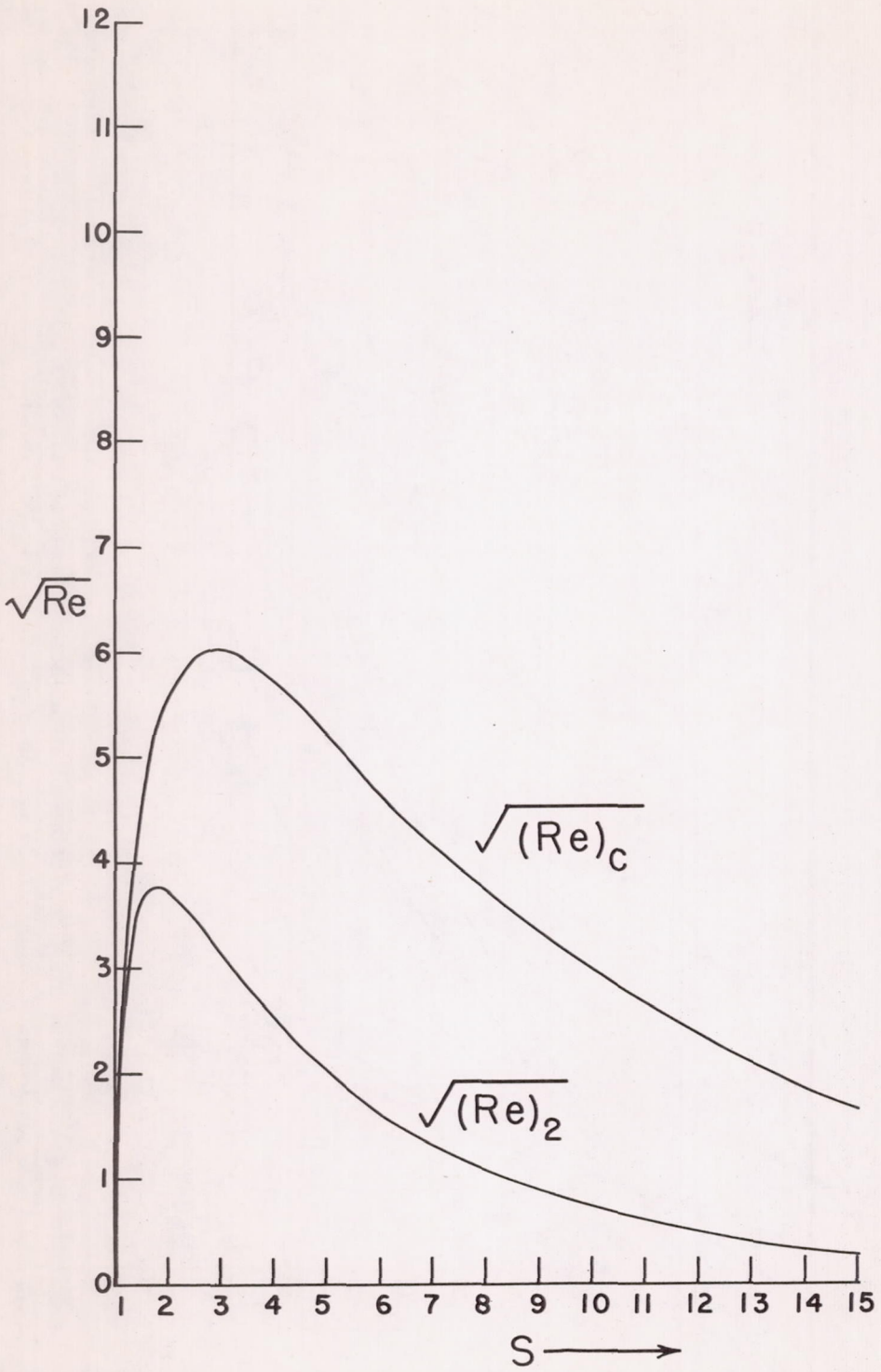

Figure 7.- Reynolds number $\sqrt{Re}$ versus shock strength. Expansion chamber partially evacuated; compression chamber at atmospheric pressure; d = 0.00015 inch (characteristic length); Air/Air.

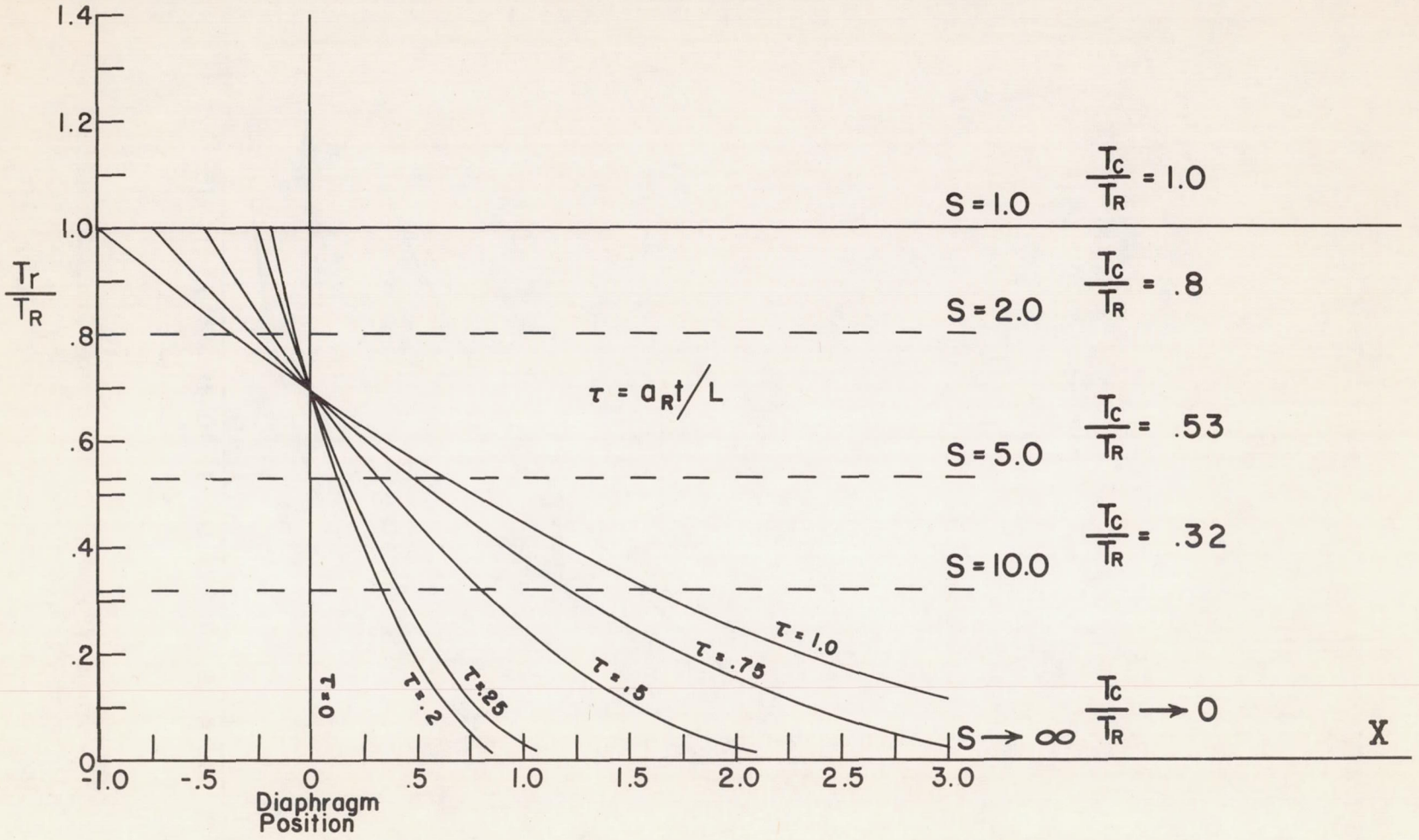

Figure 8.- Variation of temperature throughout rarefaction wave for various times after diaphragm is ruptured. $T_R = 299^\circ$ K.

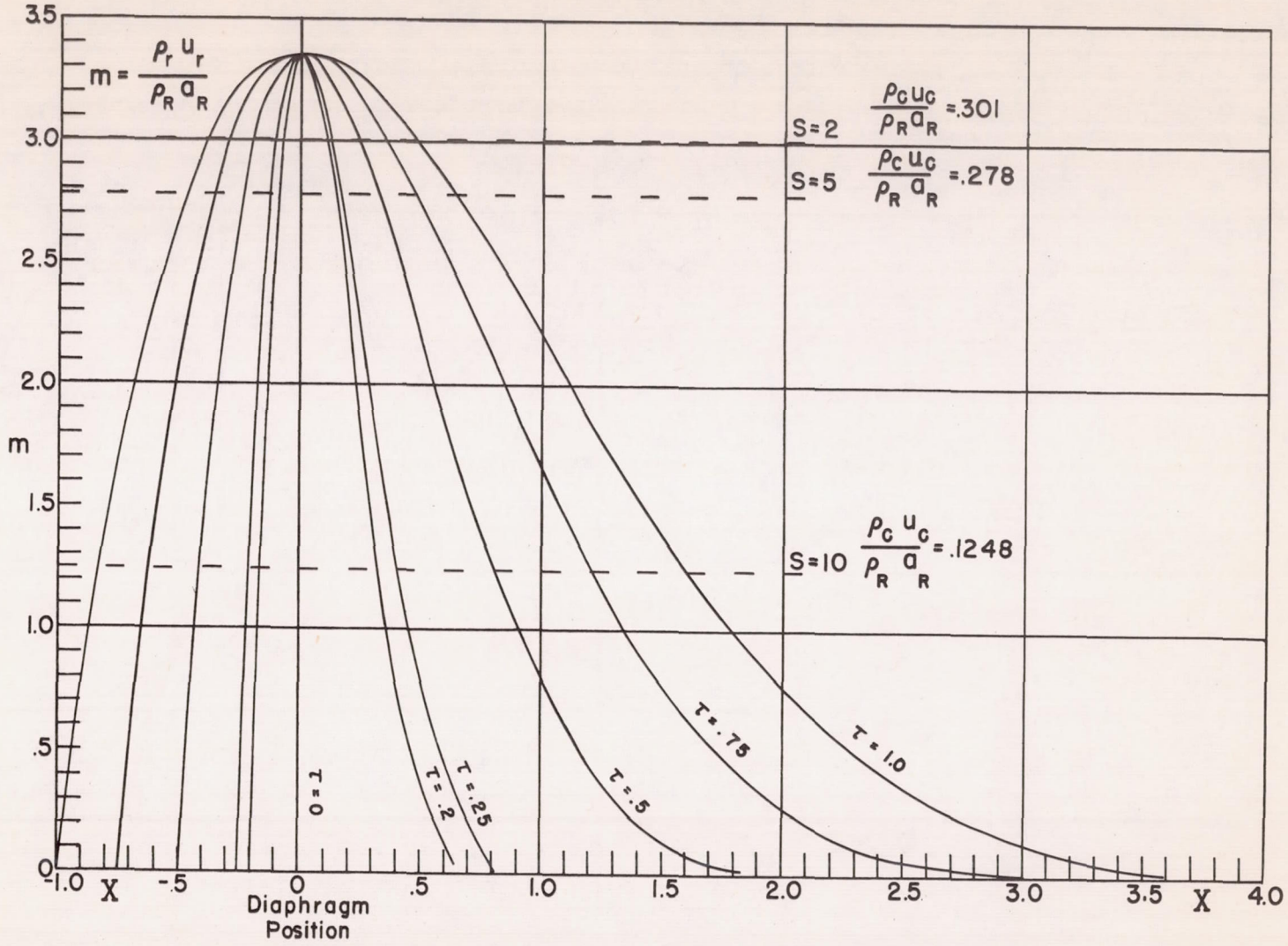

Figure 9.- Variation of mass flow throughout rarefaction wave for various times after diaphragm is ruptured.

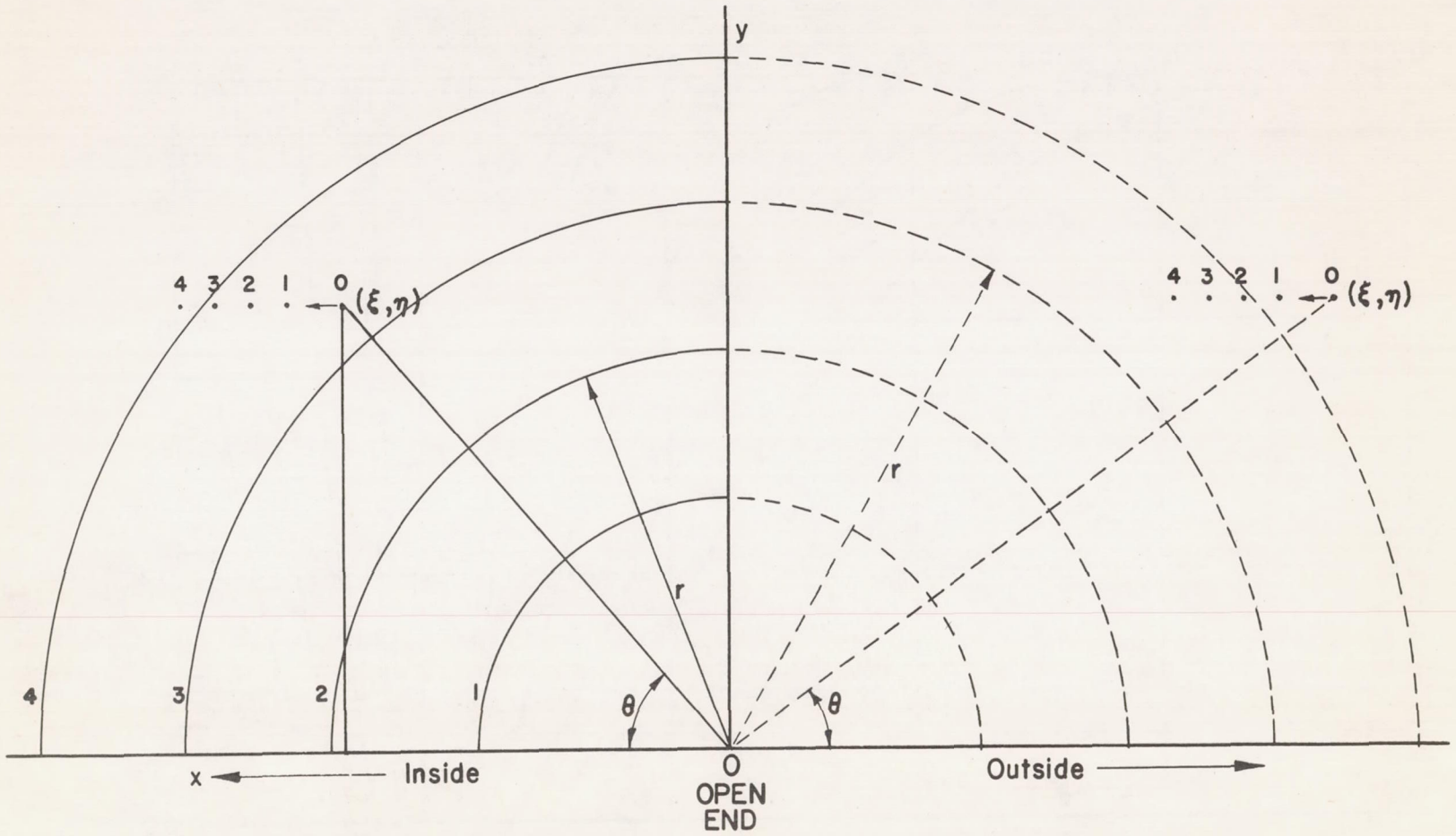

Figure 10.- Rarefaction wave generated at open end.

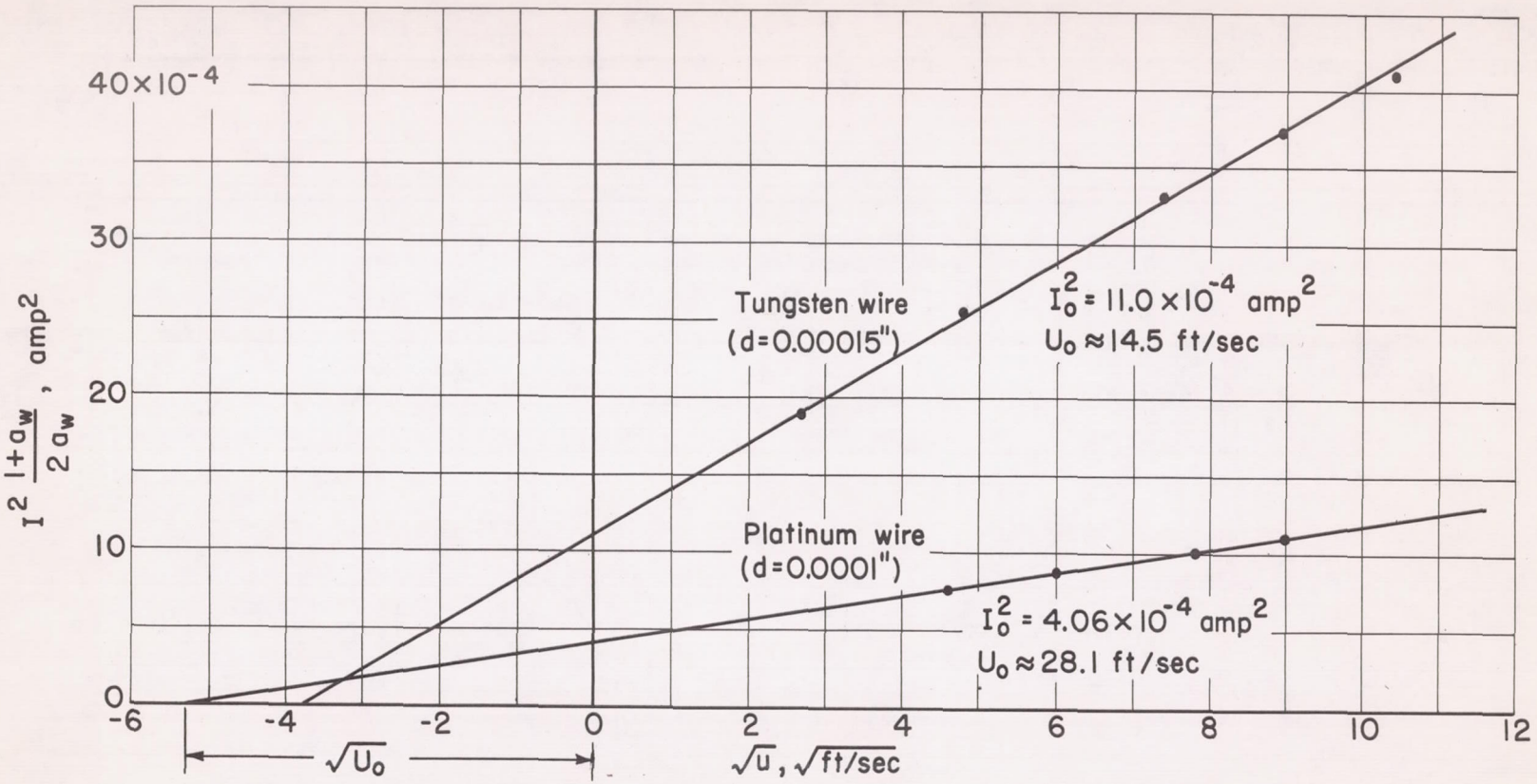

Figure 11.- Typical calibration curve.

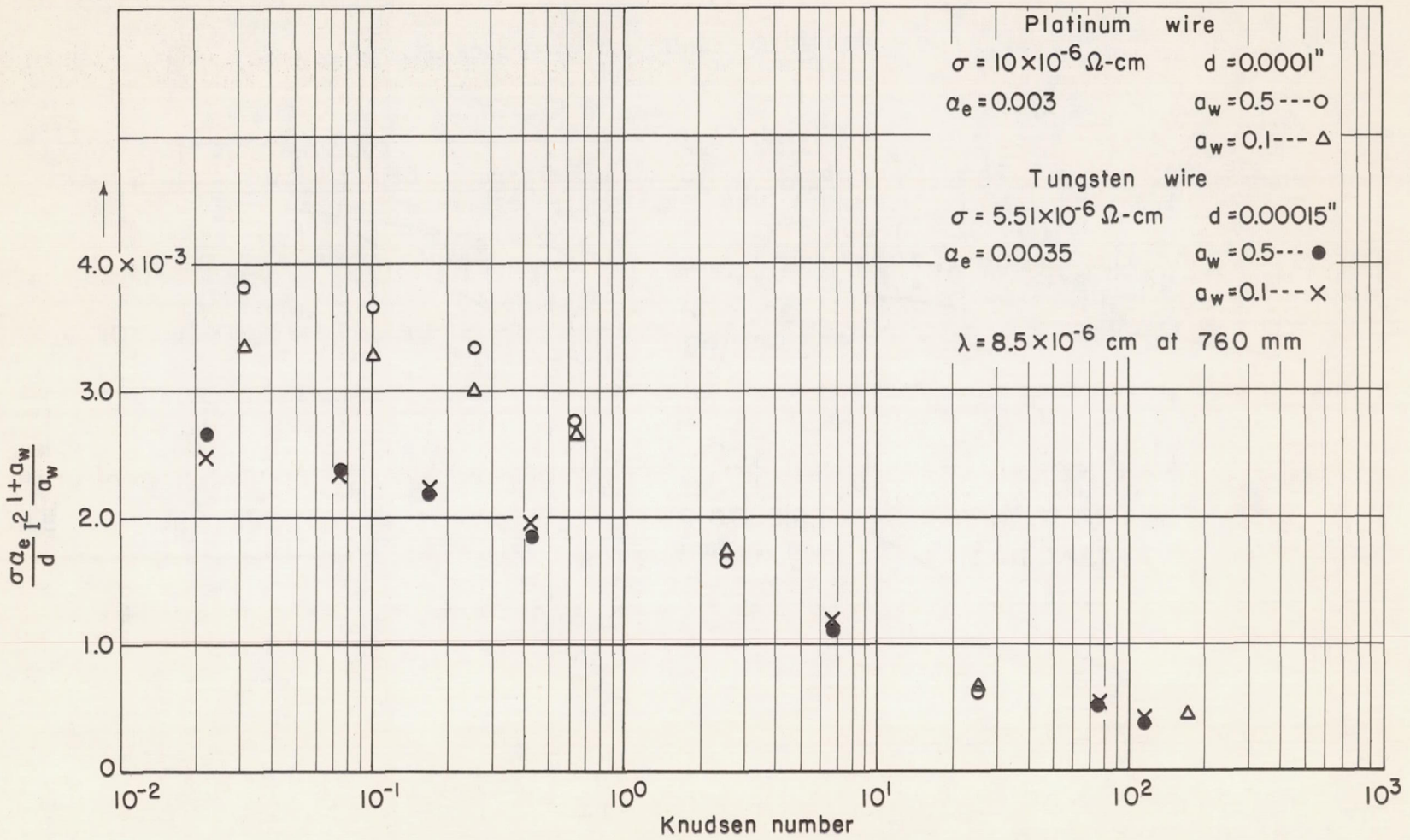

Figure 12.- Heat loss at reduced pressures in expansion chamber.

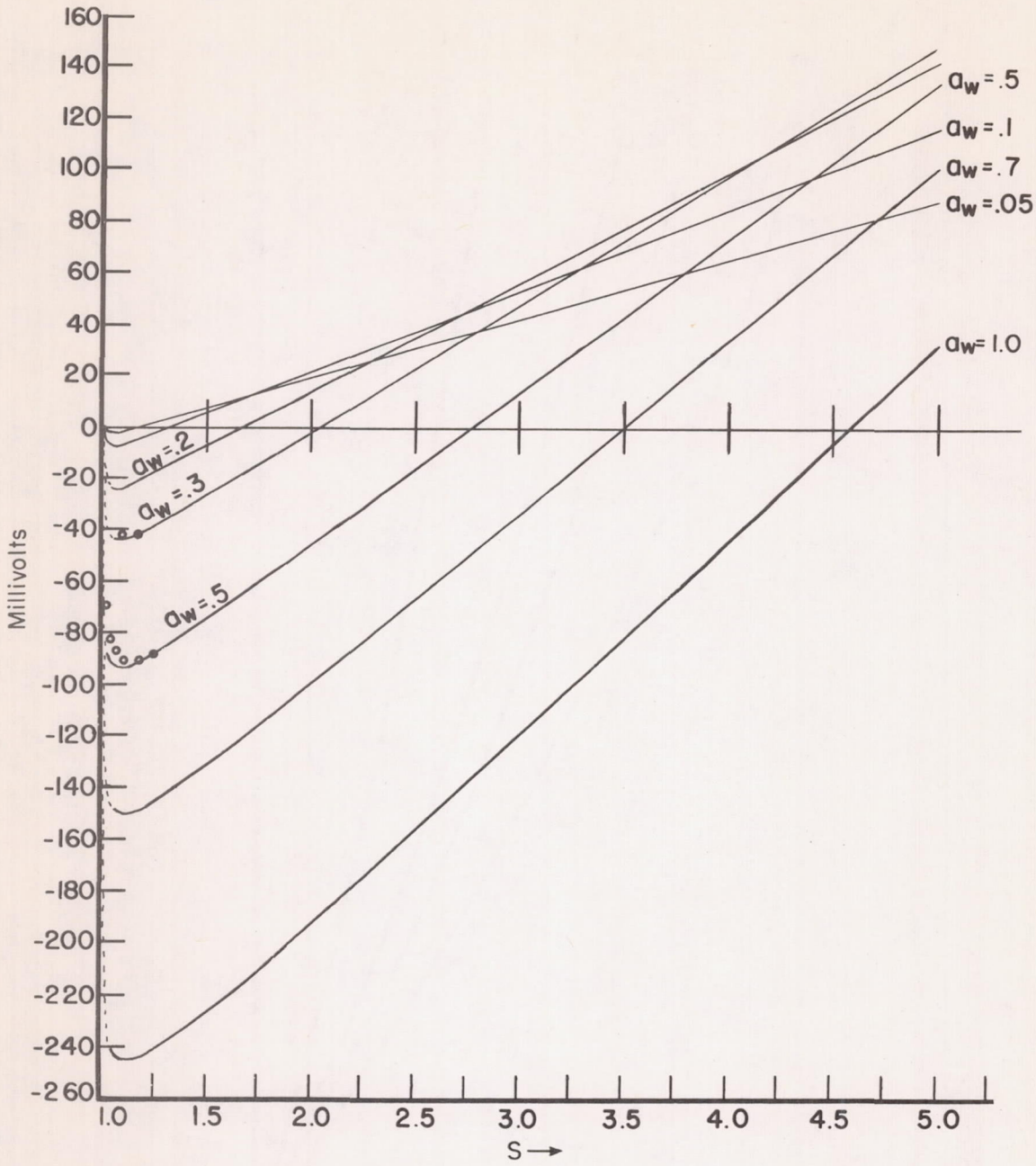

(a) Flow behind primary shock wave.

Figure 13.- Voltage signals due to response to flows. Expansion chamber at atmospheric pressure. l = 0.2 centimeter; R_o = 10 ohms; tungsten wire, d = 0.00015 inch.

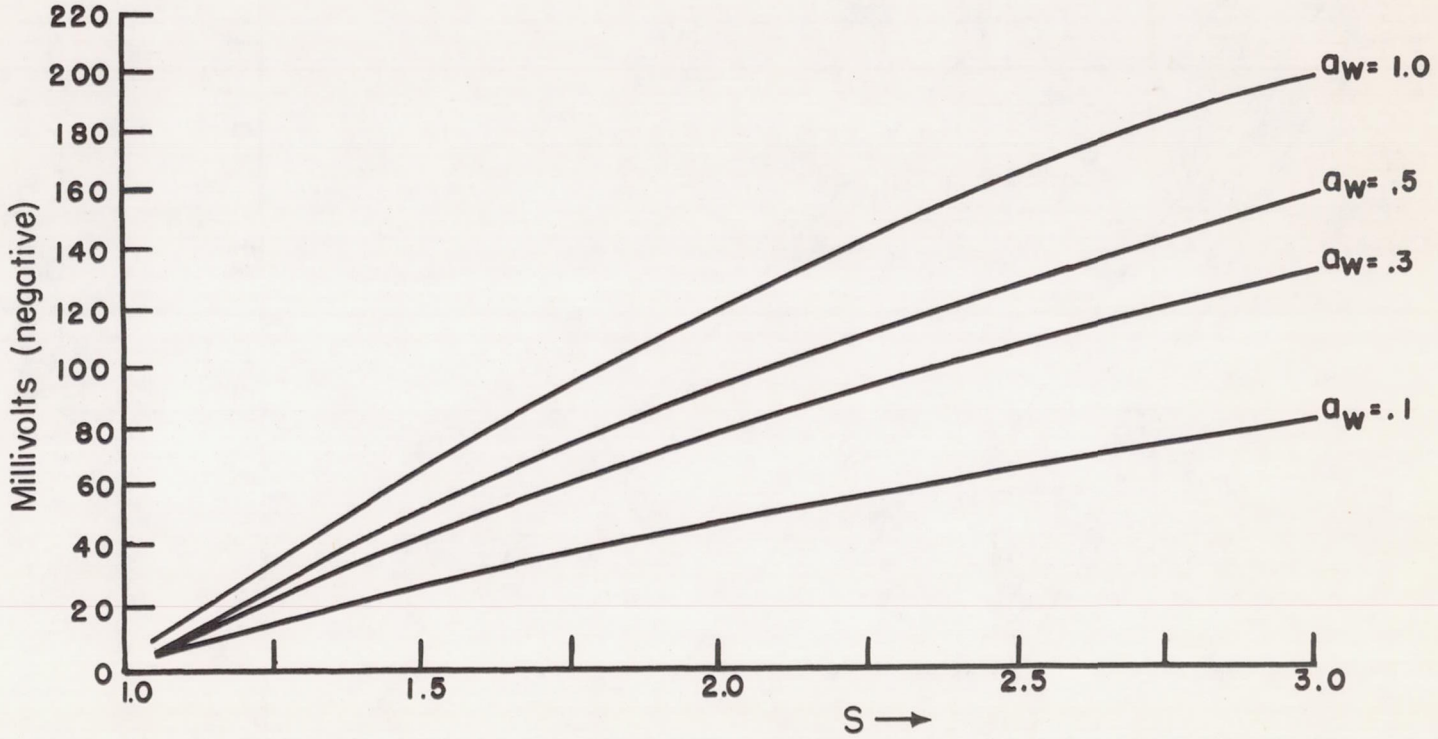

(b) Contact-surface flow.

Figure 13.- Concluded.

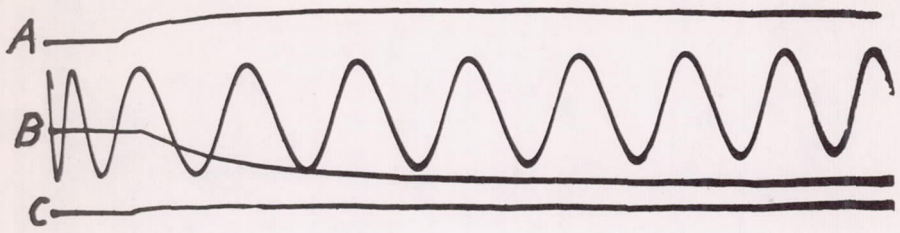

Figure 14.- "Neutral condition" in heating current. P = 1.66;
R_1 = 13.62 ohms. A: I = 4.38 milliamperes; jump upward;
R_w = 14.00 ohms. B: I = 5.08 milliamperes; jump downward;
R_w = 14.35 ohms. C: I = 4.98 milliamperes; almost no jump;
R_w = 14.18 ohms. Calibrating signal: frequency, 5-kilocycle sine wave; amplitude, 0.6 millivolt root mean square. At neutral condition (C), opposite sensitivities for temperature and mass-flow jump cancel each other.

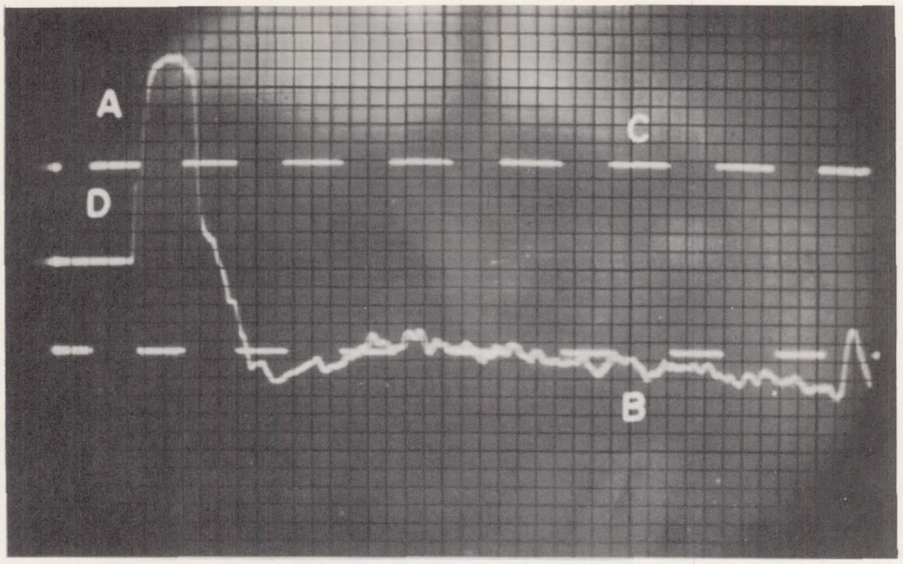

Figure 15.- Oscillogram showing hot-wire response to shock wave and contact-surface flows. (Spark triggered because of response to shock wave.) Platinum Wollaston wire, d = 0.0001 inch; P = 75; R_1 = 10.8 ohms; a_w = 0.3. A, compensated response to shock wave. B, contact surface. C, calibrating signal; frequency, 1-kilocycle square wave; amplitude, 50 millivolts. D, firing of spark.

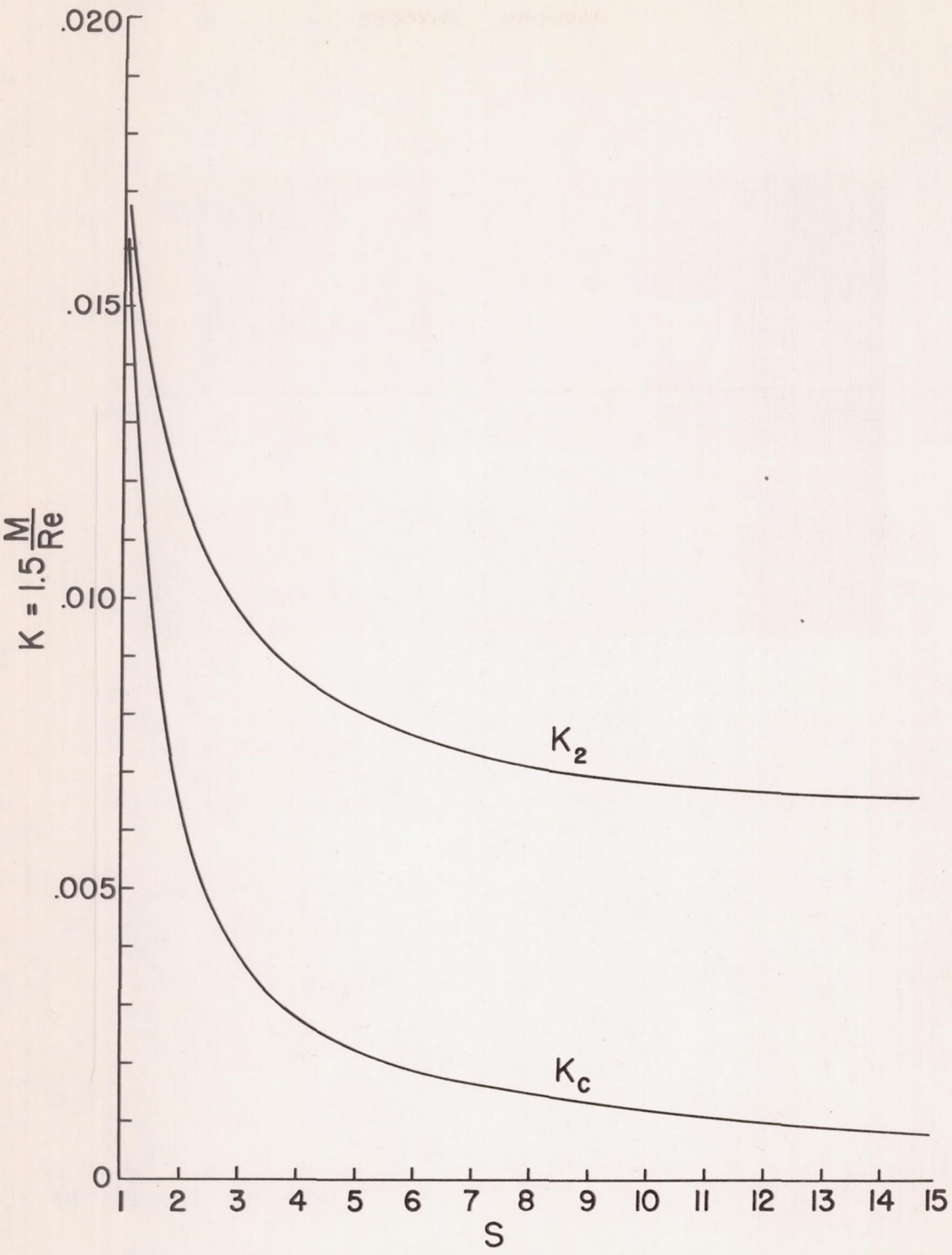

Figure 16.- Knudsen number versus shock strength. Expansion chamber at atmospheric pressure; compression chamber at higher pressure; d = 0.00015 inch (characteristic length); Air/Air.

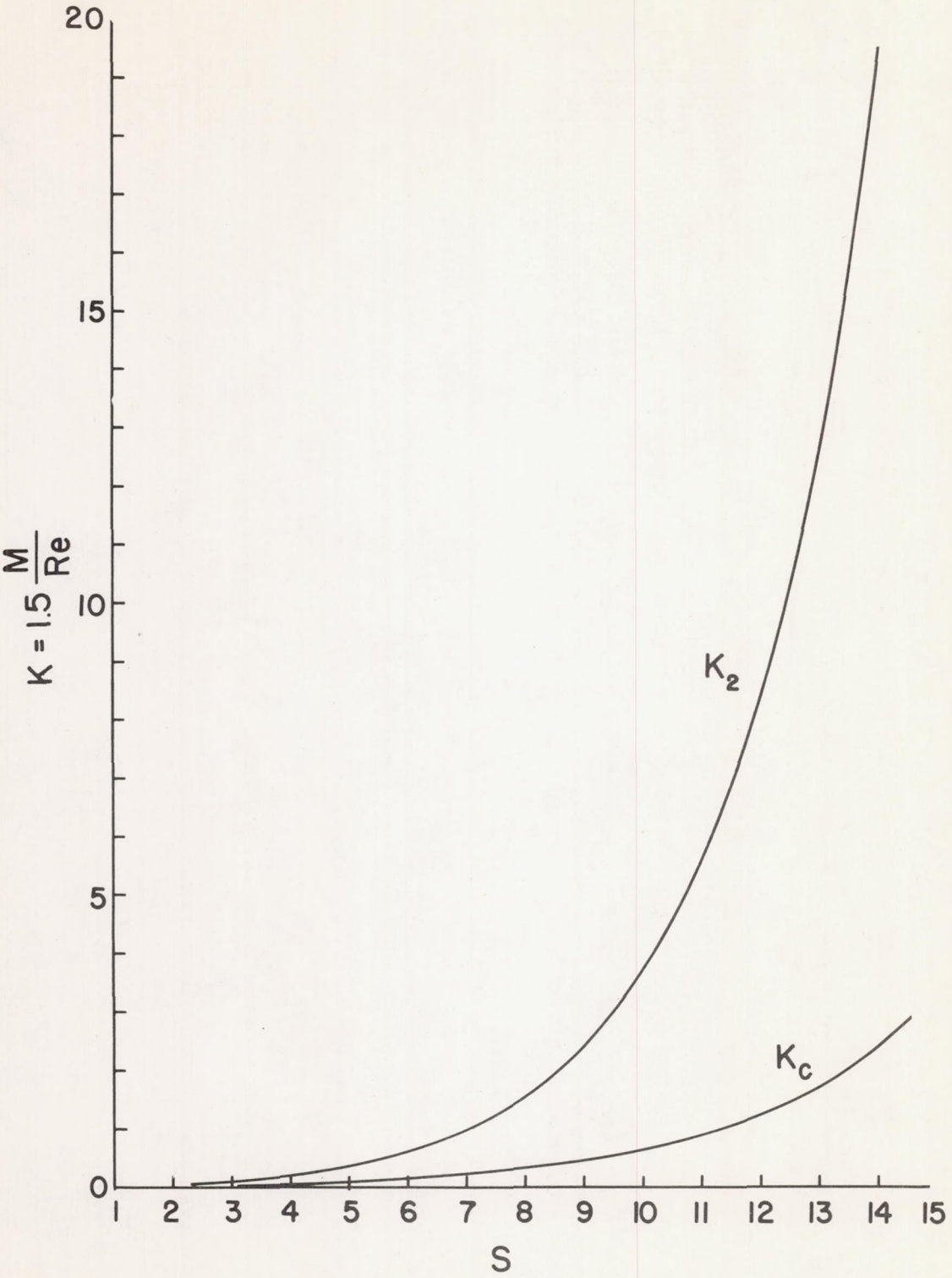

Figure 17.- Knudsen number versus shock strength. Compression chamber at atmospheric pressure; expansion chamber partially evacuated; d = 0.00015 inch (characteristic length); Air/Air.

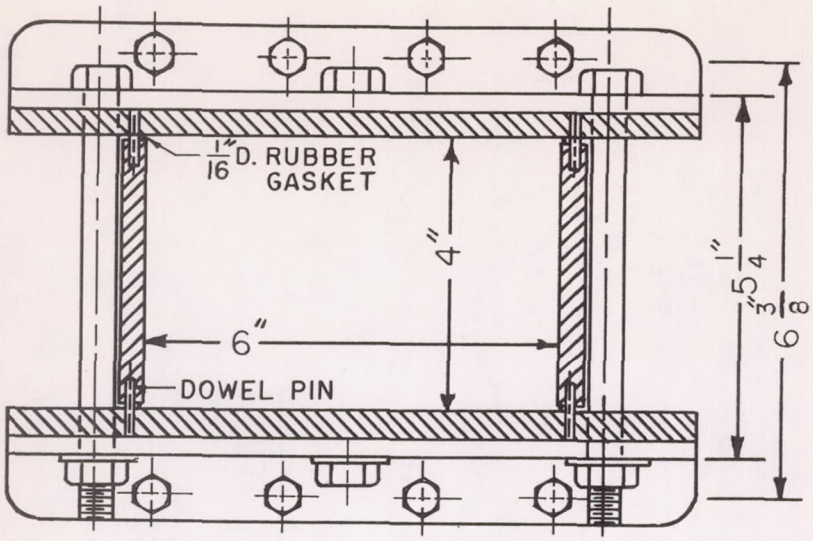

END VIEW

STEEL SECTION

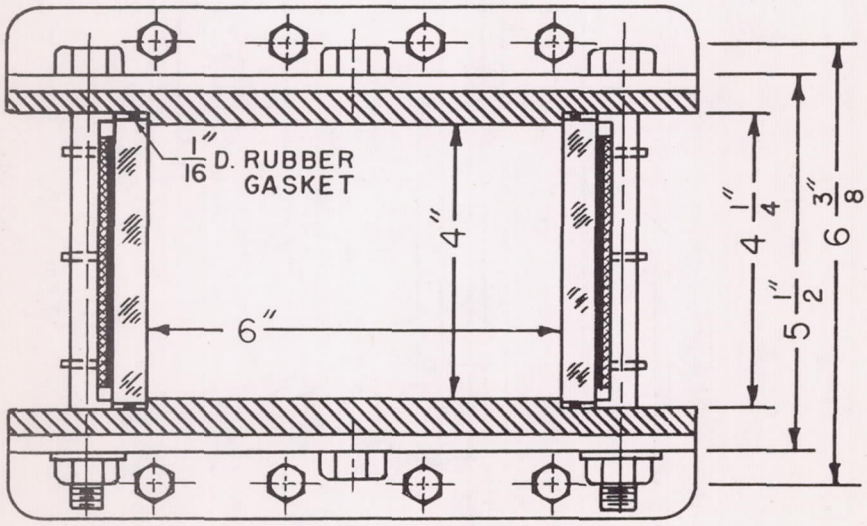

END VIEW

GLASS SECTION

Figure 18.- Shock tube.

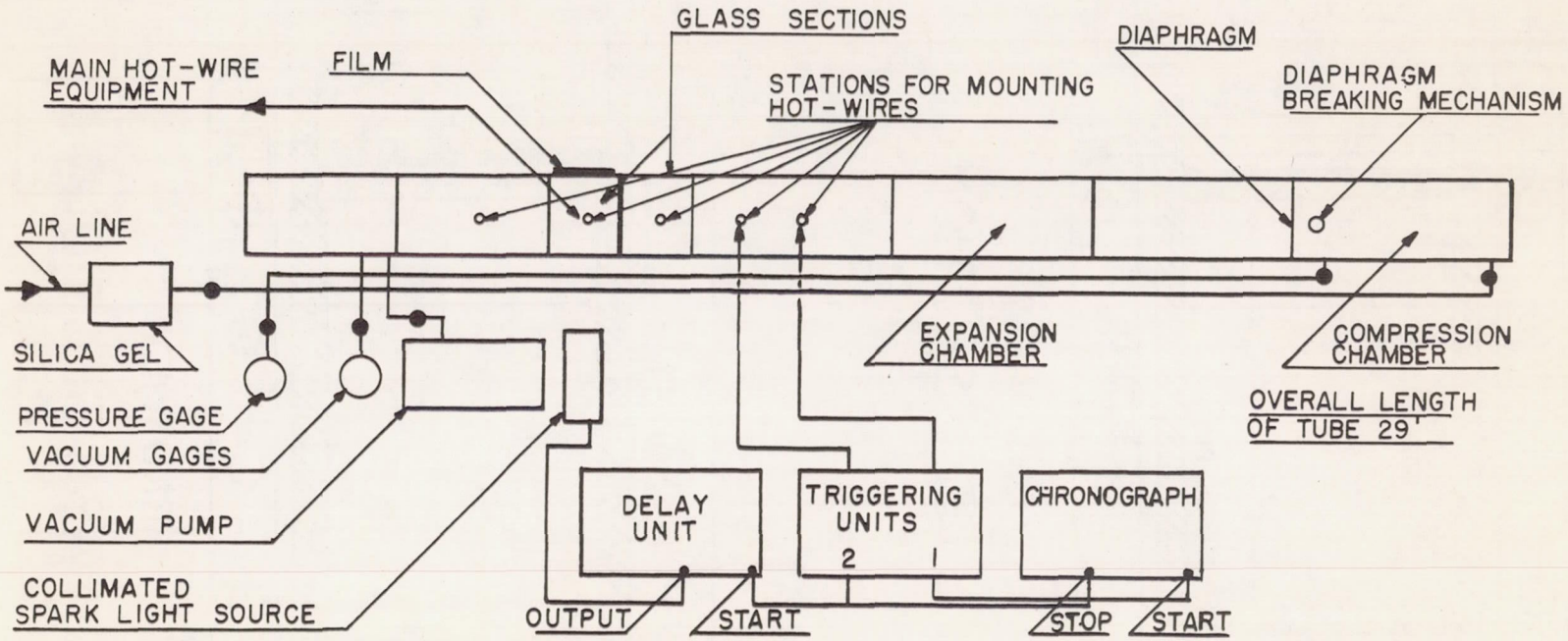

Figure 19.- General arrangement of equipment.

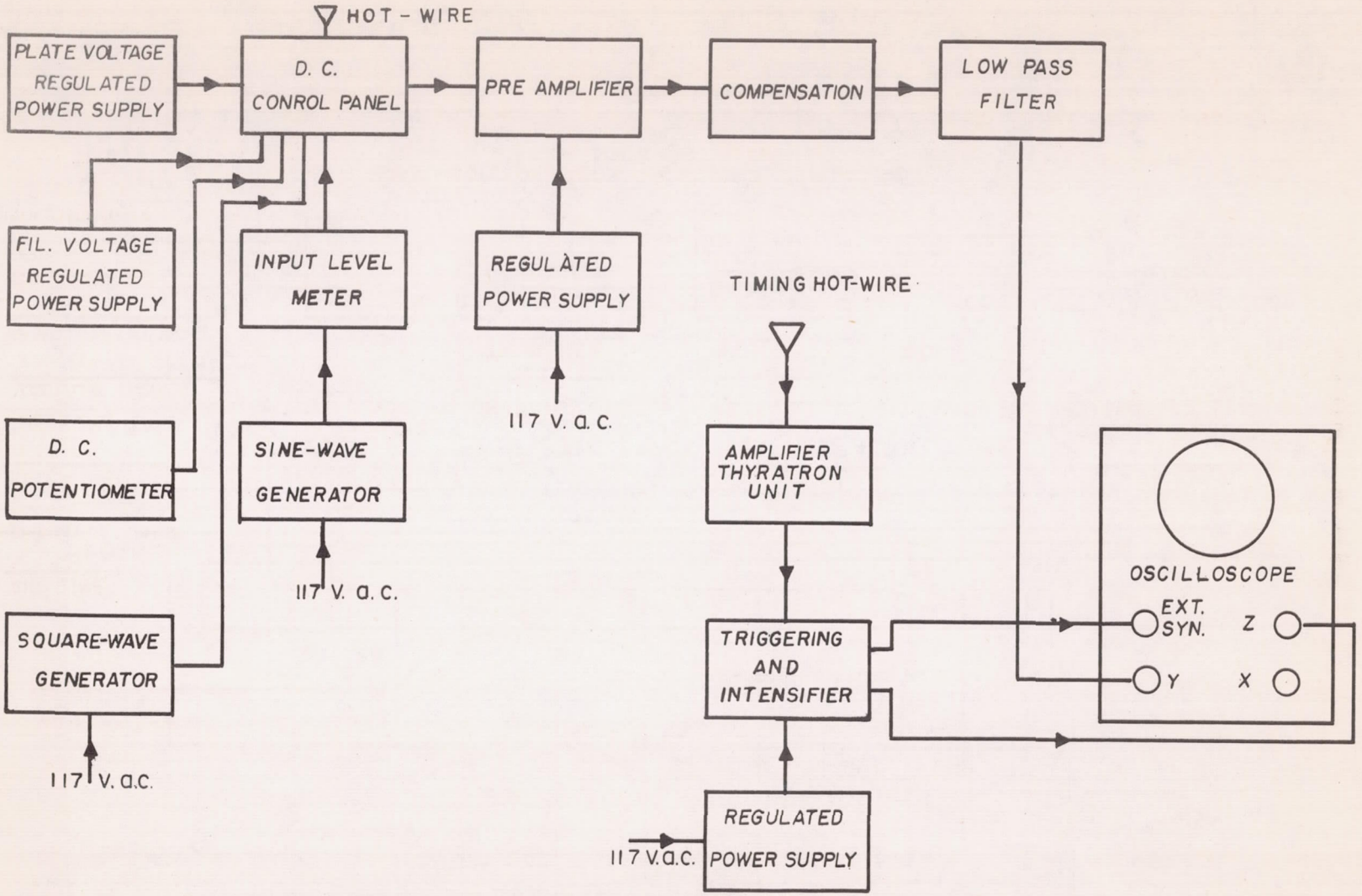

Figure 20.- Block diagram of hot-wire equipment.

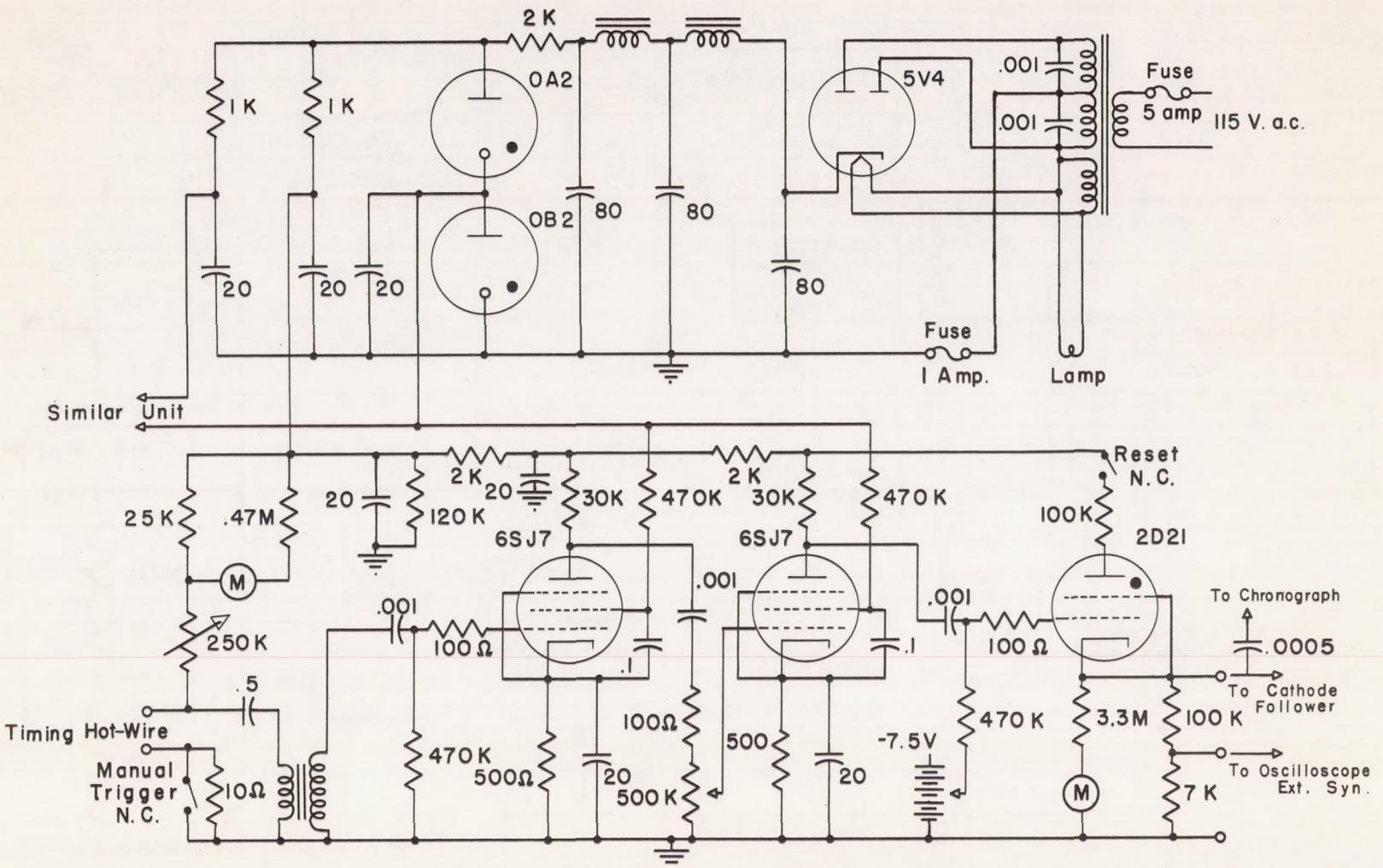

Figure 21.- Timing and triggering unit.

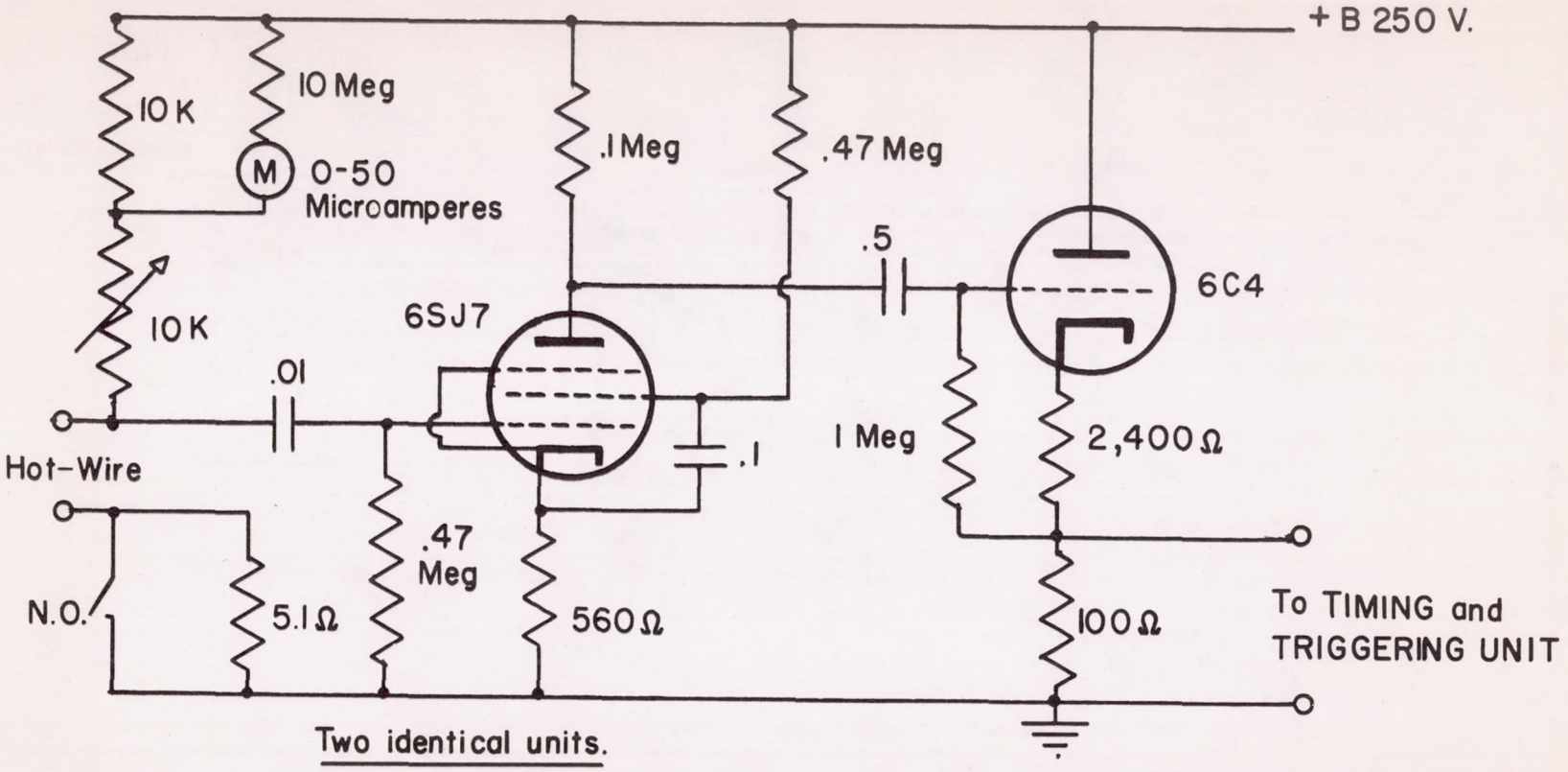

Figure 22.- Auxiliary timing and triggering unit.

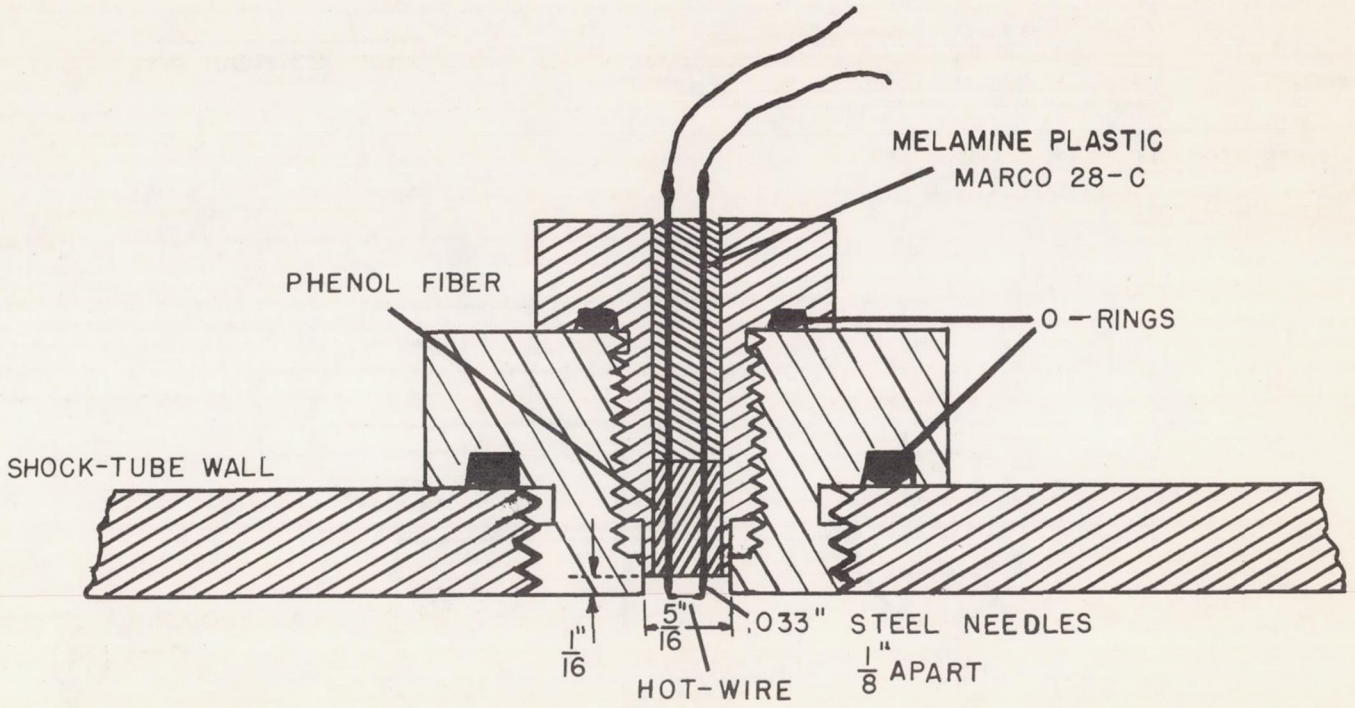

Figure 23.- Timing hot-wire probe.

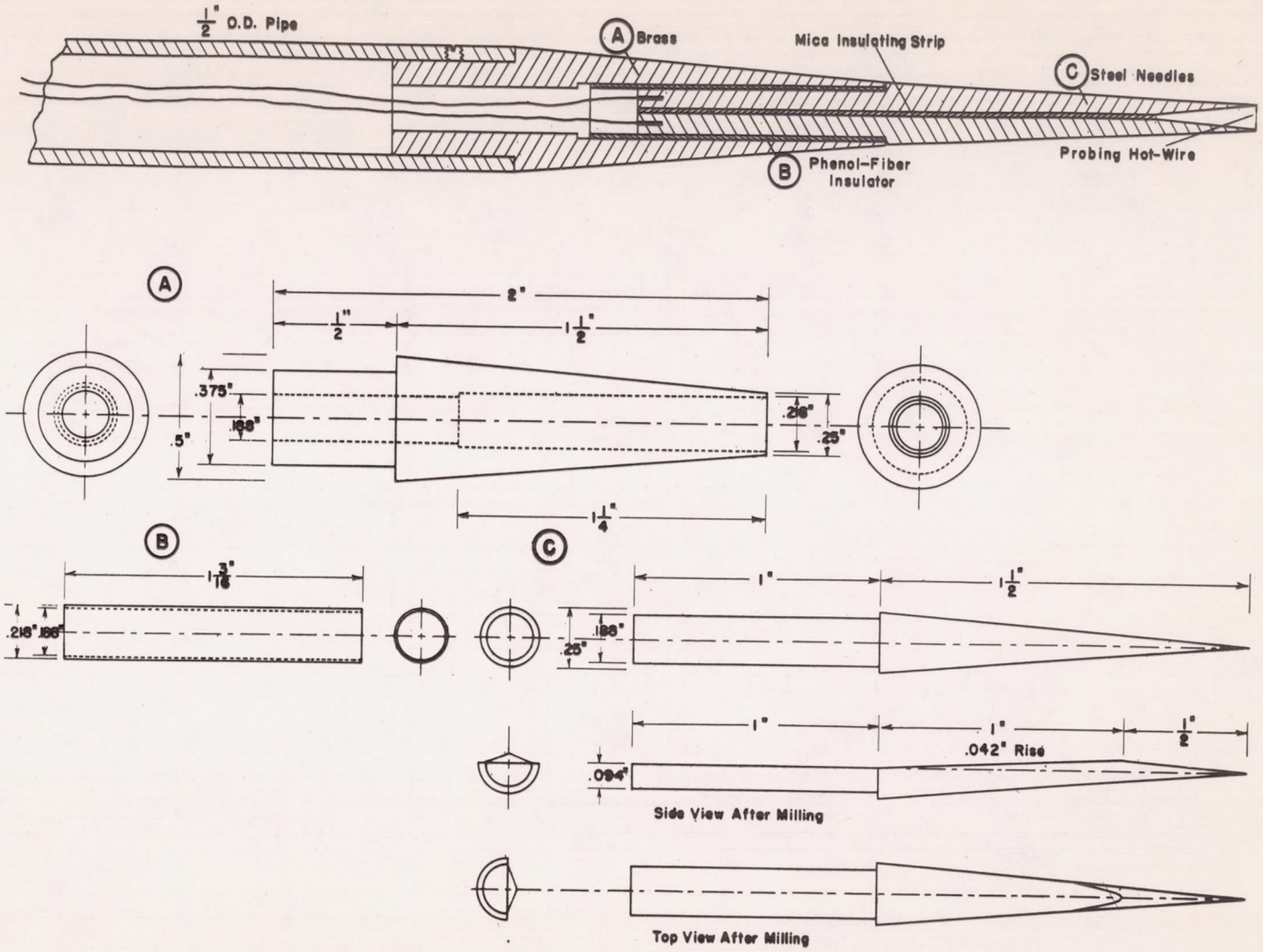

Figure 24.- Hot-wire probe.

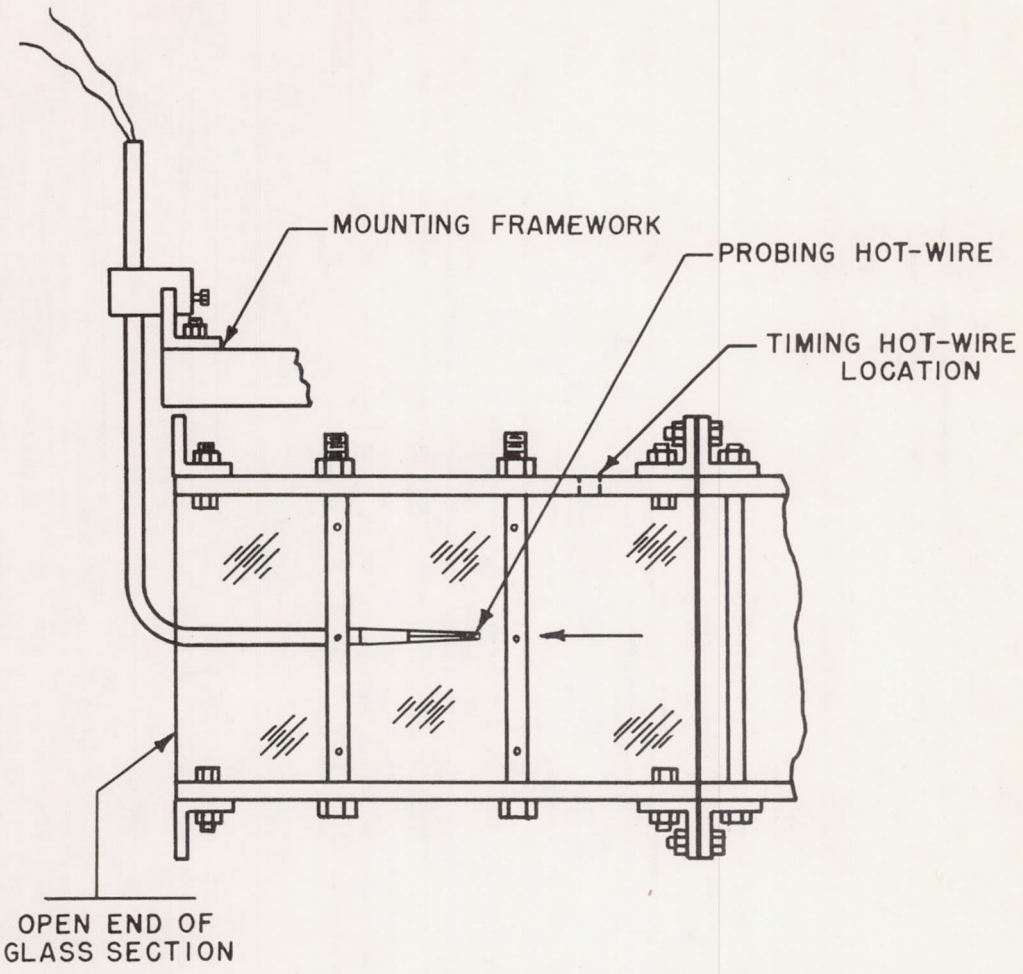

Figure 25.- Mounting of hot-wire probes.

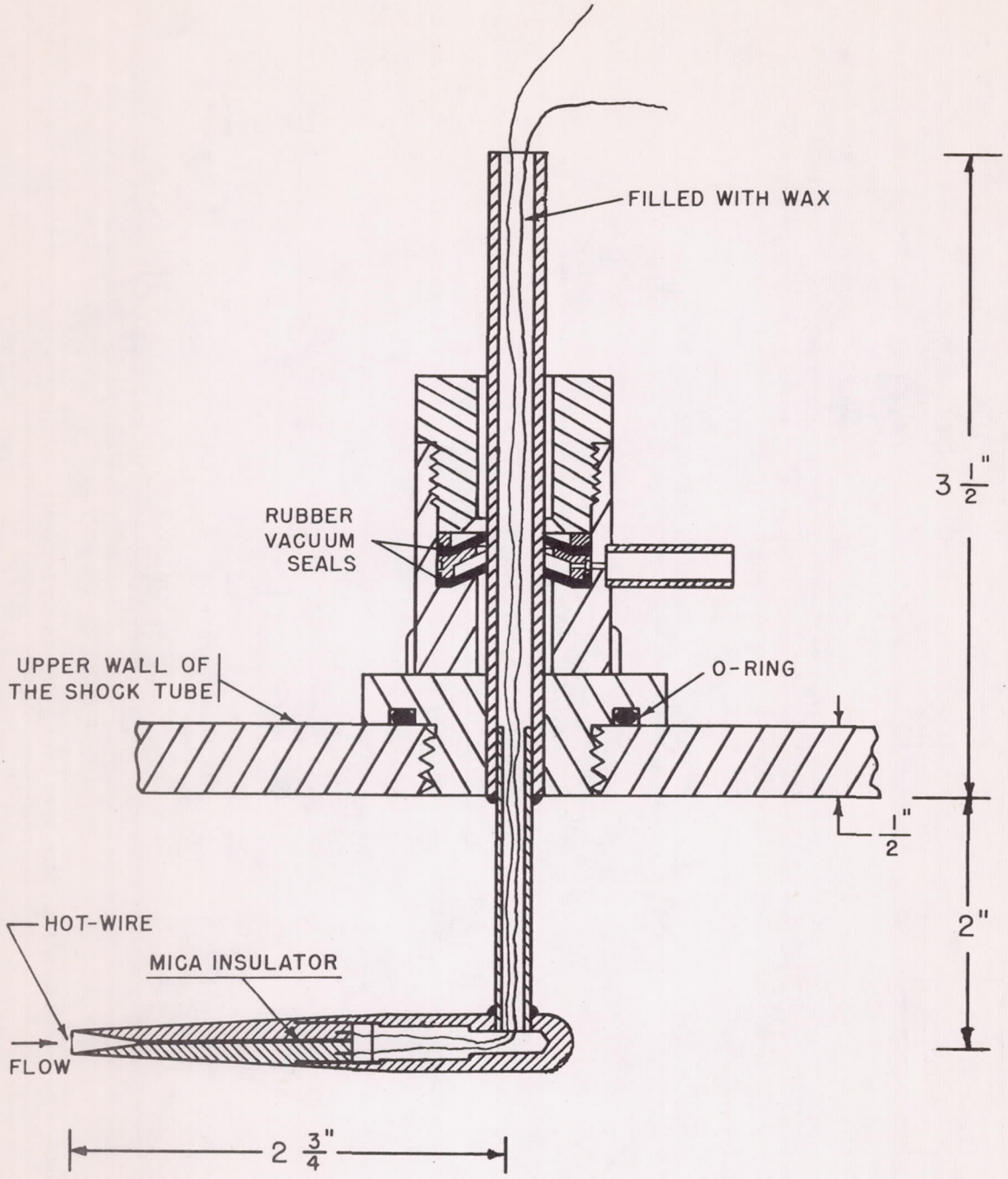

Figure 26.- Probing hot-wire with vacuum seal.

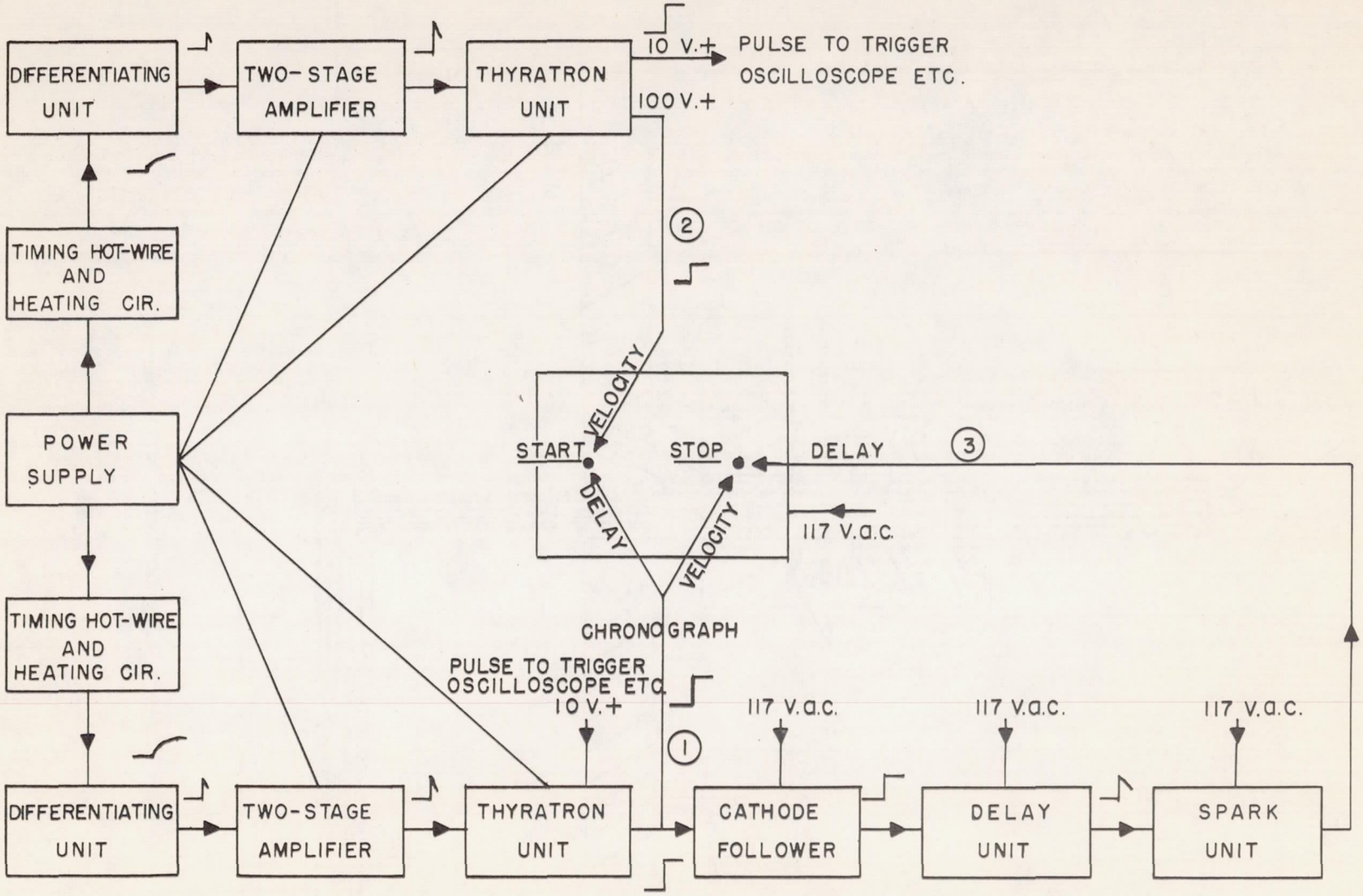

Figure 27.- Arrangement for measuring shock speeds or setting and recording time delay for shadowgraphs.

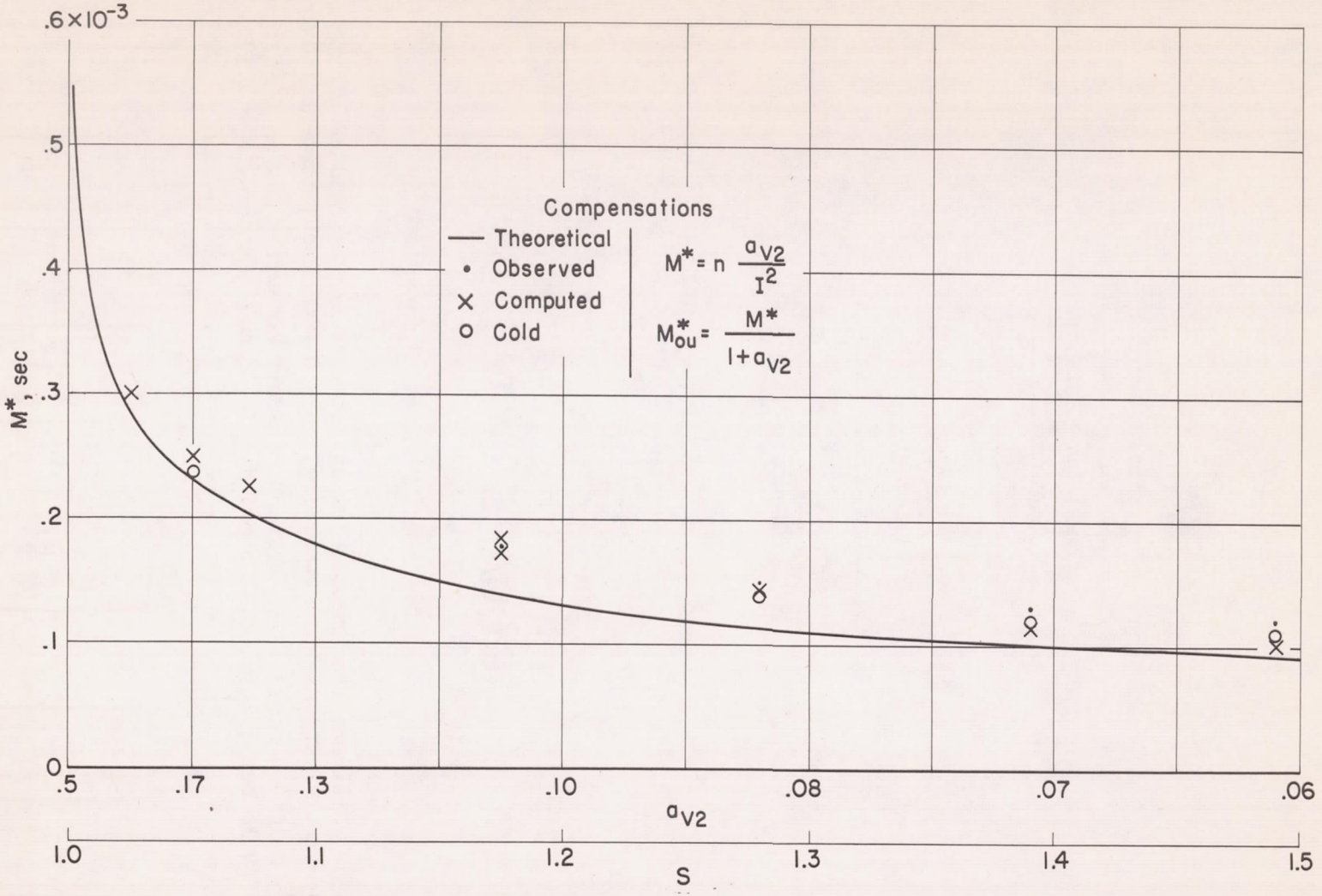

Figure 28.- Compensations versus shock strength. Platinum Wollaston wire, d = 0.0001 inch. For n, I_o, and U_o see figure 11.

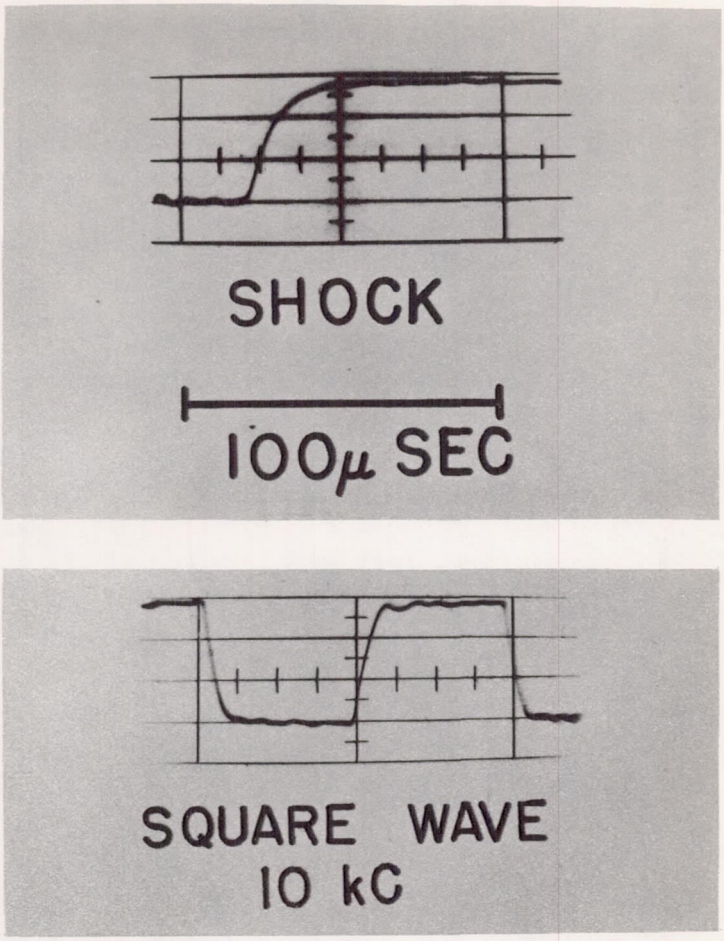

Figure 29.- Ultimate time resolution of hot-wire and associated electronic equipment. Platinum Wollaston wire, d = 0.0001 inch; compensation, 0.175×10^{-3} second; time constant of dummy hot-wire, 0.2×10^{-3} second; R_1 = 19.18 ohms; R_w = 28.77 ohms; I = 16.18 milliamperes; S = 1.175.

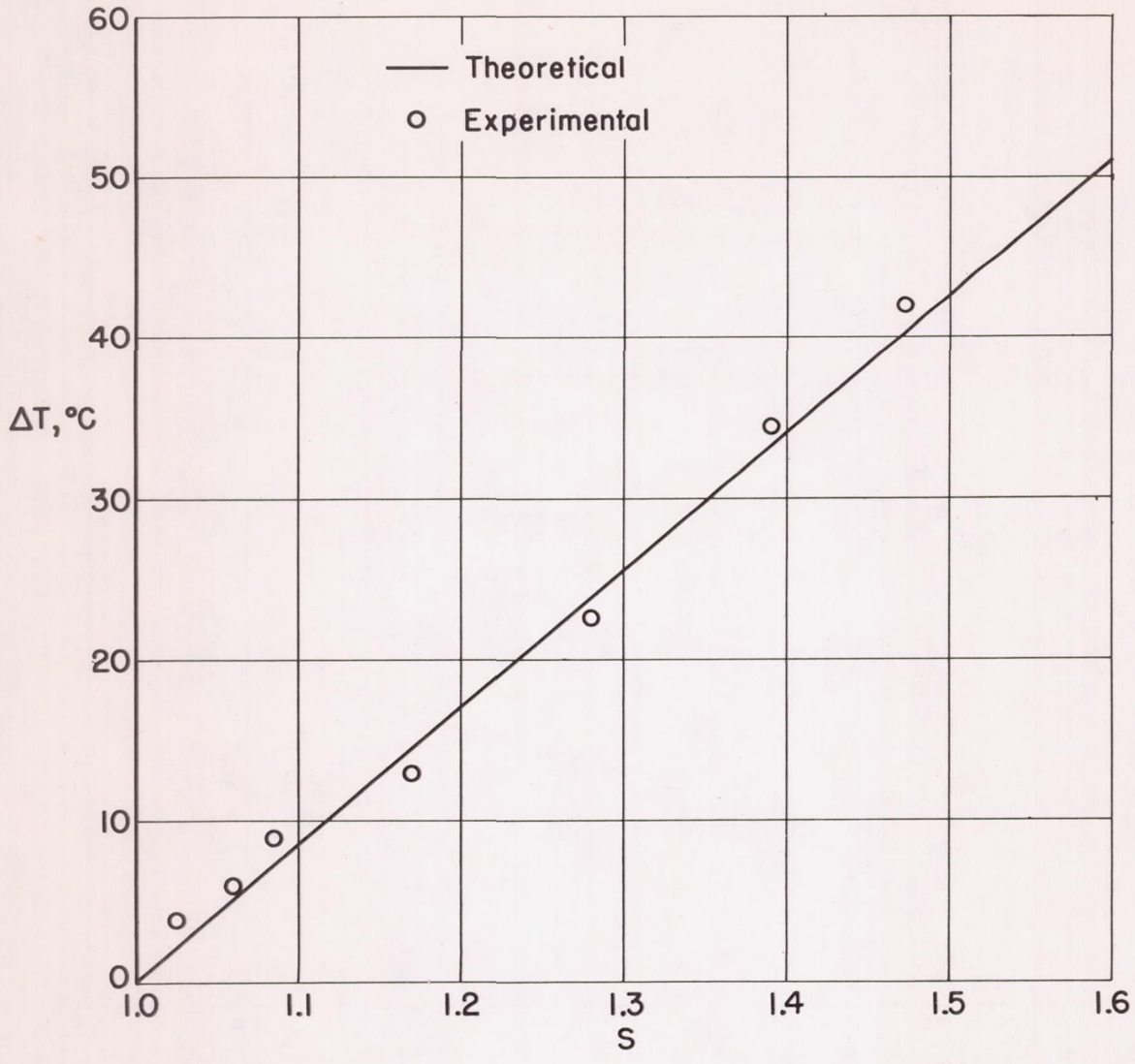

Figure 30.- Temperatures behind shock wave versus shock strength.

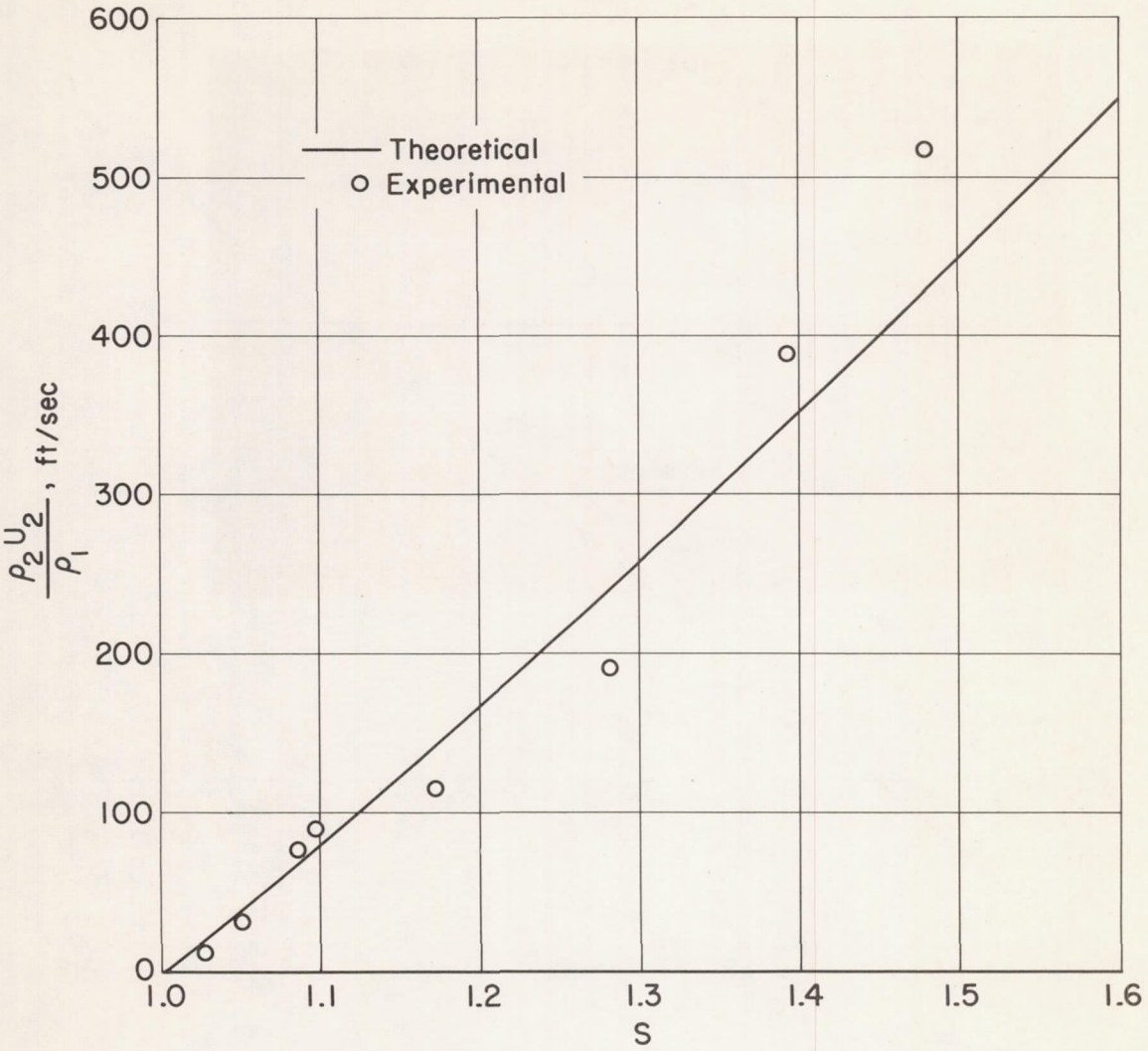

Figure 31.- Mass flow behind shock wave versus shock strength.

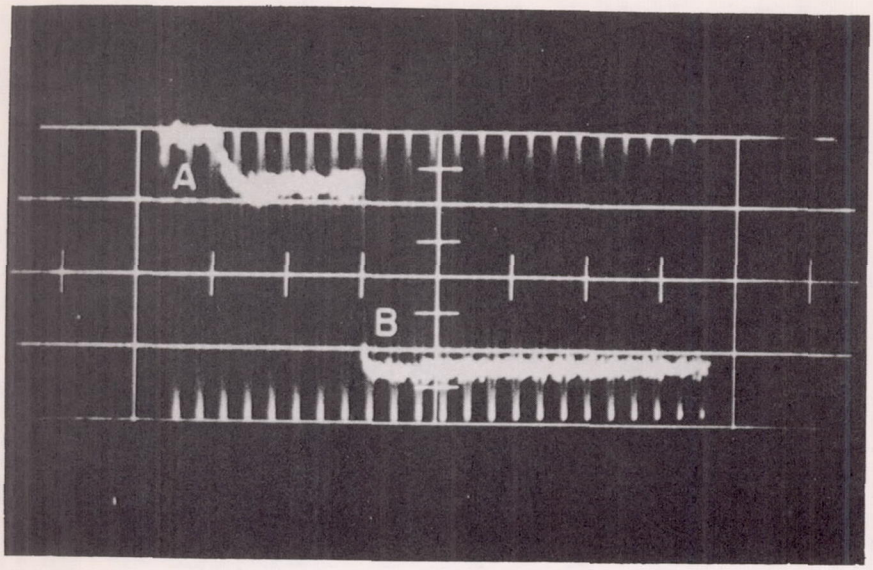

Figure 32.- Hot-wire response to shock fronts generated by use of a double diaphragm, each sheet 0.001 inch in thickness. Tungsten wire, d = 0.00015 inch; R_1 = 11.58 ohms; R_w = 17.38 ohms; I = 27.2 milliamperes; compensation, 0.24×10^{-3} second; P = 1.4. Calibrating signal: amplitude, 45 millivolts root mean square; frequency, 10 kilocycles. A, weak shock; B, strong shock.

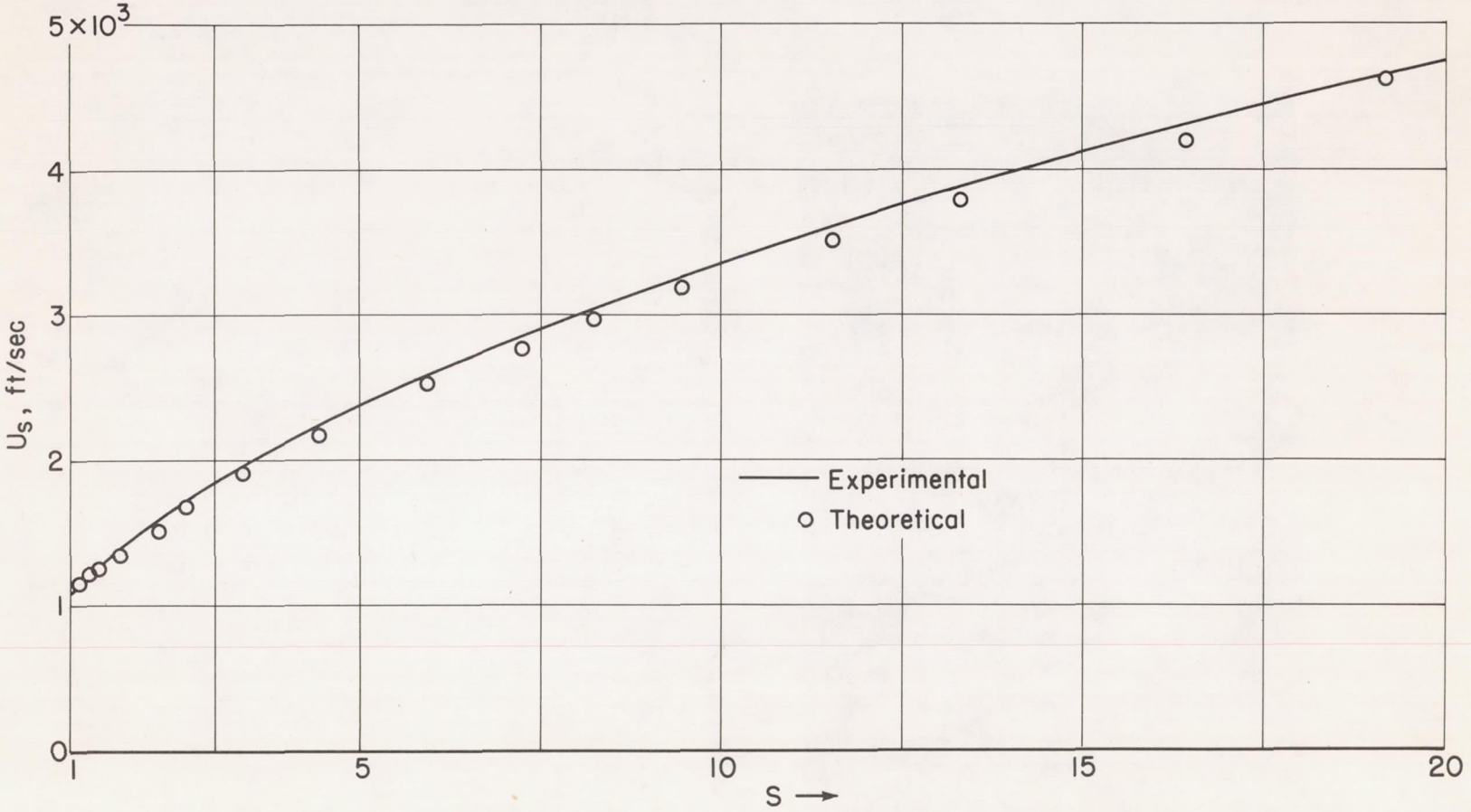

Figure 33.- Shock wave velocities as a function of shock strength (timing with hot-wire technique). a_1 = 1,141 feet per second; Air/Air.

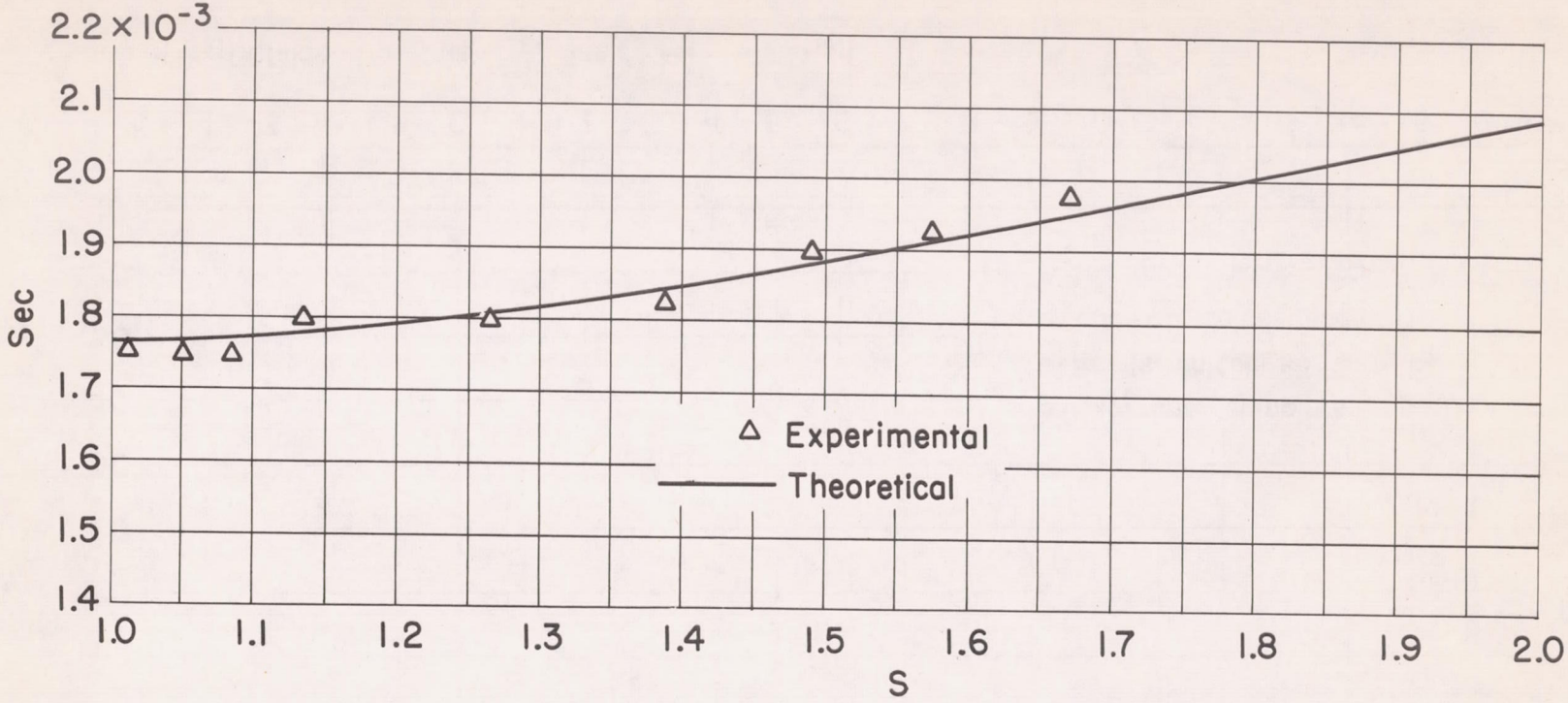

(a) Location of hot-wire 12.0 inches inside from end of shock tube.

Figure 34.- Detection and timing of rarefaction waves with hot-wire technique.

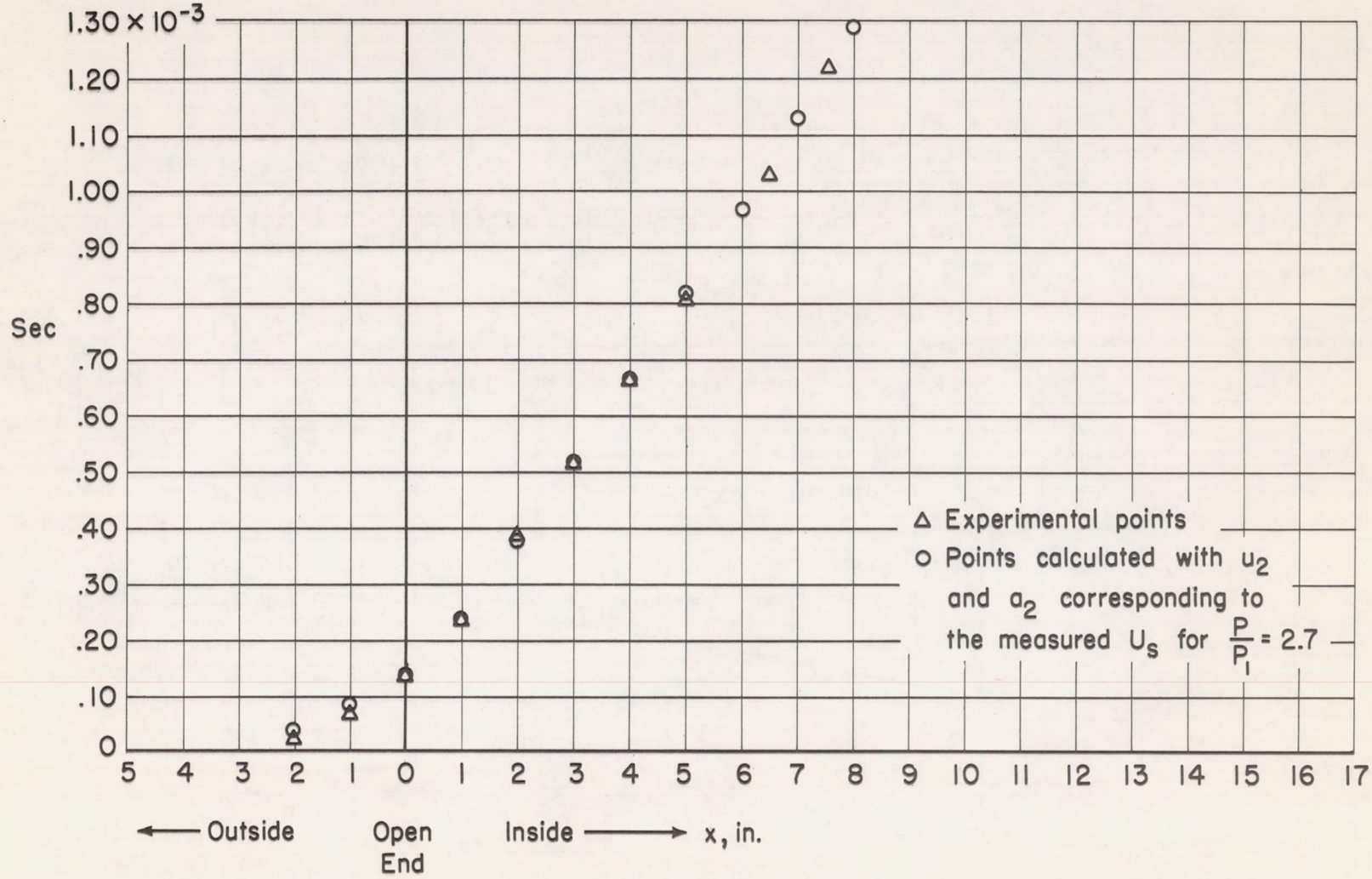

(b) Location of hot-wire varied.

Figure 34.- Concluded.

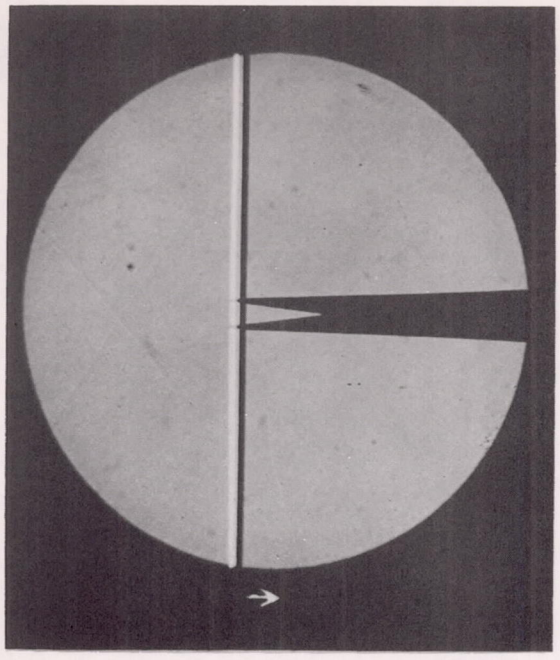

L-85636

Figure 35.- Shock front approaching hot-wire probe. S = 1.58.

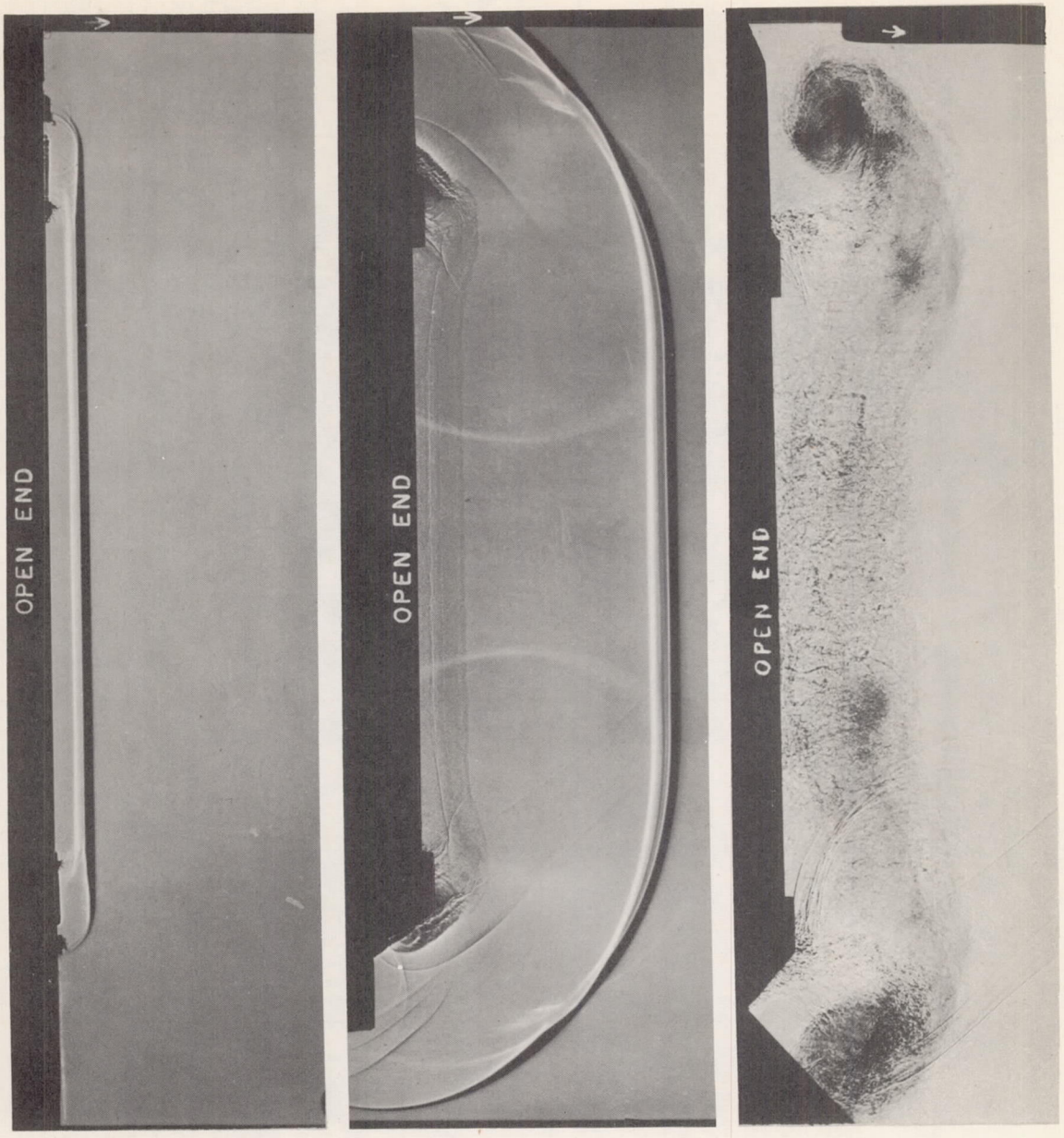

L-85637

(a) Shock front emerging from open end; S = 1.58; delay, 15×10^{-6} second.

(b) Location of shock from open end, 1.75 inches; S = 2.5; delay, 84×10^{-6} second.

(c) Location of shock from open end, 7.75 inches; S = 2.5; delay, 370×10^{-6} second.

Figure 36.- Typical shadowgraphs taken at controlled delay settings.